



The Nature Conservancy

A Model Analysis of Flow and Deposition from a Tailings Dam Failure at the Proposed Pebble Mine

Contract Number: LYNK-2018-179

March 12th, 2019

Submitted To:

The Nature Conservancy
Attention: Dave Albert
416 Harris St # 301
Juneau, AK 99801

Bristol Bay Regional Seafood Development Assn.
Attention: Andy Wink
P.O. Box 6386
Sitka, AK 99835

Submitted By:

Lynker Technologies, LLC
Cameron Wobus, Senior Scientist
3002 Bluff St., Suite 101
Boulder, Colorado 80301



Boulder, Colorado
3002 Bluff St, Suite 101
Boulder, Colorado 80301



Executive Summary

On February 20, 2019, the US Army Corps of Engineers released the draft environmental impact statement (DEIS) for the Pebble Project, a proposed copper-gold-molybdenum mine in the headwaters of the Bristol Bay watershed. The DEIS describes the potentially affected environment, the proposed project and its alternatives, and makes an effort to evaluate the environmental effects of those alternatives. While the DEIS does evaluate a number of impacts of the mine during normal operations, it does not consider the potential environmental impacts of a tailings dam failure like the ones that have recently occurred in British Columbia (Mt Polley, 2014) and Brazil (Samarco and Brumadinho, 2015 and 2019). In justifying this decision, United States Army Corps of Engineers (USACE) notes that “The probability of a full breach of the bulk or pyritic TSF tailings embankments was assessed to be extremely low” (DEIS, p. 4.27-72). As a result, “Massive, catastrophic releases that were deemed extremely unlikely were...ruled out for analysis in the EIS.” (DEIS, p. 4.27-75).

These statements in the DEIS rely entirely on the outcomes from a workshop that USACE’s third party contractor, AECOM, hosted in October of 2018, which included two representatives of USACE, one dam safety engineer from Alaska, and four representatives of the Pebble Limited Partnership (PLP). That workshop very narrowly constrained the failure analysis to consider only failures that had a reasonable chance of occurring during the 20-year operational life of the mine: “[a full tailings breach was] ruled out as remote during the 20-year operational life due to likelihood of successful detection and intervention” (AECOM, 2018). The problem with constraining the failure analysis this narrowly is that a TSF dam failure could occur at any point during the life of the dam; not just during the 20-year operational mining period.

When considering the full operational life of the tailings storage facility (TSF) impoundments, many of the aspects of the proposed tailings facility at Pebble suggest that such a failure is not “extremely unlikely”, and therefore the EIS review must consider a broader range of low probability-high consequence scenarios to be compliant with National Environmental Policy Act (NEPA) guidelines. These aspects include the following:

- The northern embankment of the larger, bulk TSF north, is approximately 164 meters high and uses the centerline construction method, even though “dams designed with downstream construction methods are less likely to fail than dams using centerline construction methods, especially under seismic shaking” (DEIS, p. 4.27-73).
- The bulk TSF is approximately ten times larger than the facilities that failed at Mt. Polley and Samarco, and is nearly unprecedented in scale relative to historical dam failures (Rico et al., 2008).
- The Pebble site receives more than 1.3 meters (52 inches) of precipitation each year, which suggests that the tailings and dam are very likely to remain wet and unstable after mine operations cease.
- There are substantial risks of seismicity at the site that could destabilize the facility via dam failure or liquefaction.

Given these clear risk factors, a full dam failure analysis falls within the NEPA mandate for understanding low-probability, high-consequence events. As the lead federal agency and the project proponent, respectively, the responsibility to conduct this analysis ultimately rests with USACE and PLP. However, in an effort to provide the public with relevant information during the DEIS public comment period, Lynker undertook a modeling study to estimate the downstream impacts of a TSF failure, if it were to occur.

We used publicly available data describing the physiography and hydrology of the region, and data published by PLP describing the proposed TSF design and other mine site characteristics, to build a model of tailings release and downstream transport. We developed our model using the FLO-2D software package, one of the few flood modeling packages capable of simulating the non-Newtonian flows that characterize tailings failures, and one that is commonly utilized by the mining industry for similar purposes (e.g., Knight Piesold, 2014; Tetra Tech, 2015). We used a comprehensive sensitivity analysis to evaluate how outcomes vary with different model parameters, and we developed a set of failure scenarios to bracket the range of potential downstream impacts for different release volumes and durations. Our results provide regulators and the public with information that will be valuable during the public comment period for the DEIS.

Under all of the scenarios tested, our model results indicate that the tailings from a dam breach would travel more than 75 kilometers (~50 miles) downstream, beyond the confluence with the Mulchatna River, where the majority

of our simulations end. Over the entire modeled reach, the mudflow fills the valley bottoms, spreading tailings across the off-channel habitat in the floodplains. The tailings within this limited model domain alone would be deposited in approximately 250 kilometers (155 miles) of streams that are mapped as salmon habitat (Johnson and Blossom, 2018), and approximately 700 kilometers (435 miles) of streams that have been identified as potentially suitable for salmon spawning and/or rearing (Woll et al., 2012). In these simulations, up to 80% of tailings are still moving through the downstream boundary of the model.

In the limited number of simulations where we expanded our model domain, the results indicate that the tailings under most scenarios would continue beyond the confluence with the Nushagak River, more than 130 kilometers (~80 miles) downstream. In these simulations, approximately 50% of the tailings are still moving through the downstream boundary of this model. Given the fine-grained nature of the material, it is extremely likely that these tailings would continue to Bristol Bay, where they would eventually settle out in the Nushagak River estuary. While we do not simulate the long-term fate of these tailings after the initial flood wave passes, the DEIS itself acknowledges that clean-up would be unrealizable in the event of a large-scale failure, and that natural attenuation would likely take decades.

With more than 130 years of sustainable harvest, Bristol Bay ranks among the most important wild salmon fisheries on earth (Hilborn et al. 2003, Knapp et al 2013). Yet the risks associated with a large-scale failure of the proposed tailings storage facility at Pebble have not been evaluated in the Draft Environmental Impact Statement that is currently under review (USACE 2019). Based on our analysis, the impacts of such a failure could be catastrophic to salmon habitat in the Nushagak watershed and should not be ignored in the EIS process.

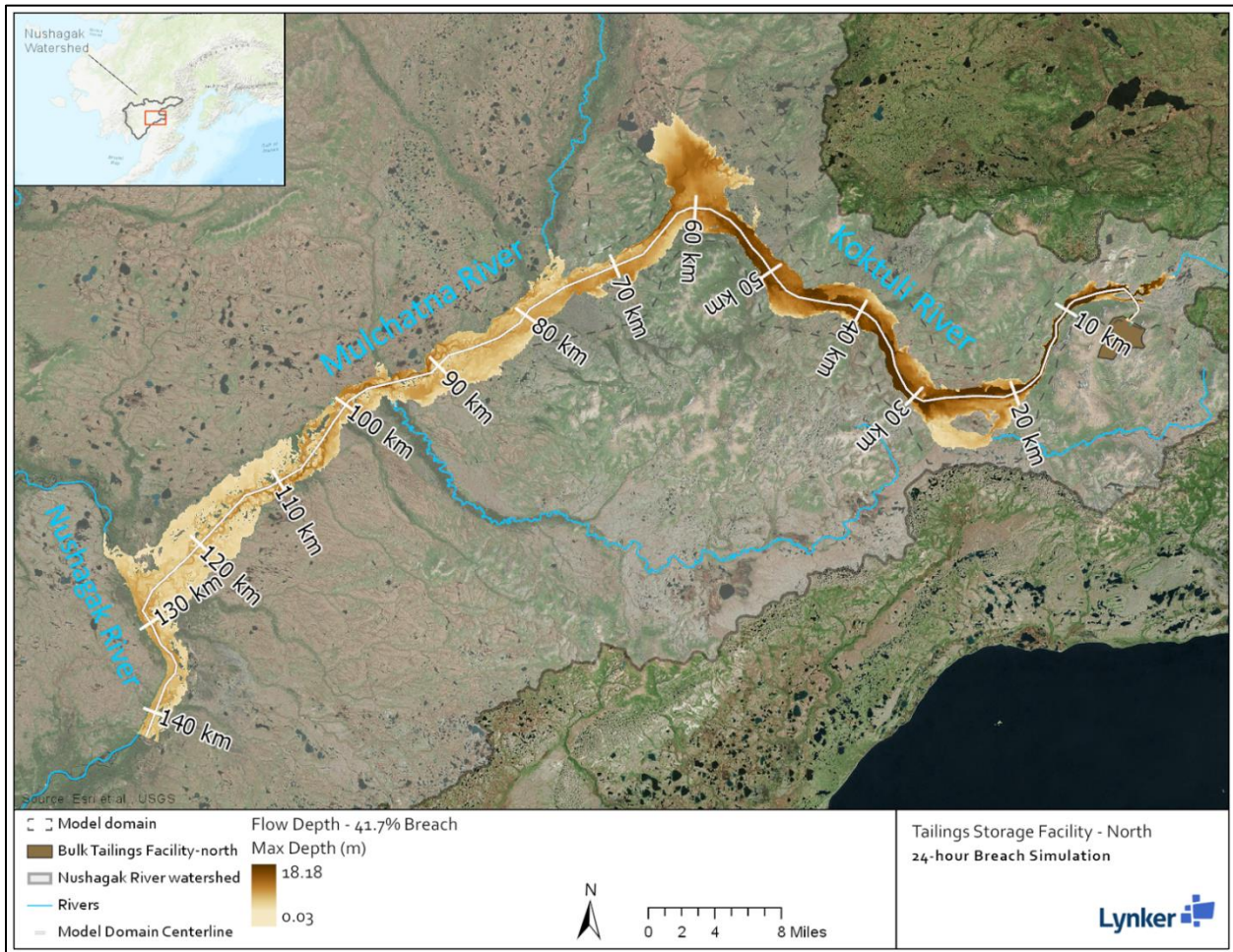


Figure ES-1. Model results from 24-hour TSF breach releasing 41.7% of tailings.

Table of Contents

1	Introduction and Background	1
1.1	Regulatory Requirements.....	1
1.2	Historical Tailings Dam Failures.....	2
1.3	Previous Work at the Pebble Site.....	2
2	Model Setup	4
2.1	Tailings Dam Failure.....	5
2.1.1	TSF Physical Properties.....	5
2.1.2	TSF Release Volume.....	5
2.1.3	Developing Breach Hydrographs.....	7
2.1.4	Dam Breach Scenarios.....	8
2.2	FLO-2D Model Setup.....	10
2.2.1	Model Domain.....	10
2.2.2	Topography and Hydrography.....	12
2.2.3	Flow Resistance.....	12
2.2.4	Mine infrastructure.....	14
2.2.5	Tailings Characteristics.....	15
2.2.6	FLO-2D Runtime Settings.....	16
3	Model Sensitivity Analysis	16
3.1	Sensitivity to Digital Elevation Model (DEM).....	17
3.2	Sensitivity to Manning’s n.....	20
3.3	Sensitivity to River Baseflow.....	23
3.4	Sensitivity to Sediment Concentration Composition.....	26
3.5	Sensitivity to Bingham Parameters.....	29
4	Dam Break Scenario Analysis	31
4.1	Koktuli River Model Results.....	32
4.1.1	Breach Volume.....	32
4.1.2	Breach Duration.....	35
4.2	Nushagak River Model Results.....	38
4.3	Impacts to Salmon Habitat.....	41
4.4	Long-term fate of tailings.....	44
5	Summary	46
6	References	46
7	Appendices	49
7.1	Additional Model Sensitivity Assessments.....	49
7.1.1	Sensitivity to Maximum Sediment Concentration.....	49
7.1.2	Laminar Flow Resistance Sensitivity.....	51
7.2	Reach-Scale Analysis of Salmon Habitat Characteristics.....	53
7.3	Report Authors and Funding.....	58

Figures

Figure ES-1. Model results from 24-hour TSF breach releasing 41.7% of tailings	b
Figure 2. Probability of dam failure throughout time.....	1
Figure 3. Map of the currently proposed PLP tailings storage facilities and mining features.....	4
Figure 4. Comparison of tailings pond capacity and calculated/observed release volume for historical breach events (historical breach data obtained from Concha Larrauri & Lall, 2018)	6
Figure 5. Comparison of dam factor and observed breach run-out distance for historical breach events (historical breach data obtained from Concha Larrauri & Lall, 2018) and the estimated Pebble bulk TSF run-out distance. Orange horizontal line shows distance to Bristol Bay for reference.....	7
Figure 6. Range of sediment concentration time series scenarios developed for input to the FLO-2D model.....	8
Figure 7. Range of TSF failure bulked hydrograph time series scenarios (variable breach durations) developed for input to the FLO-2D model	8
Figure 8. Model domain for the Koptuli River watershed model (red) and the Nushagak River watershed model (yellow) model cross-sections numbered upstream to downstream (blue circles).....	11
Figure 9. Sample grid view of the model domain with calculated flow accumulation channels	12
Figure 10. Map of Manning’s roughness polygons developed for the North Fork Koptuli to Mulchatna River model domain	13
Figure 11. Relationships between yield stress and Bingham viscosity and sediment concentration for Pebble tailings (source: PLP, 2018p)	15
Figure 12. Cross section flow accumulation plot for the 24-hour breach simulation.....	16
Figure 13: Model Sensitivity to the DEM	19
Figure 14: DEM Sensitivity Analysis – Hydrographs	19
Figure 15. Histogram of maximum flow depth with the ArcticDEM (left) and the IfSAR DEM (right).....	20
Figure 16: Model Sensitivity to Manning’s n Values.....	22
Figure 17: Hydrograph Comparison of Manning’s n Values	22
Figure 18. Histograms of the max flow depth cell values for the 0.04 (left) and 0.30 (right) Manning’s n value simulations.....	23
Figure 19: Hydrograph Comparison of Baseflow Hydrology	25
Figure 20: Hydrograph Comparison of Breach without Baseflow vs Breach with Subtracted Baseflow.....	26
Figure 21. Histograms of the max flow depth cell values for the baseflow (left) and no-baseflow (right) simulations	26
Figure 22: Max flow depth map of model sensitivity to sediment concentration distribution of breach discharge..	28
Figure 23: Sediment Concentration Distribution Sensitivity Analysis – Hydrograph.....	28
Figure 24. Histograms of the max flow depth cell values for the less viscous (left) and PLP-derived parameters (right) simulations	29
Figure 25: Max flow depth map of model sensitivity of breach discharge viscosity	30
Figure 26: Mudflow Viscosity Sensitivity Analysis – Hydrograph	31
Figure 27. Histograms of the max flow depth cell values for the less viscous (left) and PLP-derived parameters (right) simulations	31
Figure 28. Breach volumes scenario analysis of max flow depth – 10% breach volume (green) vs. 60% breach volume (orange).....	33
Figure 29. Histograms of the max flow depth cell values for the 10% (top left), 42% (top right), and 60% (bottom) breach volume simulations	34
Figure 30: Hydrographs at the Koptuli and Mulchatna Rivers comparing breach volume scenarios.....	35
Figure 31: Breach Duration Scenario Comparison – 96-hr event (top) compared to a 6-hr event (bottom).....	36
Figure 32. Histograms of the max flow depth cell values for the 6-hr (top left), 24-hr (top right), and 96-hr (bottom) breach duration simulations.....	37
Figure 33. Floodplain Hydrographs showing different breach durations.....	38
Figure 34. Example comparison of top of canopy first return vs. bare earth DEM	39
Figure 35. Max flow depth comparison between the 10% breach volume (green) and the 41.7% breach volume (orange) simulations	40
Figure 36. Histograms of the max flow depth cell values for the 41.7% breach volume (left) and 10% breach volume (right) for the Nushagak model domain simulations	41

Figure 37. Example of potential off-channel reaches (dashed blue line) visible from satellite imagery that are not represented by the AWC designated reach (solid blue line)	42
Figure 38. Map of the simulated max flow depth (41.7% breach volume) and the inundated protected anadromous fish reaches	42
Figure 39. 2015 relative production of Sockeye salmon	43
Figure 40. 2015 relative production of Chinook salmon	44
Figure 41. Example of the landscape effects of a TSF failure in Brazil.....	45
Figure 42: Max flow depth map of model sensitivity to sediment concentration of breach discharge	50
Figure 43: Sediment Concentration Sensitivity Analysis – Hydrograph	51
Figure 44. Histograms of the max flow depth cell values for the 50% (left) and 35% (right) max sediment concentration simulations	51
Figure 45: Laminar Flow Resistance Sensitivity Analysis – Hydrograph	52
Figure 46. Histograms of the max flow depth cell values for the increased laminar flow (left) and default laminar flow (right) simulations	53
Figure 47. Map of 24-hr breach inundation and Chinook Salmon spawning (top) and rearing (bottom) habitat suitability reach scores.	54
Figure 48. Map of 24-hr breach inundation and Sockeye Salmon spawning (top) and rearing (bottom) habitat suitability reach scores.	55
Figure 49. Map of 24-hr breach inundation and Coho Salmon spawning (top) and rearing (bottom) habitat suitability reach scores.	56
Figure 50. Map of 24-hr breach inundation and Pink Salmon spawning (top) and Chum Salmon spawning (bottom) habitat suitability reach scores.	57

Tables

Table 1. Summary of the calculated specifications for the PLP mining storage facilities	5
Table 2. Summary of all breach discharge scenarios developed for input to FLO-2D.....	9
Table 3: Land Use Classification and Manning’s n Values	13
Table 4: Mudflow Parameters.....	15
Table 5: FLO-2D Model Sensitivity Tests	17
Table 6: DEM Sensitivity Analysis – Model Output	18
Table 7: DEM Sensitivity Analysis – Hydrograph Output	18
Table 8: Manning’s n Sensitivity Analysis – Model Output.....	21
Table 9: Manning’s n Sensitivity Analysis – Hydrograph Output.....	21
Table 10: Drainage area and average streamflow for study area sub-basins	23
Table 11: Baseflow Sensitivity Analysis – Model Output.....	24
Table 12: Baseflow Sensitivity Analysis – Hydrograph Output	25
Table 13: Sediment Curve Sensitivity Analysis – Model Output	27
Table 14: Sediment Curve Sensitivity Analysis – Hydrograph Output	27
Table 15: Yield Stress Sensitivity Analysis – Model Output.....	29
Table 16: Yield Stress Sensitivity Analysis – Hydrograph Output.....	29
Table 17: Dam Break Scenario Analysis.....	32
Table 18: Breach Volume Scenario Analysis – Model Output.....	33
Table 19: Breach Volume Scenario Analysis – Hydrograph Output	35
Table 20: Breach Duration Scenario Analysis – Model Output	36
Table 21: Breach Duration Scenario Analysis – Hydrograph Output	38
Table 22: Nushagak River Watershed Model Scenarios.....	39
Table 23. Model Results for Nushagak Model Runs	40
Table 24: Maximum Sediment Concentration Sensitivity Analysis – Model Output.....	49
Table 25: Maximum Sediment Concentration Sensitivity Analysis – Hydrograph Output.....	49
Table 26: Laminar Flow Sensitivity Analysis – Model Output.....	52
Table 27: Laminar Flow Sensitivity Analysis – Hydrograph Output	52

1 Introduction and Background

In February of 2019, the US Army Corps of Engineers (USACE) released a draft environmental impact statement (DEIS) describing the direct, indirect and cumulative impacts of mining the Pebble Deposit in southwestern Alaska, one of the largest undeveloped copper deposits in the world. Mining this resource would require perpetual storage of billions of tons of mining waste, including tailings. These tailings would be stored in tailings storage facilities (TSFs) behind massive earthen dams, which must maintain their integrity in perpetuity to prevent contamination of the rivers downstream. A failure of one of these earthen dams could potentially cause significant harm to salmon spawning and rearing habitat in the headwaters of the Nushagak-Mulchatna River system, an important part of the Bristol Bay salmon fishery.

1.1 Regulatory Requirements

As part of the EIS process, the National Environmental Policy Act (NEPA) requires that project proponents take a “hard look” at the potential environmental impacts of their proposed action and the alternatives. NEPA requires a complete investigation into potential environmental impacts and acknowledgement of potential environmental harms. As described in NEPA (40 C.F.R. § 1502.22), the EIS’s cumulative impacts analysis must include quantified and detailed information about past, present and reasonably foreseeable future actions. “Reasonably foreseeable” includes impacts which have catastrophic consequences, even if their probability of occurrence is low.

Despite these requirements, the draft EIS for the Pebble Mine does not consider the possibility of a complete tailings dam failure at any of the proposed facilities, noting that “The probability of a full breach of the bulk or pyritic TSF tailings embankments was assessed to be extremely low” (DEIS, p. 4.27-72). This assessment of the low level of risk relies on the outcomes of a “Failure Modes and Effects Analysis” (FMEA) workshop, wherein the participants very narrowly constrained the failure analysis to consider only failures that had a reasonable chance of occurring during the 20-year operational life of the mine: “[a full tailings breach was] ruled out as remote during the 20-year operational life due to likelihood of successful detection and intervention” (AECOM, 2018).

Elsewhere in the DEIS, USACE cites a number of studies that demonstrate the probability of a TSF failure to be approximately 1 failure per 2000 dam years (Davies et al., 2000; Chambers and Higman, 2011; Peck, 2007). Based on this 1:2000 probability in any given year, Figure 2 shows how the probability of failure increases with dam lifetime. By this analysis, the probability of a tailings dam failure is approximately 1% over the 20-year operational life of the mine, and approximately 5% over a 100-year operational and post-closure timeframe (Figure 1). Because of the potentially catastrophic impacts to the fishery, these probabilities should fall well within the threshold of analysis for low-probability, high-consequence events that NEPA requires.

Other information contained in the DEIS further underscores the need for a detailed study of a TSF failure. These aspects include the following:

- The northern embankment of the bulk TSF is approximately 164 meters high and uses the centerline construction method. The DEIS states that “dams designed with downstream construction methods are less likely to fail than dams using centerline construction methods, especially under

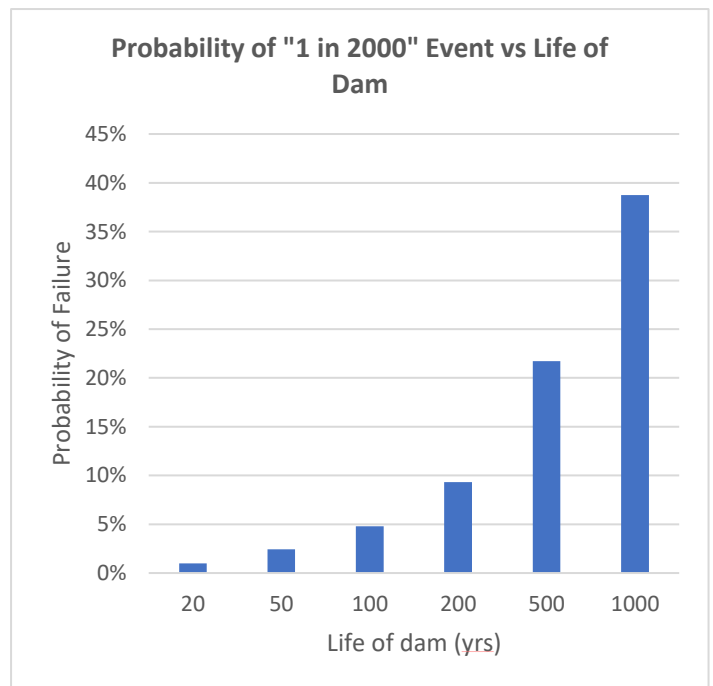


Figure 2. Probability of dam failure throughout time

seismic shaking” (DEIS, p. 4.27-73). Thus, despite the acknowledged risks, PLP is not proposing the most stable dam design for the TSF.

- The bulk TSF is approximately ten times larger than the facilities that failed at Mt. Polley and Samarco, and is nearly unprecedented in scale relative to historical dam failures (Rico et al., 2008).
- The Pebble site receives more than 1.3 meters (52 inches) of precipitation each year, which suggests that the tailings and dam are very likely to remain wet and potentially unstable after mine operations cease.

1.2 Historical Tailings Dam Failures

The most recent tailings dam failures in British Columbia and Brazil have demonstrated that even modern dams built to present-day engineering specifications can fail. Depending on the type of tailings released and the setting in which the failure occurs, these failures can have potentially disastrous effects on humans and the environment. At the Samarco mine, for example, tailings were transported more than 600 km (370 miles) downstream, leaving behind a trail of iron-rich mud that will most likely continue to be a source of contamination for decades. At the Feijao Mine, the tailings dam failure killed more than 200 people, with approximately 100 others unaccounted for at the time of this writing. While the Mt. Polley failure was limited in spatial extent because it emptied into nearby Lake Quesnel, this failure nonetheless destroyed salmon spawning habitat along Hazeltine Creek, and its full effects on the aquatic ecosystem at Quesnel Lake are not yet known.

Furthermore, while both of the recent failures in Brazil occurred on dams built using the less stable “upstream” method, the Mt. Polley dam was built using a “modified centerline” method, which is considered to be more stable. Despite this higher standard of safety, the Mt. Polley tailings dam still failed, due to geologic factors that were unknown at the time it was designed. These factors should have been recognized by Knight Piesold but were missed even under the extensive review and permitting process for the Mt. Polley mine. Knight Piesold now is the same engineering firm hired by PLP to design the tailings dam at the Pebble mine, under a dramatically accelerated EIS scheduling process compared to other mines of its size.

Finally, none of these recent tailings dam failures were “one-off” events. The Feijao dam failure was the 11th serious tailings dam failure in the last decade, and such catastrophic events are becoming more frequent, according to researchers at the non-profit World Mine Tailings Failures (WMTF, 2019). The number of incidents is projected to rise without major changes to law, regulation, and industry practices, and without new technology that substantially reduces risk and increases loss control. WMTF’s current prediction is for 19 ‘very serious’ failures between 2018 and 2027

1.3 Previous Work at the Pebble Site

As part of the Bristol Bay Watershed Assessment (USEPA, 2014), the US Environmental Protection Agency simulated downstream transport of tailings from a breach of a tailings dam at the Pebble site. In that analysis, EPA used the hydraulics package HEC-RAS to simulate the flood wave and downstream transport of tailings from a conceptual mine scenario consistent with the information available at the time. The model domain extended approximately 30 km downstream from the tailings storage facility. That analysis found that tailings would be transported far beyond the model boundary, and that the effects would likely be long-lasting:

Deposited tailings and their leachate would persist at toxic levels for decades. The acute effects of a tailings spill would extend far beyond the modeled 30-km (18.6 mi) distance downstream (USEPA, 2014, p. 9-45)

Although the USEPA analysis indicated far-reaching impacts from a TSF dam failure, the Draft EIS does not consider the possibility of a dam failure occurring. Instead, the DEIS contains a very narrow spill analysis that is based entirely on decisions made during an October 2018 FMEA workshop.¹ At that workshop, it was determined that a complete breach of a TSF dam would not be analyzed because its probability of occurrence was too remote

¹ The “Failure Modes and Effects Analysis” workshop in Anchorage on October 24-25, 2018 was run by AECOM. In addition to AECOM personnel, the meeting included two representatives of USACE, one dam safety engineer from Alaska, and four representatives of PLP. The workshop very narrowly defined the analysis to consider only potential failures that had a reasonable chance of occurring over the 20-year operational life of the mine.

during the 20-year operational life of the mine. Instead, Knight Piesold, on behalf of PLP, simulated the impacts of two very limited failures: one failure of the tailings delivery pipeline to the bulk TSF (Knight Piesold, 2018o) and a 6 foot breach of the 300' dam impounding the potentially acid generating (PAG) tailings facility that was assumed to stop after a small amount of tailings and water drained from the PAG TSF (Knight Piesold, 2018p). The pipeline breach described in Knight Piesold (2018o) does not represent a true TSF failure; as shown below, the volume of tailings released in this scenario is approximately 10,000 times smaller than what would be expected from a full tailings dam failure. Similarly, the 0.87 million tons released in the pyritic TSF failure simulation is approximately 60 times smaller than the approximately 52 million tons that empirical data would indicate could be released from an impoundment of this size (Rico et al., 2008; Laurrali and Lall, 2018).

As the lead federal agency and the project proponent, respectively, the responsibility to conduct an analysis of the impacts of a TSF dam failure event ultimately rests with USACE and PLP. However, in an effort to provide the public with relevant information during the DEIS public comment period, Lynker undertook this modeling study to estimate the downstream impacts of a TSF failure, if it were to occur. Our modeling extends the USEPA (2014) analysis in two important ways. First, because the USEPA model domain was not large enough to simulate the fate of tailings more than 30km downstream, we extended our modeling domain approximately 140 km down the Kaktuli river system, to just below the confluence between the Mulchatna and the Nushagak River. And second, because the material released from a tailings dam failure typically has a very high sediment concentration with a substantially different rheology than a clear flood flow, we simulated the TSF failures at Pebble as a non-Newtonian flow using the modeling package FLO-2D (e.g., Orman et al., 2017; Knight Piesold, 2014). USEPA (2014) used HEC-RAS for their modeling, while acknowledging the limitations of using HEC-RAS for highly sediment-laden/non-Newtonian flows.

As with the USEPA (2014) study, the goal of our modeling is not to predict exactly where sediment released from a TSF failure would go; uncertainties related to both model parameters and the failure scenario itself are both too broad to develop a predictive model. Rather, our goal is to simulate a range of plausible failure scenarios based on both site-specific characteristics and general observations from other TSF failures in the recent past, and to use this range of parameters and scenarios to bracket the types of impacts that might be expected. Our modeling provides a more complete analysis of the direct, indirect and cumulative impacts of a TSF failure at the proposed mine than what is currently included in the DEIS. USACE could incorporate our results directly into the DEIS and develop a more robust consequence analysis that acknowledges these impacts, or they could develop their own model to simulate a TSF failure. In either case, based on the outcomes of our study, the current DEIS clearly requires more analysis that acknowledges the potential impacts of a tailings dam failure.

2 Model Setup

We built our TSF failure and transport model using the FLO-2D software package, a two-dimensional hydrologic and hydraulic model that can be used to simulate sediment transport, urban hydrology, and mudflows from dam failures. We selected this code due to its ability to simulate non-Newtonian flows, which are created by landslides, mud flows, debris flows, and other sediment laden flows, including spills from tailings ponds. Because the physics of non-Newtonian flows are fundamentally different than those for clearwater flows, most of the other hydrodynamic codes available are not well-suited to these types of simulations (e.g., Orman et al., 2017). FLO-2D has also recently been used by mining companies and their consultants to simulate tailings dam failures in other settings (e.g., Knight Piesold, 2014; Tetra Tech, 2015), demonstrating that the code is well-regarded by the mining industry.

We parameterized the model using publicly available information for the Pebble deposit area, information contained in PLP’s mine permit application, and subsequent information released as part of the ongoing mine permitting process. Figure 3 provides a map of the proposed mining infrastructure outlined in the current PLP permit application. This report largely focuses on modeling the potential impacts of dam failure from the bulk TSF North. The sections below summarize the model inputs, parameters, and scenarios we developed to explore the range of potential impacts from a tailings dam failure.

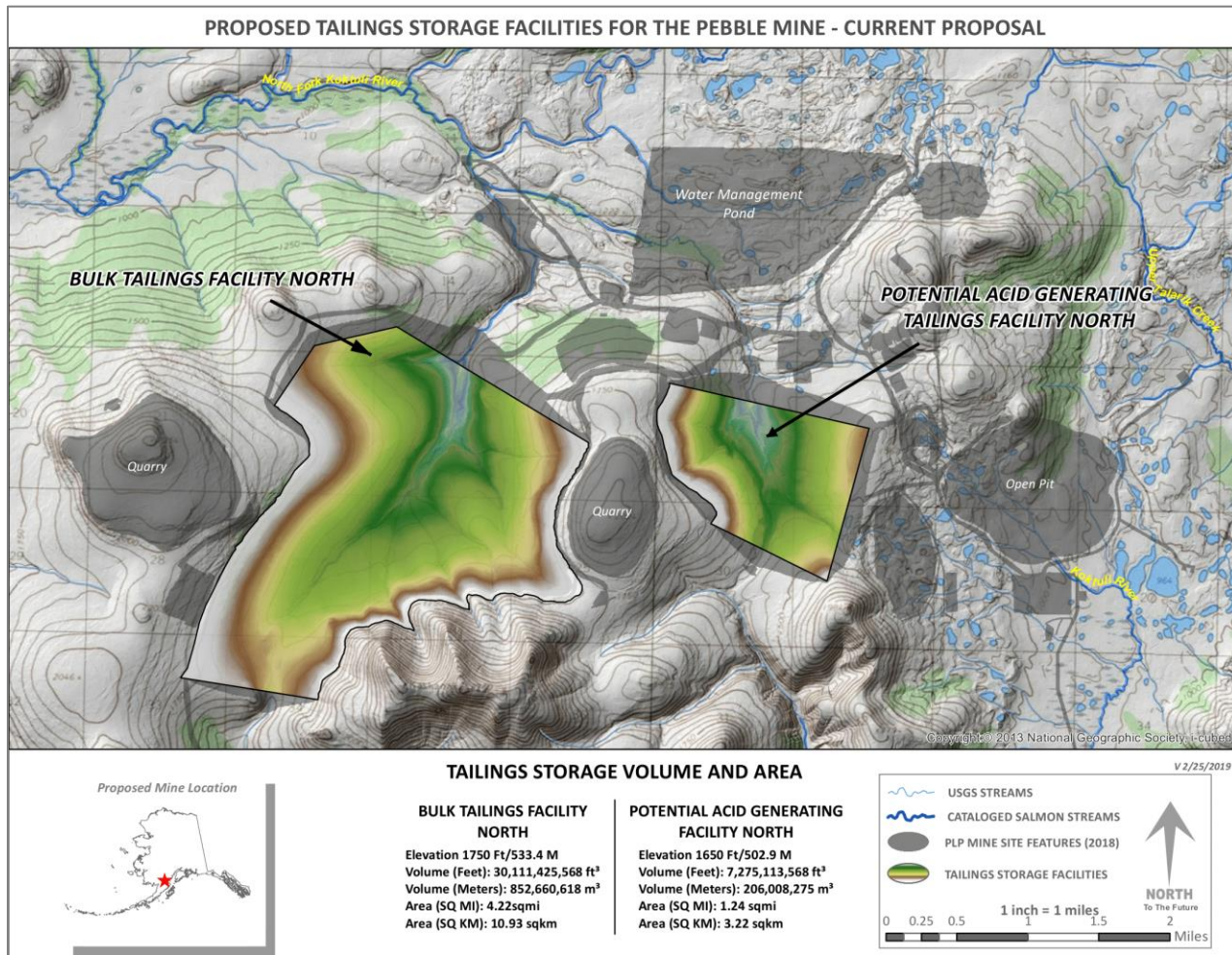


Figure 3. Map of the currently proposed PLP tailings storage facilities and mining features

2.1 Tailings Dam Failure

This section summarizes the parameters used for the tailings dam failure modeling. It includes both physical properties of the tailings releases (e.g., size of the impoundment, volume released) and the properties of the release itself (e.g., the release flow rate through time as the tailings are released).

2.1.1 TSF Physical Properties

The mine site layout for the preferred alternative is shown as Figure 2-4 in the DEIS. To calculate the dam height and storage capacity of the proposed tailings storage facilities, The Nature Conservancy developed a digitized polygon shapefile of the bulk TSF and the pyritic TSF. Using the contour lines as control, the horizontal geometry of each TSF was generated in ArcGIS. Next, the volume computations were produced in QT modeler using dam elevations derived from the elevation contours in the PDF map in RFI062. Calculations were derived using the EAGLE_Lattice_v011 DEM provided by PLP. This is a 12-foot resolution (horizontal) DEM covering the mine site footprint and projected to AK State Plane. Before deciding to use it for the TSF volume computations, the Pebble DEM was compared with other publicly-available DEM's available at the time and was found to be the most appropriate for the volume calculations in terms of coverage and resolution. The contours we generated with the Pebble DEM appear to have the same detail and artifacts as those presented in PLP's maps, likely indicating that PLP was using the same Eagle_Lattice DEM for their own TSF computations. Shortly after starting this modeling project, a 5-meter IfSAR DEM data became available for the study area. The IfSAR DEM has a much larger coverage area which provided a more expansive and detailed (finer spatial resolution) surface for input to the project FLO-2D model domain.

Table 1 summarizes the calculated physical specifications of the mining storage facilities based on the information available from PLP at the time of this study. Note that this modeling study only explores the TSF failure results from the Bulk Tailings North facility; however, it is important to note the other facilities proposed in the current permit, as well as in a full buildout scenario. A failure at any of these facilities carries its own set of downstream consequences and should be fully explored.

Table 1. Summary of the calculated specifications for the PLP mining storage facilities

Facility	Buildout Scenario	Dam Height (meters)	Elevation (meters)	Surface Area (km ²)	Volume Capacity top of dam (m ³)	Freeboard (meters)	Adj Volume Capacity (m ³) ¹
Bulk Tailings North*	Current Permit	164.6	533.4	10.93	8.53E+08	3	8.20E+08
Bulk Tailings South	Full Buildout	279.5	571.5	13.62	1.77E+09	3	1.73E+09
PAG Tailings North	Current Permit	109.4	502.9	3.22	2.06E+08	3	1.96E+08
PAG Tailings South	Full Buildout	190.2	502.9	5.98	4.04E+08	3	3.86E+08

*All modeling scenarios developed in this study were generated for the **Bulk Tailings North TSF**

¹Adjusted volume capacity = top of dam volume capacity – estimated freeboard volume

2.1.2 TSF Release Volume

Based on an extensive literature review of tailings dam breach calculations, we developed a range of feasible breach variables to bound the uncertainty of the impacts from a tailings dam failure. Rather than relying on a single deterministic breach, we examined a range of breach scenarios by varying characteristics such as total volume released, breach duration, hydrograph shape, and sediment concentration.

To generate a range of possible breach scenarios, we used the database of tailings dam failures outlined in Concha Larrauri & Lall, (2018), which expands on the database originally published by Rico et al. (2008). This database outlines the estimated tailings volumes released from 28 historical TSF breach events, including the Mt. Polley and Samarco spills. This database provided the framework for determining a feasible range of breach release volumes (Figure 4).

To calculate an initial estimate of TSF breach release volume, we used the empirically derived equation from Rico et al. (2008) that examined the relationship between the total tailings impoundment volume and the total released tailings volume:

$$V_f = 0.354V_t^{1.008} \quad (\text{Eqn. 1})$$

Here V_f is the total breach release volume; and V_t is the impoundment capacity. Depending on the size of the impoundment, this equation implies that the expected tailings release volume from a TSF failure is approximately 35-45% of the total tailings impoundment volume.

For the proposed bulk TSF at Pebble, this equation results in an expected breach volume of 41.7% of the impoundment capacity. This 41.7% breach volume is used as our baseline release volume throughout many of our model simulations in the sections that follow. Figure 4 below shows this estimated breach volume equation based on historical breach events, plotted on a logarithmic scale. The estimated breach event for the bulk TSF is plotted in the upper right corner of this figure, and represents a tailings release that would be approximately 10 times larger than either Samarco or Mt. Polley. Also shown in Figure 2 are the minimum and maximum breach volumes analyzed in this study as part of our scenario analysis. Note that the “pipeline rupture” scenario chosen as the TSF failure scenario in the DEIS is approximately 10,000 times smaller than what would be indicated by the Rico et al. (2008) empirical data.

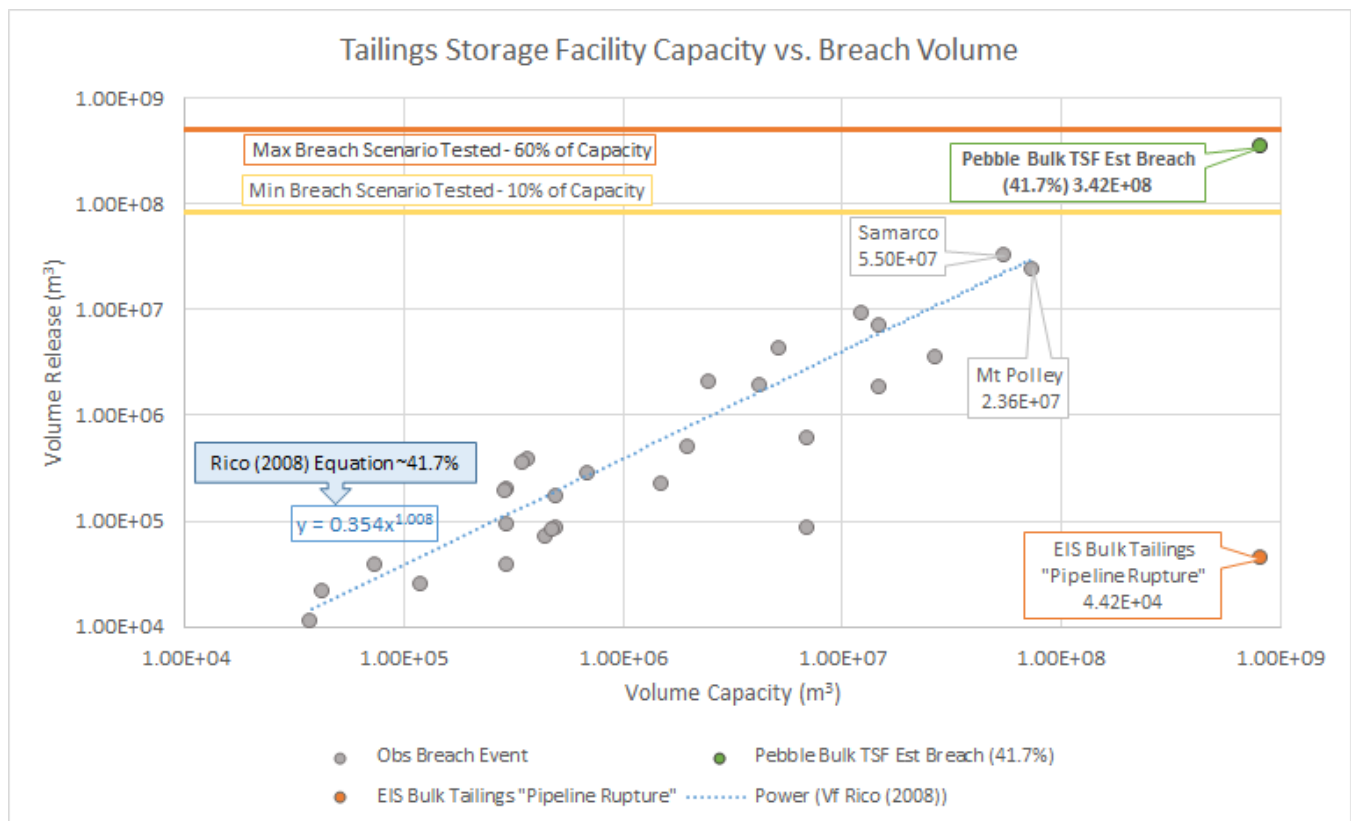


Figure 4. Comparison of tailings pond capacity and calculated/observed release volume for historical breach events (historical breach data obtained from Concha Larrauri & Lall, 2018)

A secondary empirical analysis of dam failure flood run-out distance is provided in Figure 5 below. This analysis can be used to approximate the distance downstream that tailings discharge would be expected to travel. Using the dam height and breach volume (referred to as “dam factor”), Concha Larrauri & Lall, (2018) derived the empirical equation shown in Figure 5 for historical dam failures. Using this equation, the estimated run-out distance calculated for the bulk TSF facility is approximately 680km. Bristol Bay is approximately 340km

downstream from the BTN, so this estimate indicates that tailings released from a full bulk TSF dam failure would be expected to reach Bristol Bay (for reference: the bulk TSF is 336 km from Bristol Bay).

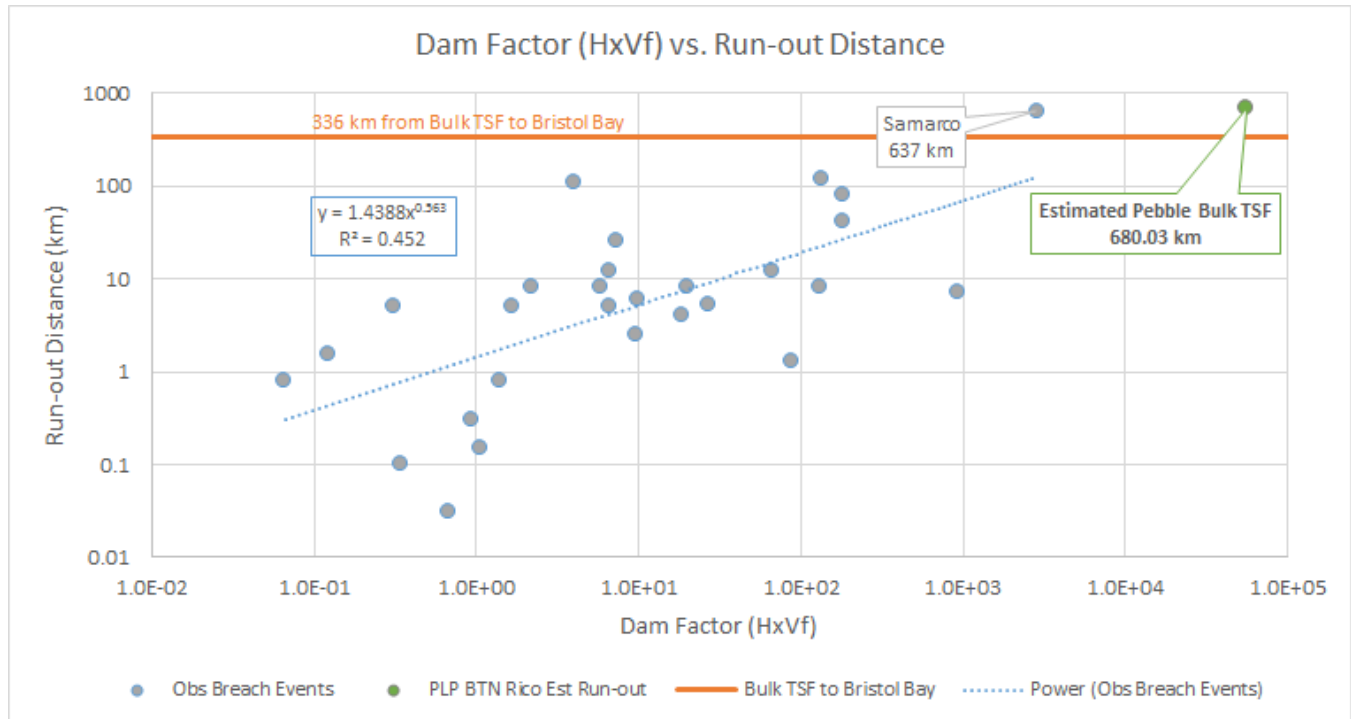


Figure 5. Comparison of dam factor and observed breach run-out distance for historical breach events (historical breach data obtained from Concha Larrauri & Lall, 2018) and the estimated Pebble bulk TSF run-out distance. Orange horizontal line shows distance to Bristol Bay for reference

2.1.3 Developing Breach Hydrographs

To generate the TSF failure inflow input files compatible with FLO-2D, we used the “Tailings Dam Failure Volume Estimate Tool” (TDFVET) developed by O’Brien et al. (2015) to generate scalable unit hydrograph and sediment concentration time series data. We then scaled each unit hydrograph with a prescribed total breach volume, to generate the full suite of failure scenarios for our analysis. Starting with the total breach volumes as summarized in Section 3.1.2, we examined a range of feasible peak outflow rates and breach duration times. As a starting point, we used the Rico et al. (2008) relationship between peak discharge and dam factor to calculate a set of peak discharge values to define the inflow hydrograph:

$$Q_{max} = 10.5 H^{1.87} \quad (\text{Eqn. 2})$$

where Q_{max} is the peak discharge and H is the dam factor (“dam height” x “release volume”). Equation 2 results in an estimated peak discharge of 32,100 m³/s for a bulk TSF failure that releases 41.7% of the total volume, as calculated in Section 3.1.2. Based on a combination of this peak discharge rate and the total release volume, the TDFVET unit hydrograph requires an 11-hour breach duration to match both the peak flow and the total flow. To further explore the sensitivity of the breach duration to the downstream impacts, we also developed alternative scenarios using a range of prescribed event durations (i.e. 6-hr, 11-hr, 24-hr, 48-hr, 96-hr).

We also developed a range of sediment concentration timeseries corresponding to the breach volume hydrograph. We explored the maximum and average sediment concentrations for TSF breach mudflows based on a literature review of historical events and field experiments (Julien & Leon S., 2000; Major & Pierson, 1992; J. S. O’Brien et al., 1993; Jim S. O’Brien & Julien, 1988). The FLO-2D reference manual also states that “For a mudflow event, the average sediment concentration generally ranges between 20% and 35% by volume with

peak concentrations approaching 50%” and “For concentrations less than 20% by volume, the flow will behave like a water flood”.

Figure 6 outlines three different sediment concentration scenarios that were developed for the sensitivity analysis. The sediment concentration model input is defined as the ratio of the total discharge made up of tailings material with water comprising the remaining portion. Figure 7 illustrates a sample of the bulked (sediment + water) hydrograph scenarios (variable breach durations) that were developed from the processes outlined above.

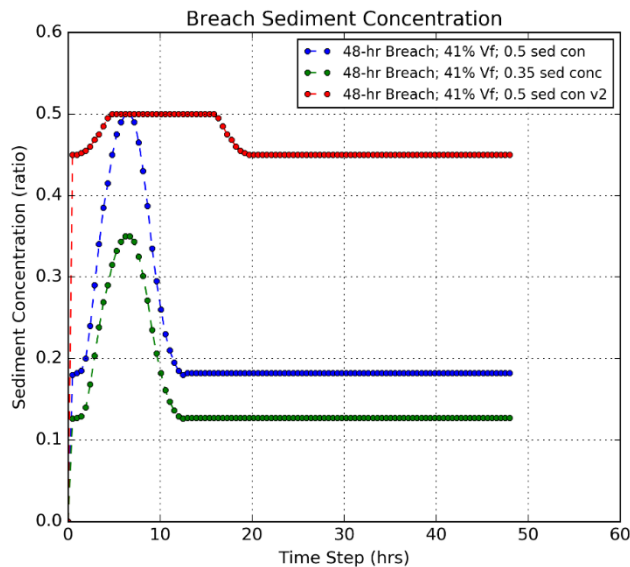


Figure 6. Range of sediment concentration time series scenarios developed for input to the FLO-2D model

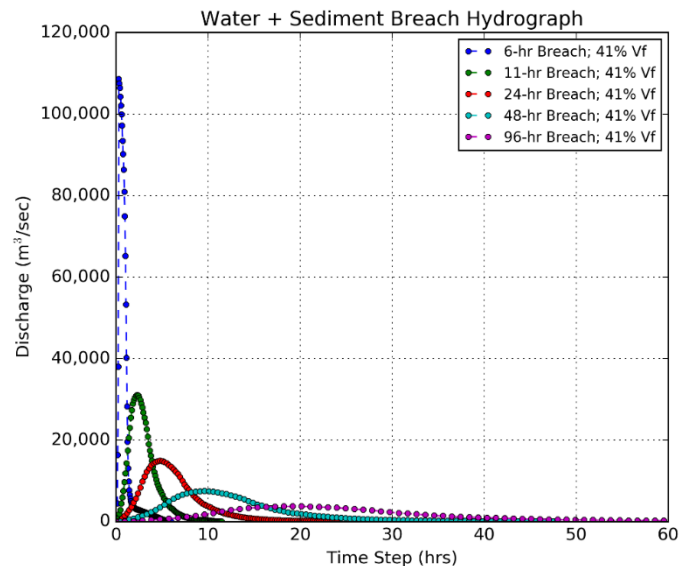


Figure 7. Range of TSF failure bulked hydrograph time series scenarios (variable breach durations) developed for input to the FLO-2D model

2.1.4 Dam Breach Scenarios

Using the information outlined above, we developed a series of breach failure hydrographs to be input to the FLO-2D model as the breach discharge. These scenarios were developed to examine both a reasonable range of potential dam failure scenarios and to examine the FLO-2D model output sensitivity to variable flow characteristics. Table 2 summarizes the different breach discharge hydrographs we developed, each of which will be summarized in the following sections.

Table 2. Summary of all breach discharge scenarios developed for input to FLO-2D

Scenario	Breach Volume (million m ³)	Breach Volume as percent of Dam Capacity (%)	Peak Flow of Bulk Discharge (m ³ /s)	Breach Duration (hours)	Max Sediment Conc (%)	Total Sediment Conc (%)	Discharge Water Vol (million m ³)	Discharge Sed Vol (million m ³)
Variable Breach Durations								
6-hr Breach ¹	342	41.7	108,540	6	50	37	213.8	128.2
11-hr Breach*	342	41.7	31,027	11	50	28	246.2	95.7
24-hr Breach*	342	41.7	14,867	24	50	28	246.2	95.7
48-hr Breach	342	41.7	7,434	48	50	28	246.2	95.7
96-hr Breach	342	41.7	3,717	96	50	28	246.2	95.7
Variable Max Sediment Concentration								
35% max sediment concentration	342	41.7	7,434	48	35	20	275.0	67.0
50% max sediment concentration	342	41.7	7,434	48	50	28	246.2	95.7
Variable Breach Volumes								
10% of Rico	82	10	3,560	24	50	28	59.0	23.0
60% of Rico	491	60	21,385	24	50	28	354.2	137.7
Variable Sediment Concentration Composition								
standard sediment concentration	342	41.7	7,434	48	50	28	246.2	95.7
increased sediment concentration	342	41.7	7,434	48	50	49	174.4	167.5

*Empirical estimates of breach release volume and peak discharge from the bulk TSF dam failure indicate the **11-hr to 24-hr event** scenarios would be the most likely outcome given the currently available data and assumptions.

¹The 6-hr breach scenario was configured with a more dramatic rising limb and peak which results in a different water/sediment composition compared to the event hydrograph used for the 11-hr to 96-hr simulations.

2.2 FLO-2D Model Setup

This section summarizes the setup and configuration of the overland flood model FLO-2D. FLO-2D represents physical properties of the land surface (e.g. surface roughness, topography) to simulate mud and debris flow progression between model grid elements.

2.2.1 Model Domain

FLO-2D uses a grid network over the model study area to perform cell-to-cell flow calculations. We developed the initial model domain boundary by using the full extent of the best available topographic data. The model domain was further refined through an iterative process of reducing the boundary to maximize computation time while also ensuring all flood simulations are contained within the extent of the domain (i.e., ensuring that inundation does not reach the edge of the model boundary). Our initial model domain was built from the headwaters of the North and South Fork Koktuli Rivers to the confluence with the Mulchatna River (red boundary in Figure 8). In each of the TSF failure scenarios developed using this model domain, tailings transport continued beyond the downstream edge of this model boundary. As a result, we developed a larger model domain that extended further downstream to the confluence between the Mulchatna and the Nushagak (yellow boundary in Figure 8), to estimate the fate of tailings transport beyond the Koktuli/Mulchatna confluence. As summarized below, limitations to the available topographic data required that we use different base topographic data for these two model domains.

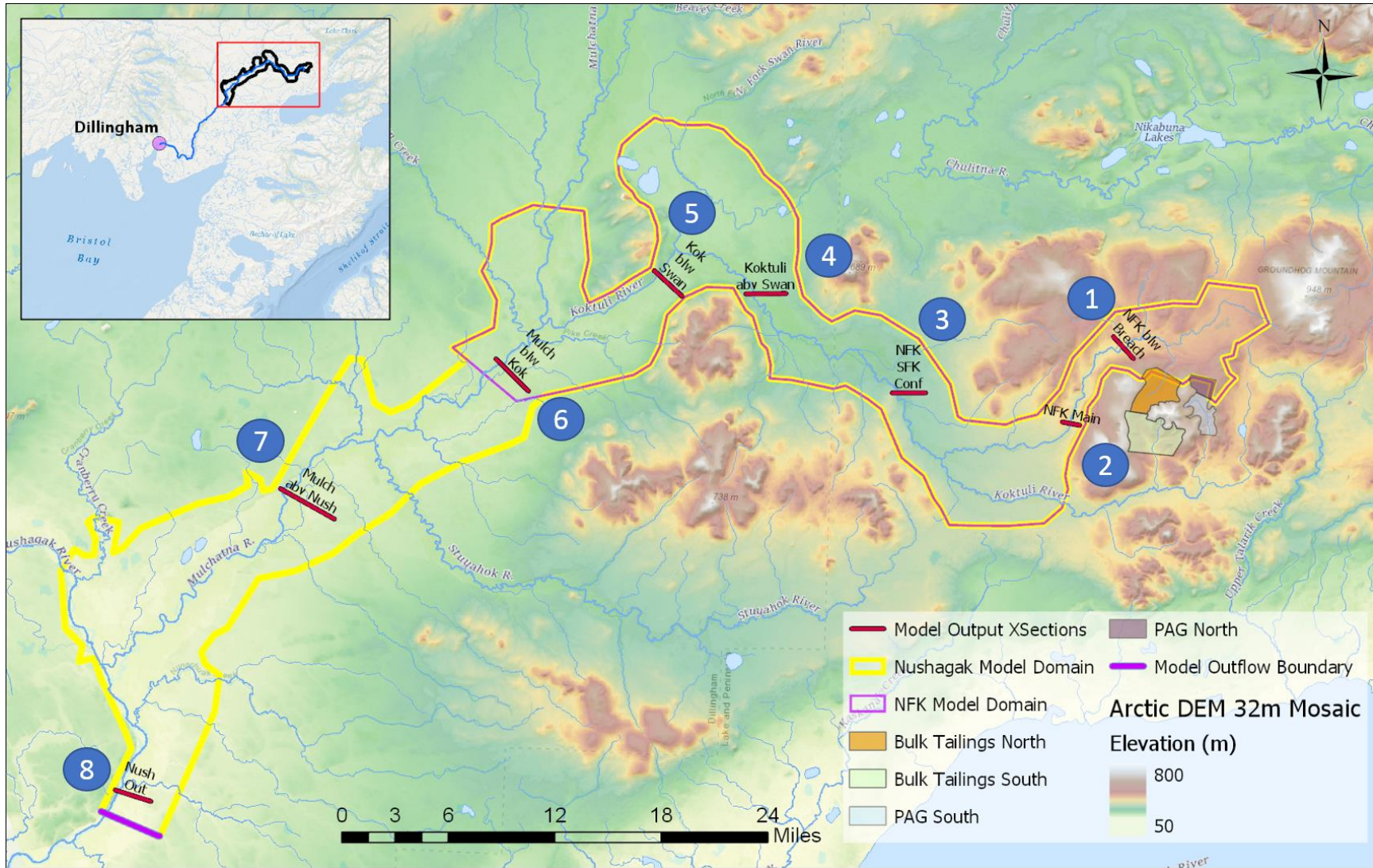


Figure 8. Model domain for the Kaktuli River watershed model (red) and the Nushagak River watershed model (yellow) model cross-sections numbered upstream to downstream (blue circles)

2.2.2 Topography and Hydrography

FLO-2D uses a gridded computation solver to distribute flows over the model land surface, which means the quality of the underlying terrain dataset influences the accuracy of the modeled outputs. For the smaller “NFK Model Domain”, we used a 5-meter resolution digital elevation model (DEM) generated from interferometric synthetic aperture radar (IfSAR) as the underlying topography for the FLO-2D model. The processing steps undertaken for this DEM were as follows. First, because we required a relatively coarse FLO-2D grid in order to simulate failures over our full model domain, we down-sampled this DEM to a 30-meter resolution, using nearest neighbor resampling. To define channels that were consistent with the model topography, we then filled pits in this 30-meter DEM and generated flow direction and flow accumulation arrays from the filled DEM. We then selected a flow accumulation area threshold of 1 km² and assigned all flow accumulation values larger than this to be defined as “channels”. The IfSAR DEM is limited in that the data does not represent the bathymetry within river channels; therefore, to ensure that these channels created conduits for flow in the model, we then “burned-in” each of these cells to the model topography by subtracting 0.5 meters from the DEM value for each of those cells. Finally, we re-gridded the DEM within the FLO-2D model domain to a 60-meter resolution using a minimum value re-sampling algorithm to ensure hydrologic connectivity is maintained.

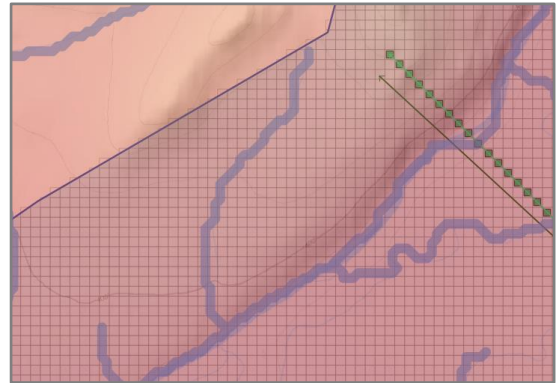


Figure 9. Sample grid view of the model domain with calculated flow accumulation channels

A 2-meter DEM mosaic for Alaska, called [ArcticDEM](#), is also available at the Polar Geospatial Center, a collaboration between the National Geospatial-Intelligence Agency and the National Science Foundation². The modeled DEM is a product of stereo pairs of 2-meter resolution imagery obtained by DigitalGlobe commercial satellites. We obtained the 32-meter mosaiced dataset for the study area. To use this DEM, we filled depressions, calculated flow direction, and flow accumulation from the dataset to ensure hydrologic connectivity. We identified small data gaps in the grid (typically located in areas of open water) and filled these pits using a raster statistics function to average the grid cell values within a 120-meter radius. We then followed the same processing steps used for the 5-meter IfSAR data, as summarized above. The primary disadvantage of the ArcticDEM is the top of canopy imagery return - which means the elevation data represents the height of any vegetation and not a true “bare earth” elevation. This limitation plays a role in the higher resolution details of the modeled flood extent; however, we retained the results from this model to provide a qualitative analysis of impacts from a TSF failure on the broader Nushagak watershed.

2.2.3 Flow Resistance

The hydrography of the Pebble deposit area is characterized by wide, vegetated alluvial valleys with sinuous, gravel and sand-bedded channels winding through the valley bottoms. To simulate this hydrologic condition in the model domain, we assigned a smoother roughness value (Manning’s n) to the “channel” cells than the surrounding cells. A Manning’s n value of 0.04 was selected for the “channel” cells, which matches the value used for Pebble planning studies (Knight Piesold Ltd., 2018b,c). Manning’s n values for the remaining model floodplain were selected based on land use classification for Alaska from the National Land Cover Database (NLCD) 2011 dataset (Homer et al., 2015). Land within the model domain was classified as either dwarf shrub, shrub/scrub, open water or forest, and assigned the appropriate Manning’s n values. Other land cover types within the model domain (barren land, sedge/herbaceous, emergent herbaceous wetlands, and woody wetlands) were ignored due to their small percentage of land cover within the model domain. Since FLO-2D is a 2D model, and the Manning equation assumes steady, uniform flow, Manning’s n values used for overland flow along the floodplain are higher than typical Manning n values. The values used for the model were recommended from the FLO-2D documentation as adapted from U.S. Army Corps of Engineers HEC-1 manuals, as summarized in Table 3 (FLO-

² The Arctic DEM was provided by the Polar Geospatial Center under NSF-OPP awards 1043681, 1559691, and 1542736

2D, 2017 Table 1, chapter 4). The final roughness values assigned to the smaller model domain are shown in Figure 10.

Table 3: Land Use Classification and Manning's n Values

NLCD 2011 Land Class	NLCD ID	NLCD Description ¹	Manning's n Value
Dwarf shrub	51	Shrubs less than 20 centimeters tall	0.15
Shrub/scrub	52	Shrubs less than 5 meters tall	0.25
Open water	11	Open water	0.04
Deciduous forest	41	Trees greater than 5 meters tall with seasonal change	0.30
Evergreen forest	42	Trees greater than 5 meters tall that maintain their leaves all year	0.30
Mixed forest	43	Trees generally greater than 5 meters tall that is a mix of deciduous and evergreen trees	0.30

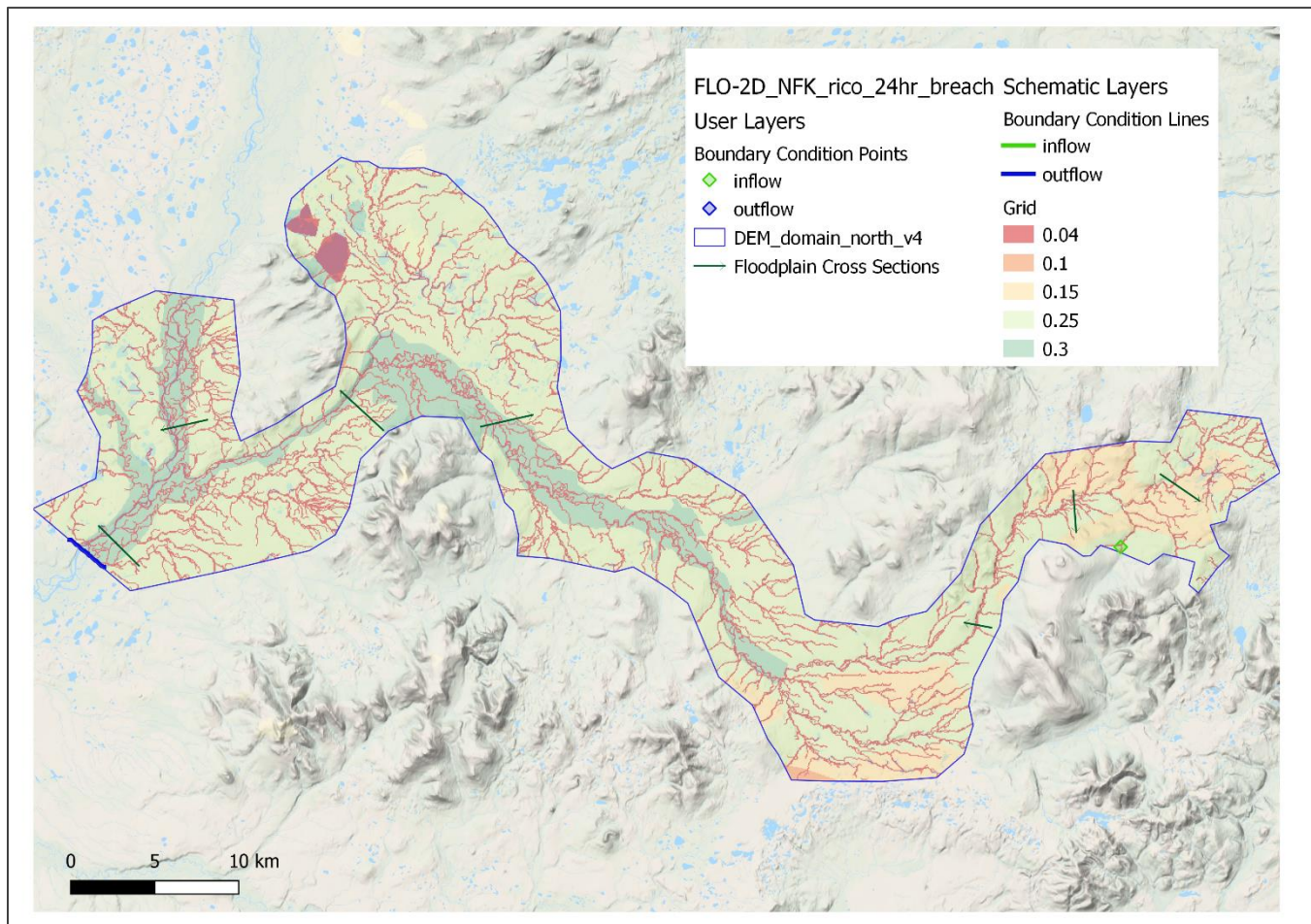


Figure 10. Map of Manning's roughness polygons developed for the North Fork Koktuli to Mulchatna River model domain

In the case of high sediment concentrations (mudflows) the dispersive stress increases due to increased particle interactions, which increases the flow resistance (n_{td}). FLO-2D estimates this increased flow resistance by modifying the turbulent flow resistance n value (n_t) with an exponential function that includes the sediment concentration (C_v) as shown in Equation 3 (FLO-2D, 2017):

$$n_{td} = n_t b e^{mC_v} \quad (\text{Eqn. 3})$$

where n_{td} is the modified flow resistance, n_t is the turbulent flow resistance n value, b is a coefficient (0.0538), m is an exponent (6.0896), and C_v is the sediment concentration. Thus, the modified flow resistance parameter (n_{td}) reflects turbulent and dispersive stresses arising from high sediment concentrations. This modified n value replaces the typical n value in the calculation of the turbulent-dispersive slope (S_{td}) approximated from the Manning's Equation as shown in Equation 4 (FLO-2D, 2017):

$$S_{td} = \frac{n_{td}^2 V^2}{h^{4/3}} \quad (\text{Eqn. 4})$$

where V is the velocity, and h is the hydraulic radius. The turbulent-dispersive slope is one part of a three-part formula for the calculation of shear stress by the FLO-2D model. The total friction slope (S_f) is the sum of the yield slope (S_y), the viscous slope (S_v) and the turbulent-dispersive slope (S_{td}) as shown in Equation 5 (FLO-2D, 2017).

$$S_f = S_y + S_v + S_{td} \quad (\text{Eqn. 5})$$

In its expanded form, the total frictional slope has the following components (see Equation 6) (FLO-2D, 2017):

$$S_f = \frac{\tau_y}{\gamma_m h} + \frac{K \eta V}{8 \gamma_m h^2} + \frac{n_{td}^2 V^2}{h^{4/3}} \quad (\text{Eqn. 6})$$

where τ_y is the yield stress (see Section 2.2.5), γ_m is the specific weight of the fluid matrix, K is the laminar flow resistance (see Section 2.2.5), and η is the viscosity (see Section 2.2.5).

2.2.4 Mine infrastructure

PLP's permit application specifies a 1.1 billion ton bulk tailings storage facility in the upper reaches of the North Fork Kottuli, with a 155 million ton pyritic tailings storage cell immediately to the east. However, the scenario for which PLP has submitted its permits represents only a small fraction of the total mineable resource at Pebble. Thus, it is likely that the full mine buildout will include substantially larger tailings impoundments than what is contained in the initial permit application. Over the course of the EIS preparation, USACE requested further information from PLP on what a full mine buildout scenario would look like. In this scenario, there are two additional tailings impoundments, with a larger bulk TSF and a larger pyritic TSF than those in the initial proposal.

Because the "Bulk Tailings North" facility does not change between the mine plan in the permit application and the full buildout scenario, we focused our modeling on simulating failures from this bulk TSF (which could occur in either the permit mine or in the full mine buildout). Note that while we do not assign a probability to the potential failure of this tailings dam, the probability of failure for the mine site as a whole must increase in the full buildout scenario where there are four tailings storage facilities rather than two.

2.2.5 Tailings Characteristics

For mudflow simulations in FLO-2D, the tailings are characterized as a non-Newtonian fluid. Fluid motion for these non-Newtonian fluids is controlled both by the fluid stresses that dominate in clear water flows, and by the interactions among fine-grained sediment particles within the fluid. As a result, the equations of motion for these fluids are dependent on the sediment concentration, which is tracked dynamically within the model. The sediment concentration-dependent parameters describing the fluid properties in the model are the yield stress, τ_y , and the Bingham viscosity, K_B or η . Based on laboratory experiments, both of these fluid properties can be expressed as exponential functions of the sediment concentration, with two parameters, α and β , defining the shape of this relationship (Equations 7 and 8):

$$\tau_y = \alpha_2 e^{\beta_2 C_v} \quad (\text{Eqn. 7})$$

$$n = \alpha_1 e^{\beta_1 C_v} \quad (\text{Eqn. 8})$$

FLO-2D includes a table with a set of experimentally-derived values for α and β , based on experiments with a range of different materials. For our modeling, we included runs that used average parameter values from these laboratory experiments, as well as site-specific results from PLP representing Bulk Tails-East, G and Bulk Tails-East 80G + 20Y (Knight Piesold, 2018p; Figure 10) to ensure that our modeling results explored a wide range of parameter space. Table 4 summarizes the parameter values estimated from Figure 11 as well as the modified values used within the sensitivity simulations.

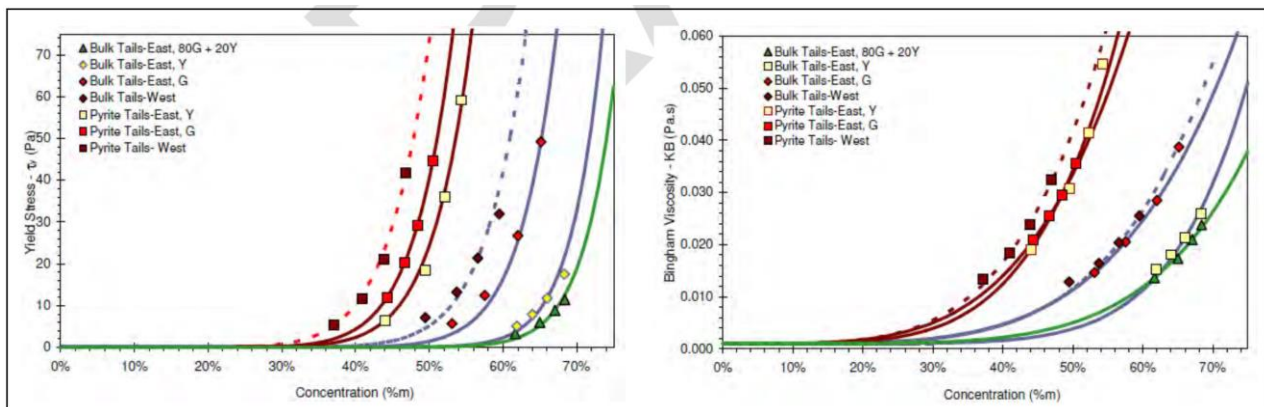


Figure 11. Relationships between yield stress and Bingham viscosity and sediment concentration for Pebble tailings (source: PLP, 2018p)

Table 4: Mudflow Parameters

Parameter	¹ Estimated PLP Values	² Sensitivity Test 1	Sensitivity Test 2
Viscosity vs Sediment Concentration	Coefficient: 0.011 Exponent: 8.5	<u>Coefficient: 0.015</u> <u>Exponent: 6.0</u>	Coefficient: 0.011 Exponent: 8.5
Yield Stress vs Sediment Concentration	Coefficient: 0.4 Exponent: 17	<u>Coefficient: 0.17</u> <u>Exponent: 14.5</u>	Coefficient: 0.4 Exponent: 17
Sediment specific gravity	2.65	2.65	2.65
Laminar flow resistance	2480	2480	<u>4960</u>

¹Represents estimates from PLP site-specific results: Bulk Tails-East, G

²Represents estimates from PLP site-specific results: Bulk Tails-East, 80G + 20Y

2.2.6 FLO-2D Runtime Settings

An analysis of discharge hydrographs and flow accumulation calculations throughout the model domain was used to identify the model runtime needed to reach a steady state (discharge through the model outlet approaches zero as illustrated in Figure 12). The smaller model domain (bulk TSF to Mulchatna) simulations were configured with a 200-hour runtime and the larger model domain (bulk TSF to Nushagak) was configured with a 500 hour runtime. Within each simulation the bulk TSF breach discharge hydrograph is input at the start of the simulation. The only exception to the runtime configuration was the baseflow + breach simulation for the smaller model domain which used a 300-hour runtime to allow baseflow to reach a steady state within the channel network (0-200 hours) prior to introducing the bulk TSF breach discharge. Model outputs from each simulation were evaluated to ensure the model maintained the mass balance and numerical stability throughout. FLO-2D uses an internal variable timestep calculation, and we configured all simulations to generate 0.5-hour tabulated outputs for all post-simulation analysis.

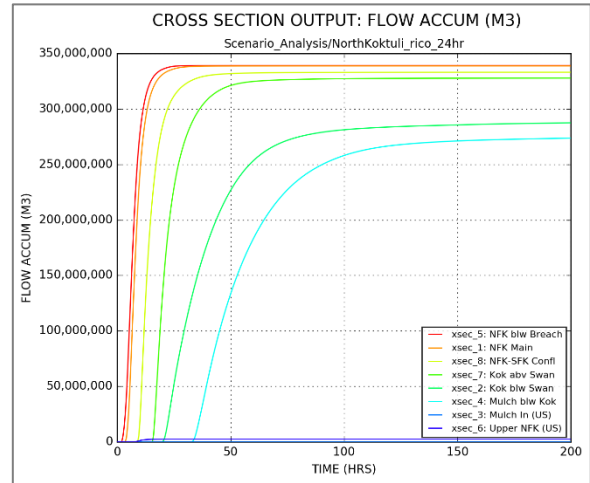


Figure 12. Cross section flow accumulation plot for the 24-hour breach simulation

3 Model Sensitivity Analysis

The FLO-2D modeling was conducted in two stages: model sensitivity testing and dam break scenario analyses. The sensitivity analysis attempts to define the most sensitive model parameters to understand their range of impact on the final model results. The dam break scenario analysis attempts to define or bracket the uncertainty around what a tailings dam breach might look like, considering both the timing and volume of the breach.

The model sensitivity analysis involved changing parameters within the FLO-2D model to evaluate the impacts of those changes on the model output or model results. The parameter sensitivity was evaluated by comparing model outputs with several different metrics including floodplain storage (tailings stored on the floodplain at the end of the model run), total outflow volume (tailings exiting the model domain), and maximum inundated area or areal extent of the tailings breach. We also analyzed the results at two cross-sections in the model, the Kuktuli River above the Swan River (downstream of the confluence of the north and south fork of the Kuktuli River) and the Mulchatna River (downstream of the confluence with the Kuktuli River). These cross-sections are shown as cross-section number 4 and number 6, respectively, in Figure 8. The cross-sections were used to show the tailings discharge hydrograph progression, which provide a summary of the timing and magnitude of the floodwave as it travels downstream.

The model sensitivity tests that were completed are listed in Table 5, along with their relative sensitivity classification determined from the model outputs characterized above. The sensitivity tests are discussed in more detail throughout Section 3, with some tests located within the report appendix.

Table 5: FLO-2D Model Sensitivity Tests

Sensitivity Test	% Difference in Inundated Area	% Difference in Outflow Volume	Sensitivity	Location in Report
DEM	0.7%	6.5%	Moderately sensitive	Section 4.1
Manning's n values	19.7%	12.2%	Highly sensitive	Section 4.2
River baseflow	6.2%	NA ¹	Slightly sensitive	Section 4.3
Sediment concentration distribution (sed composition)	10.4%	170.0%	Highly sensitive	Section 4.4
Mudflow yield stress (Bingham parameters)	2.3%	13.1%	Moderately sensitive	Section 4.5
Maximum sediment concentration	3.0%	12.7%	Moderately sensitive	Appendix
Laminar flow resistance	1.0%	4.6%	Insensitive	Appendix

¹River baseflow simulations are comparing models with differing inflow volume

3.1 Sensitivity to Digital Elevation Model (DEM)

The initial model domain extended from the bulk TSF to just downstream of the confluence of the Kuktuli and Mulchatna rivers (approximately 83 river km total). This model domain was chosen because it was approximately the extent of the available high resolution IfSAR DEM³. However, our initial model runs demonstrated that the majority of the tailings were flowing beyond the limits of this domain. Thus, it became clear that in order to better characterize the risks of a TSF failure, a larger DEM was needed. We extended our initial model to the Nushagak River (to a total of approximately 142 km downstream of the bulk TSF. We used the lower-resolution ArcticDEM (see Section 2.2.2) for this larger FLO-2D model domain.

To evaluate the sensitivity of our results to the DEM, we ran identical TSF failure scenarios over the IfSAR and ArcticDEMs and compared model outcomes. A sensitivity analysis comparing the performance of the two model domains showed that they behaved similarly, but the IfSAR DEM simulation produced more distinguished channel reaches, with slightly less flow stored on the floodplain (Table 6). Although the timing and magnitude of the peak flow was similar between the two models at the Kuktuli River upstream of Swan River, the peak of the flow in the ArcticDEM model is approximately 680 m³/s or 25% less than that of the IfSAR DEM model at the Mulchatna River (see Table 7 and Figure 14). A comparison of the two maximum flow inundation maps shows that the IfSAR DEM more clearly defines the braided channel network, noted by the deeper colors of red along the channel (see Figure 13).

³ The Alaska USGS is in the process of processing IfSAR data to create a 5-meter seamless DEM across the entire state. At the time of this writing, the spatial limits of the high-resolution DEM were just below the Kuktuli-Mulchatna confluence.

Table 6: DEM Sensitivity Analysis – Model Output

Model Run	Bulked Breach Volume (million m ³)	Bulked Floodplain Storage (million m ³)	Bulked Outflow Volume (million m ³)	Storage as a % of Inflow	Outflow as a % of Inflow	Maximum Inundated Area (km ²)
IfSAR DEM	341.9	69.6	272.4	20.4%	79.7%	255.9
ArcticDEM	341.9	86.3	255.7	25.2%	74.8%	257.6

Table 7: DEM Sensitivity Analysis – Hydrograph Output

Model Run	Koktuli River upstream of Swan River			Mulchatna River		
	Maximum Discharge (m ³ /s)	Time to Maximum Discharge (hours)	Total Discharge Volume (million m ³)	Maximum Discharge (m ³ /s)	Time to Maximum Discharge (hours)	Total Discharge Volume (million m ³)
IfSAR DEM	9,788	17.6	328.4	2,723	38.0	274.7
ArcticDEM	10,054.6	17.0	326.2	2,043	40.4	257.6

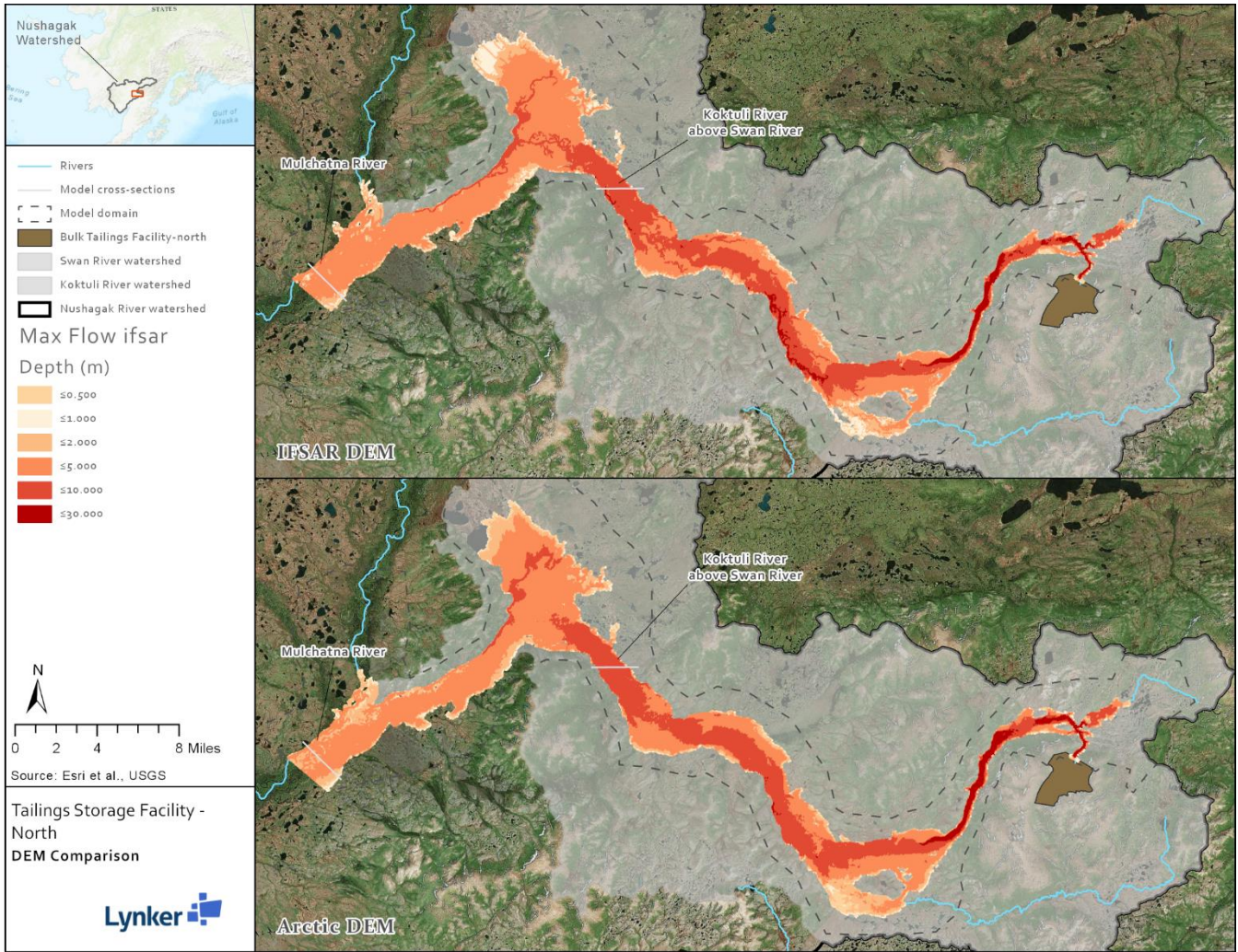


Figure 13: Model Sensitivity to the DEM

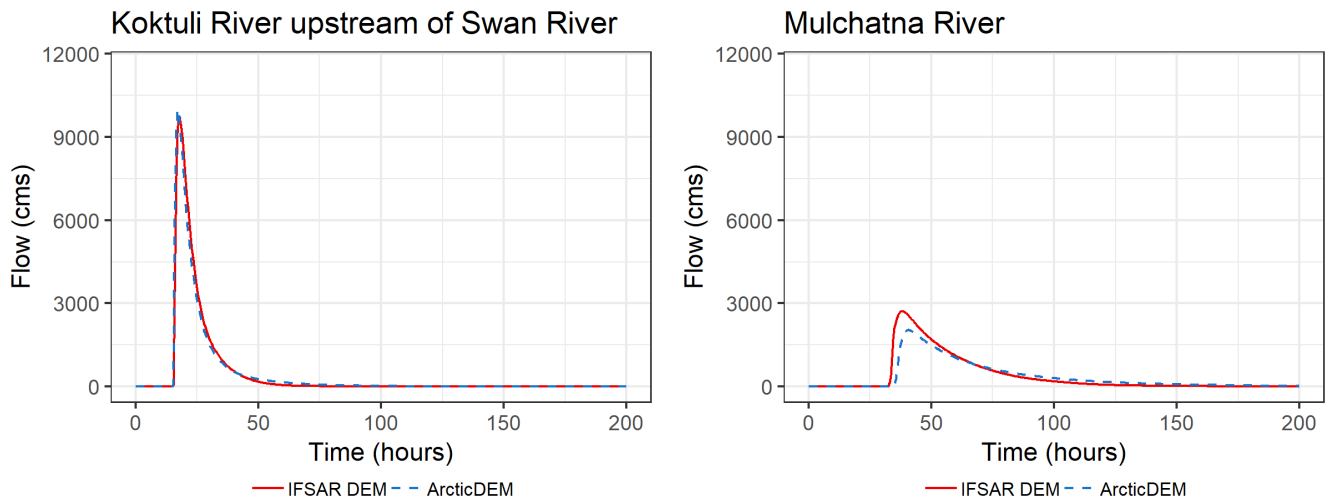


Figure 14: DEM Sensitivity Analysis – Hydrographs

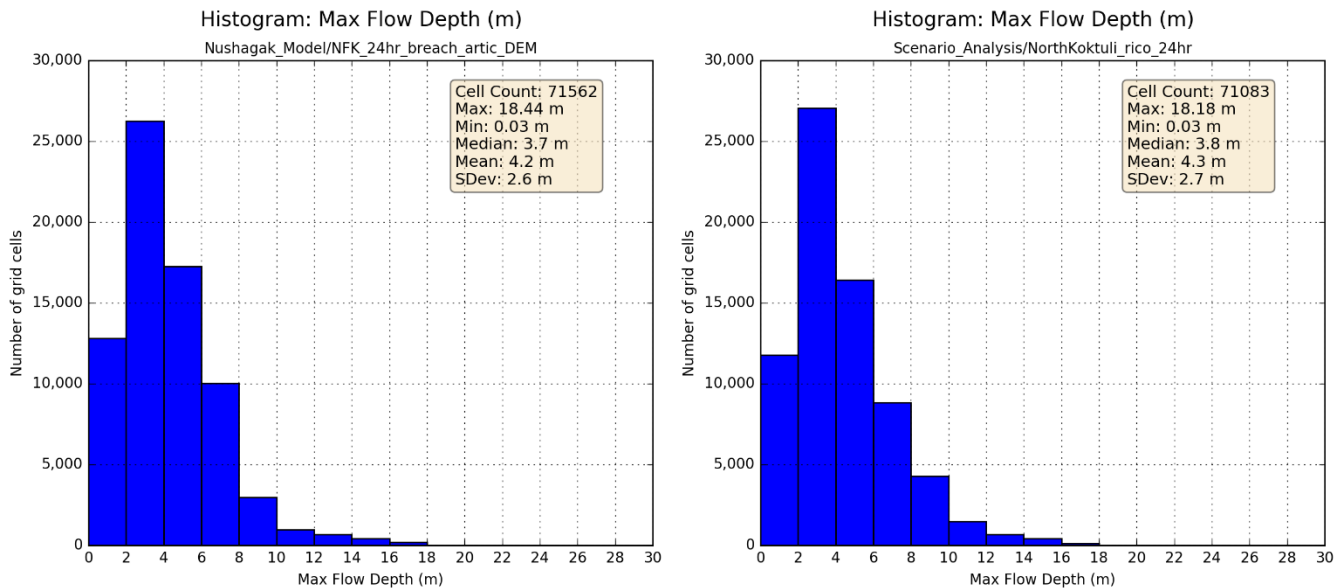


Figure 15. Histogram of maximum flow depth with the ArcticDEM (left) and the IfSAR DEM (right)

3.2 Sensitivity to Manning’s n

Manning’s n is a simplified metric that represents how rough a landscape is: a smoother landscape (lower Manning’s n; an extreme example would be a concrete channel) will convey flow more easily, whereas a rougher landscape (higher Manning’s n; an extreme example would be a mountain stream choked with boulders and logs) will provide more resistance to flow. Typically, Manning’s n is derived by observing the features on the landscape and using lookup tables from hydraulics textbooks to assign values. While we used this approach for the majority of our model runs (see Figure 9), we also explored model sensitivity to the choice of Manning’s n.

Based on the landscape features in the Nushagak-Mulchatna watershed, an appropriate range of Manning’s n values is between approximately 0.04 (low roughness assigned to channel flow) and 0.30 (high roughness assigned to denser floodplain vegetation). We developed two model runs that were identical in all respects except Manning’s n: in the first run, all grid cells were assigned a Manning’s n value of 0.04, and in the second run all grid cells were assigned a Manning’s n value of 0.30. Manning’s n values of 0.04 produced a fast hydrograph with a high peak flow. However, Manning’s n values of 0.30 deposited more sediment storage on the floodplain as less mudflow was transported out of (downstream) the model domain. The changes in Manning’s n values affected the timing and magnitude of the tailings floodwave, as well as the floodplain inundation area. With a Manning’s n value of 0.04, 82% of the outflow left the model (18% stored on the floodplain) leaving an inundated area of 219 km². With a Manning’s n value of 0.30, 72% of the outflow left the model (28% stored on the floodplain), leaving a larger inundated area of 262 km² (see Table 8). The difference in inundated areas and flow depths are shown in Figure 16, while the difference in hydrographs is shown in Table 9 and Figure 17. The maximum flow depth histograms show the Manning’s n of 0.04 produced shallower depths, with an average depth of 3.5 meters. The Manning’s n of 0.30 produced greater depths (maximum of 4.8 meters) and a higher average depth of 4.6 meters (see Figure 18).

Table 8: Manning's n Sensitivity Analysis – Model Output

Model Run	Bulked Breach Volume (million m ³)	Bulked Floodplain Storage (million m ³)	Bulked Outflow Volume (million m ³)	Storage as a % of Inflow	Outflow as a % of Inflow	Maximum Inundated Area (km ²)
Manning's n = 0.04	341.9	62.5	279.4	18.3%	81.7%	219.2
Manning's n = 0.30	341.9	96.5	245.4	28.2%	71.8%	262.2

Table 9: Manning's n Sensitivity Analysis – Hydrograph Output

Model Run	Koktuli River upstream of Swan River			Mulchatna River		
	Maximum Discharge (m ³ /s)	Time to Maximum Discharge (hours)	Total Discharge Volume (million m ³)	Maximum Discharge (m ³ /s)	Time to Maximum Discharge (hours)	Total Discharge Volume (million m ³)
Manning's n = 0.04	20,800	9.2	335.3	6,910	17.0	280.5
Manning's n = 0.30	5,780	25.1	319.5	1,280	63.1	249.5

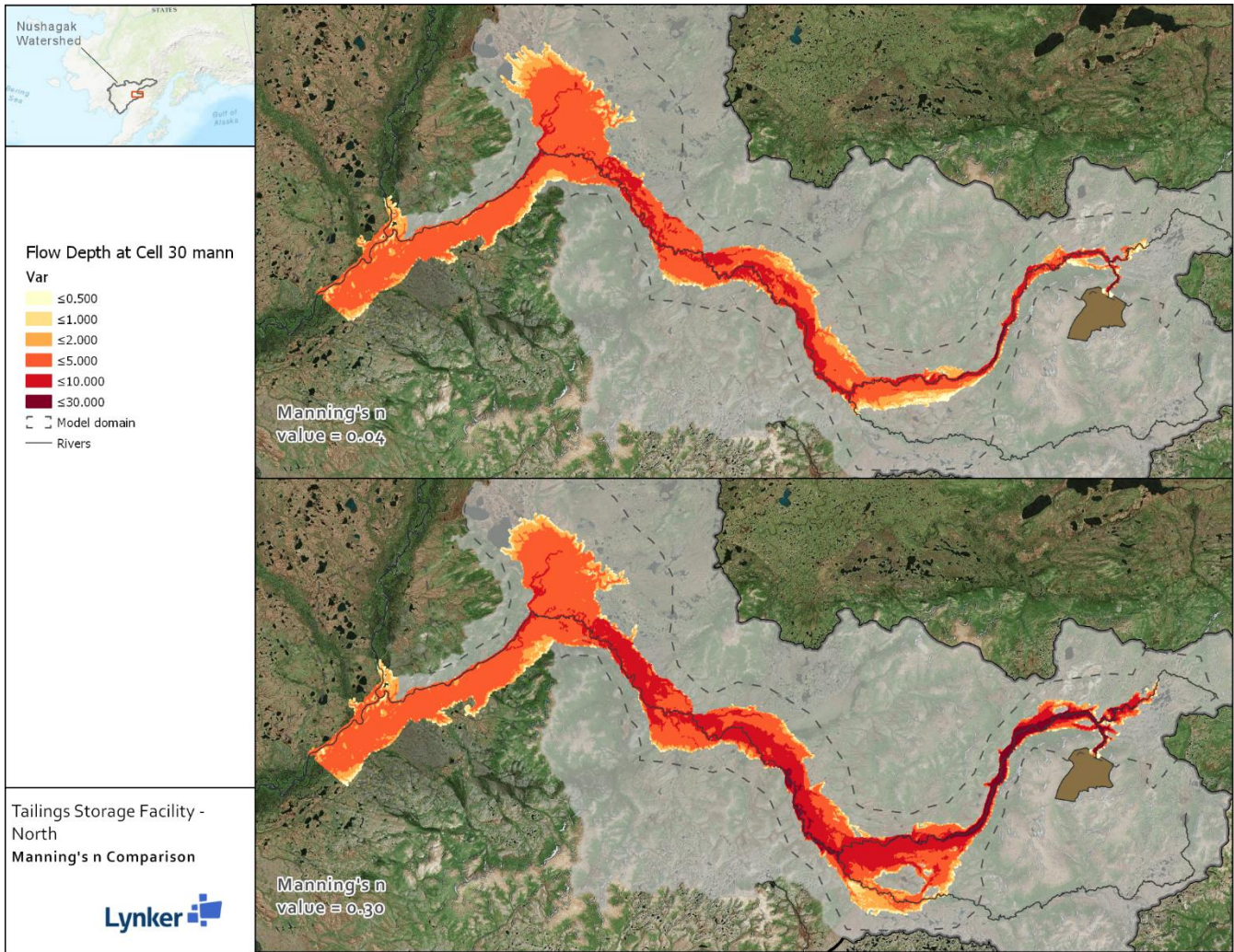


Figure 16: Model Sensitivity to Manning's n Values

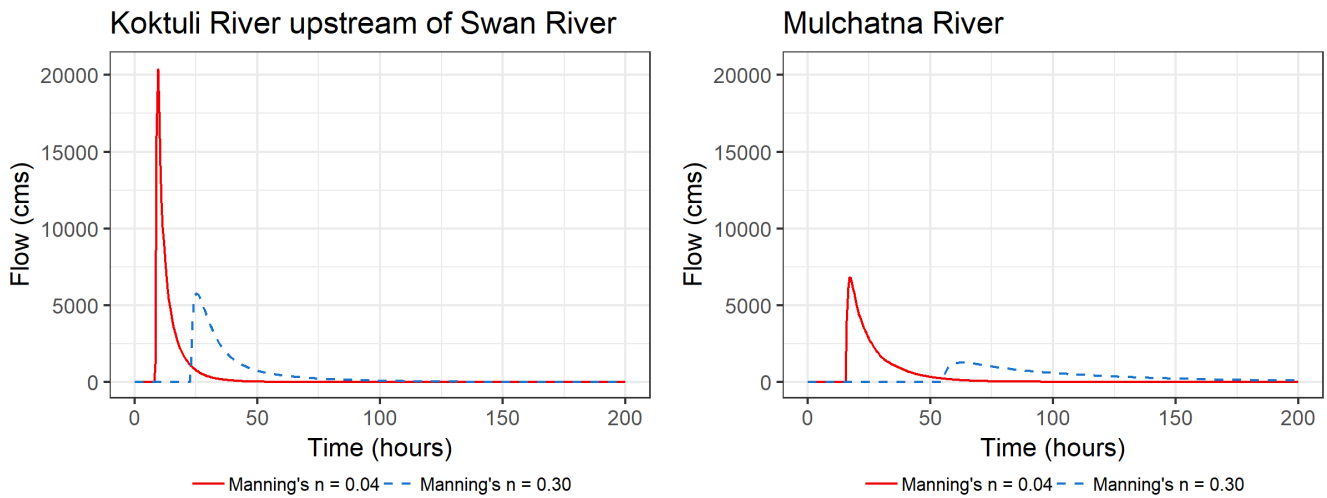


Figure 17: Hydrograph Comparison of Manning's n Values

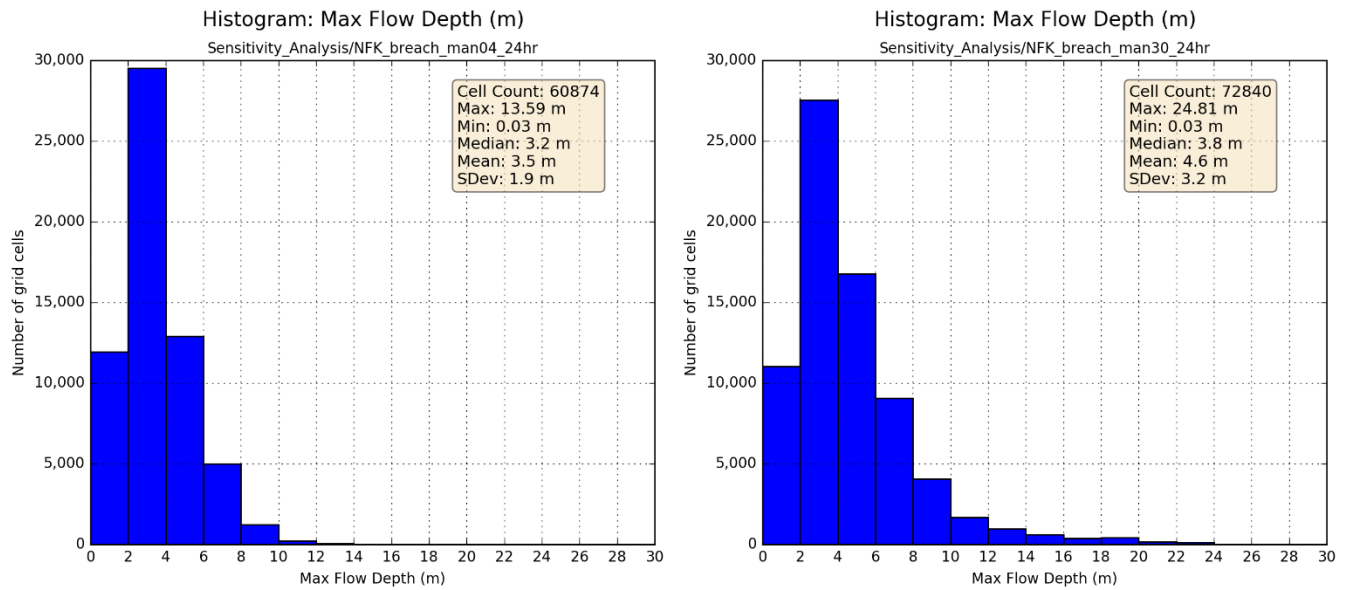


Figure 18. Histograms of the max flow depth cell values for the 0.04 (left) and 0.30 (right) Manning's n value simulations

3.3 Sensitivity to River Baseflow

To ensure a physically realistic model representation, we developed a baseflow hydrology scenario for the major channels throughout the model domain. We calculated average daily streamflow throughout the existing channel network using the USGS gage records for three gages in the model domain. Using the observed streamflow data and drainage area values, we estimated inflow magnitudes for the Swan River as well as the ungaged portion of the Koptuli River. This we accomplished by area-weighting the average flows from the North Fork and South Fork gages. We also modified the average daily inflow value for the Mulchatna River USGS gage to determine the Mulchatna inflow above the confluence with the Koptuli River (the Mulchatna USGS gage is located ~20km downstream of the confluence). We estimated the upstream Mulchatna inflow by subtracting the total estimated flow from the Koptuli system from the gaged flow on the Mulchatna.

Table 10: Drainage area and average streamflow for study area sub-basins

Inflow Name	Data Source	Drainage Area (sq. mi)	Average Streamflow (cms)
North Fork Koptuli Headwater	USGS Gage	106	7.0
South Fork Koptuli Headwater	USGS Gage	69.1	5.3
Koptuli Local Inflow (DS of NFK & SFK Confluence)	Area-weighted flow calculation	279.3	19.65 (distributed among 3 tributary reaches)
Swan River	Area-weighted flow calculation	180	12.7
Mulchatna River (US of Koptuli & Mulchatna Confluence)	USGS Gage (area-weighted adjustment)	2650.6	124.1

The tailings breach model was run with underlying baseflow included in the rivers prior to the breach to analyze how sensitive the model results were to baseflow conditions in the river network. Using the climatological estimates of streamflow from the North Fork Kaktuli, South Fork Kaktuli, mainstem Kaktuli, Swan, and Mulchatna Rivers, we incorporated 7 additional inflow points throughout the model domain to account for the baseline streamflow in the system. A model simulation was configured to run for 200 hours with constant streamflow inputs from the inflow points. After 200 hours the dam breach hydrograph was injected into the model and the simulation continued on for an additional 100 hours (total simulation time of 300 hours). Results from this “breach with baseflow” simulation were evaluated against the simulation without any baseline hydrologic inputs – “breach without baseflow”. To better understand the effects of baseflow in the river on the transport of the tailing breach, a model run of “baseflow only” was also completed. This was a 300-hour simulation of only the 7 inflow points flowing through the model grid. The “baseflow only” scenario was subtracted from the “breach with baseflow” scenario to isolate the effects river baseflow has on the transport of the tailings breach. The “breach without baseflow” and the “breach with subtracted baseflow” show the model sensitivity to including baseflow in the rivers.

The results of the baseflow sensitivity test show that the model is slightly sensitive to having baseflow incorporated into the model run. The breach with baseflow subtracted has 84 million m³ of tailings stored on the floodplain and 258 million m³ of tailings flowing out of the model domain, while the breach without baseflow has 87 million m³ of tailings stored on the floodplain and 255 million m³ of tailings flowing out of the model domain (see Table 11).

Table 11: Baseflow Sensitivity Analysis – Model Output

Model Run	Bulked Breach Volume (million m ³)	Bulked Floodplain Storage (million m ³) ¹	Bulked Outflow Volume (million m ³)	Storage as a % of Inflow	Outflow as a % of Inflow	Maximum Inundated Area (km ²)
Model Sensitivity Runs						
Baseflow only	182.1	27.7	154.4	15.2%	84.8%	53.9
Breach with baseflow	524.0	111.3	412.7	21.2%	78.8%	272.9
Baseflow Sensitivity Comparison						
Breach without baseflow	341.9	87.1	254.8	25.5%	74.5%	255.9
Breach with subtracted baseflow	341.9	83.6	258.3	24.4%	75.6%	---

¹Bulked floodplain storage includes all volume that remains in the model domain (within both the channel and floodplain). Note that the baseflow model includes additional flow volume from the baseflow component compared to the breach only simulation (no baseflow). This introduces differences to the floodplain storage and outflow volume comparisons.

The hydrographs are very similar for the “breach without baseflow” scenario and the “breach with subtracted baseflow” scenario, with total discharge volumes of 328 million m³ and 330 million m³, respectively at the Kaktuli River upstream of Swan River. The total discharge volume is also very similar at the Mulchatna River, with 259 million m³ for the “breach without baseflow” scenario and 260 million m³ for the “breach with subtracted baseflow” scenario (see Table 12).

Table 12: Baseflow Sensitivity Analysis – Hydrograph Output

Model Run	Koktuli River upstream of Swan River			Mulchatna River		
	Maximum Discharge (m ³ /s)	Time to Maximum Discharge (hours)	Total Discharge Volume (million m ³)	Maximum Discharge (m ³ /s)	Time to Maximum Discharge (hours)	Total Discharge Volume (million m ³)
Model Sensitivity Runs						
Baseflow only	26	298.6	21.8	169	210.0	158.9
Breach with baseflow	9,670	217.7	352.3	2,770	238.7	418.7
Baseflow Sensitivity Comparison						
Breach without baseflow	9,790	17.6	327.9	2,720	38.0	258.7
Breach with subtracted baseflow	9,650	17.7	330.5	2,600	38.7	259.9

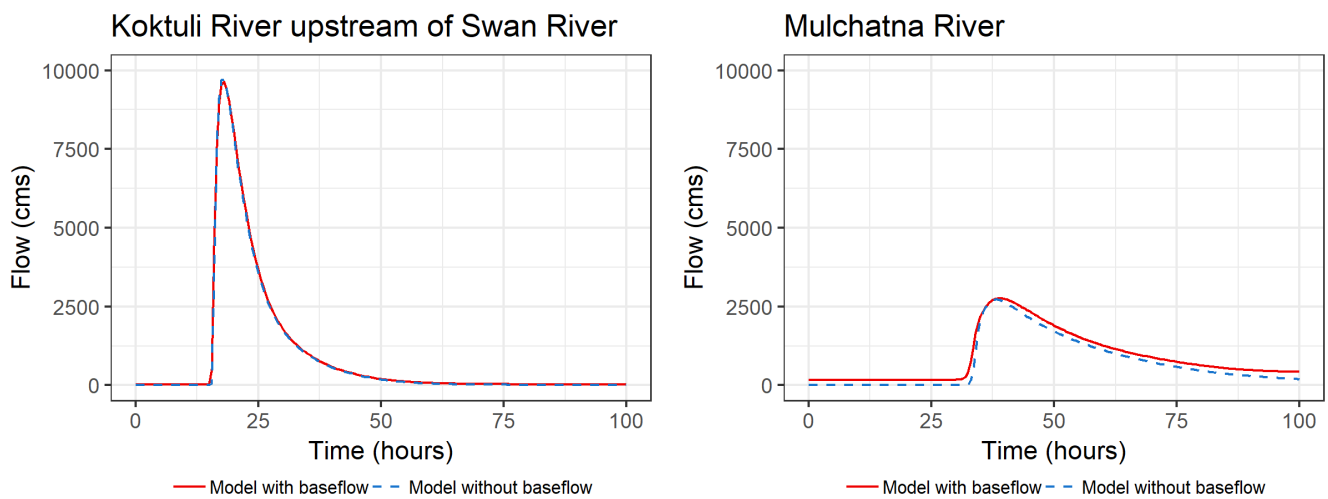


Figure 19: Hydrograph Comparison of Baseflow Hydrology

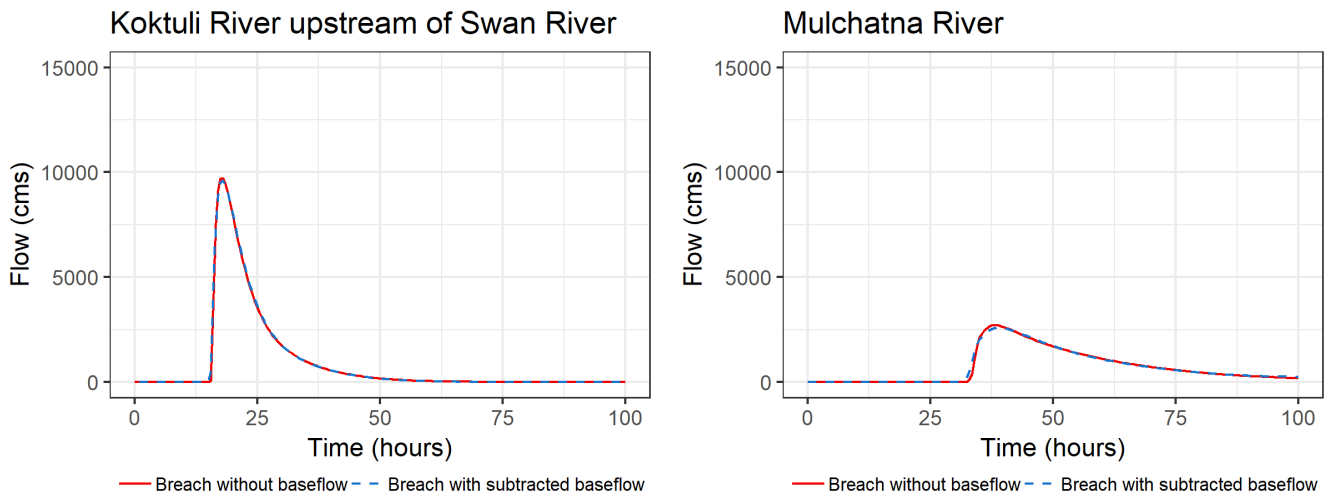


Figure 20: Hydrograph Comparison of Breach without Baseflow vs Breach with Subtracted Baseflow

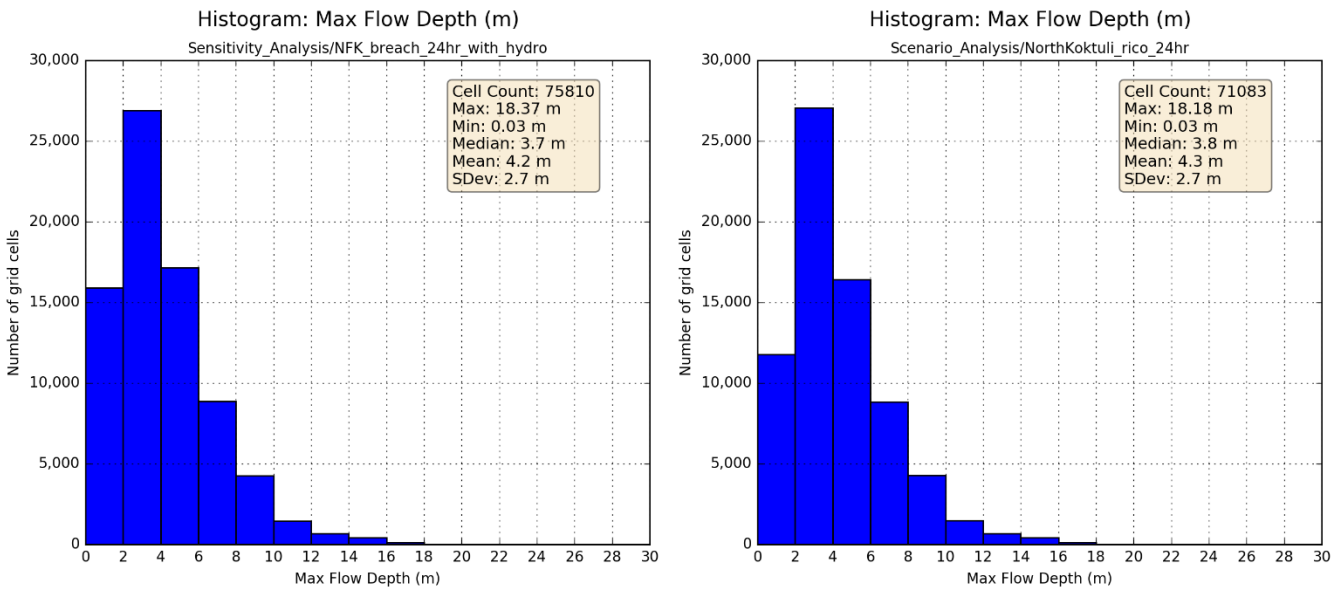


Figure 21. Histograms of the max flow depth cell values for the baseflow (left) and no-baseflow (right) simulations

3.4 Sensitivity to Sediment Concentration Composition

A second sensitivity analysis was developed to examine the impacts of modifying the sediment concentration distribution. By altering the time series distribution of the sediment concentration values, the total sediment portion of bulked discharge is modified. By applying a more sustained sediment concentration hydrograph (Figure 6 – blue vs. red line), the average composition of the bulked discharge was increased to 49% from the standard value of 28%. Both scenarios have a peak sediment concentration value of 50%, and both scenarios represent a total discharge volume of 341 million m³ distributed over a 48-hour breach event.

Results in Table 13 show significantly more breach volume stored in the floodplain for the increased sediment concentration simulation (240.2 million m³) compared to the standard sediment concentration simulation (67.2 million m³). Peak discharge values and time to maximum discharge values in Table 14 indicate the increased

sediment concentration simulation results in a slower moving flow and more prolonged discharge hydrograph (Figure 23). Overall the maximum flow depth inundation map (Figure 22) shows similar a similar footprint of the inundated area apart from the area below the Koptuli and Mulchatna River confluence.

Table 13: Sediment Curve Sensitivity Analysis – Model Output

Model Run	Bulked Breach Volume (million m ³)	Bulked Floodplain Storage (million m ³)	Bulked Outflow Volume (million m ³)	Storage as a % of Inflow	Outflow as a % of Inflow	Maximum Inundated Area (km ²)
Increased sediment concentration distribution	341.9	240.2	101.8	70.2%	29.8%	206.5
Standard sediment concentration distribution	341.9	67.2	274.7	19.7%	80.4%	228.0

Table 14: Sediment Curve Sensitivity Analysis – Hydrograph Output

Model Run	Koptuli River upstream of Swan River			Mulchatna River		
	Maximum Discharge (m ³ /s)	Time to Maximum Discharge (hours)	Total Discharge Volume (million m ³)	Maximum Discharge (m ³ /s)	Time to Maximum Discharge (hours)	Total Discharge Volume (million m ³)
Increased sediment concentration distribution	5267	26.6	299.9	409	91.6	109.2
Standard sediment concentration distribution	7869	23.5	332.3	2658	46.1	276.8

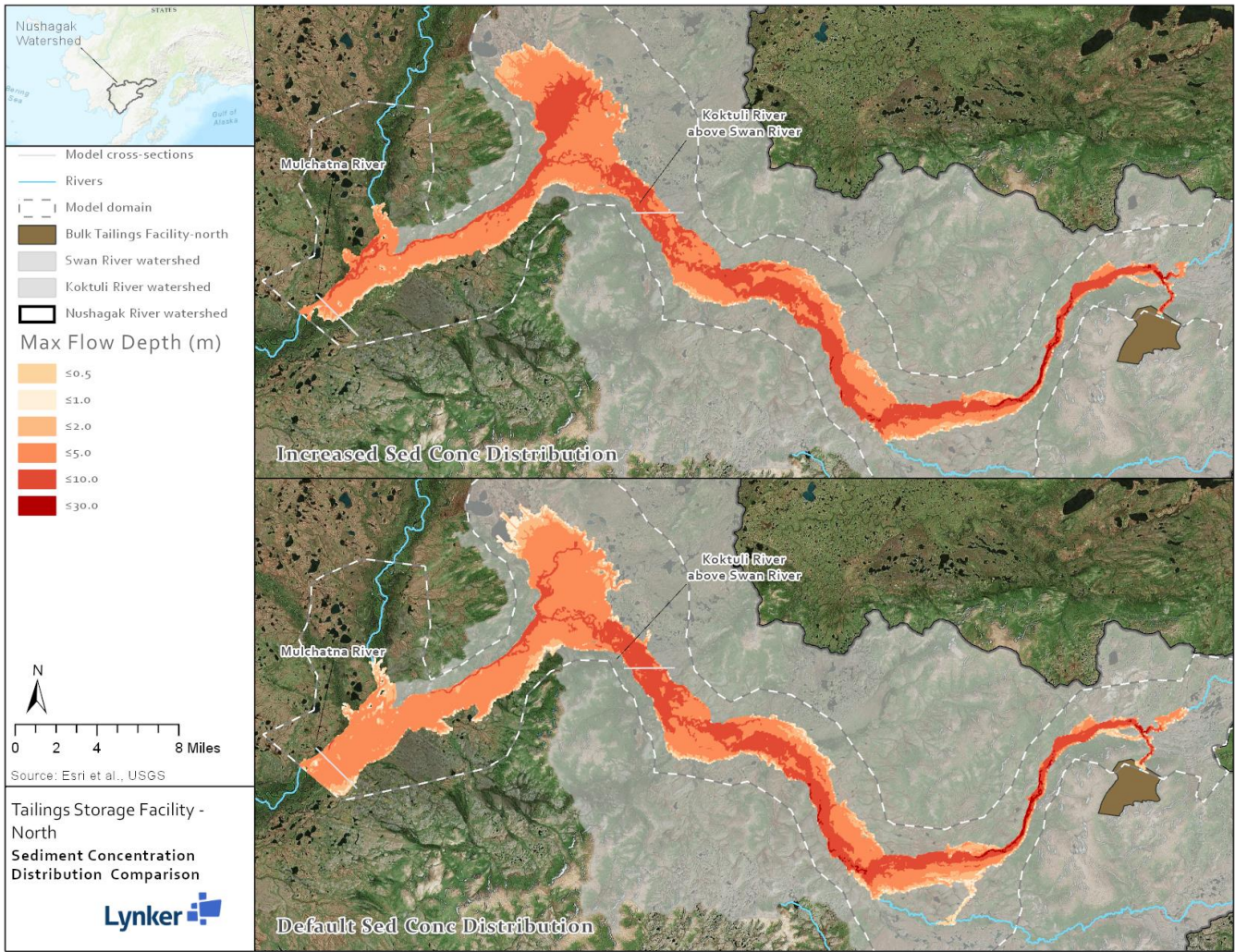


Figure 22: Max flow depth map of model sensitivity to sediment concentration distribution of breach discharge

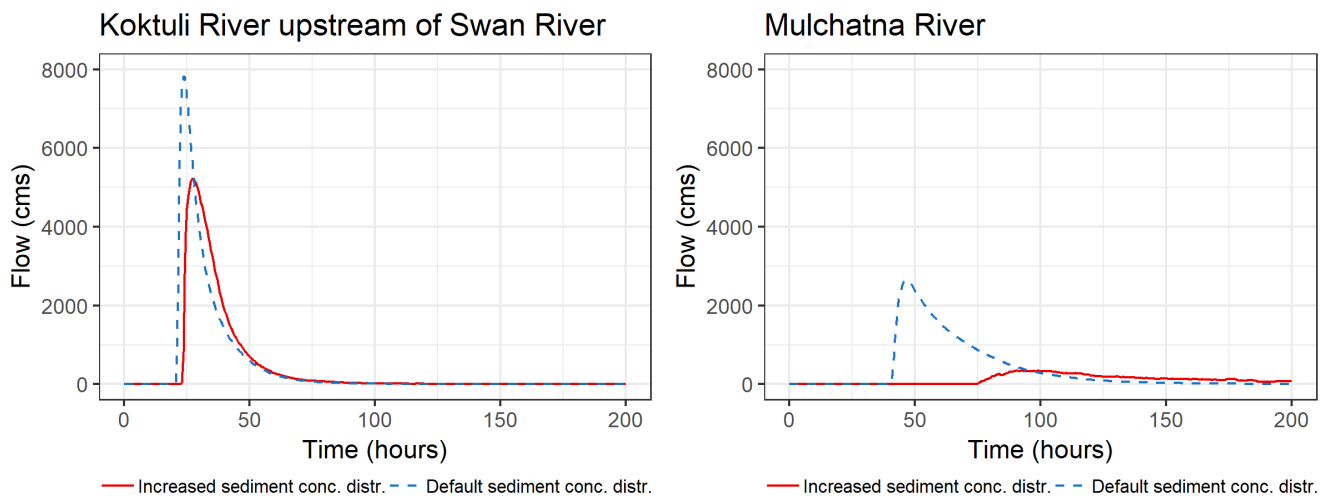


Figure 23: Sediment Concentration Distribution Sensitivity Analysis – Hydrograph

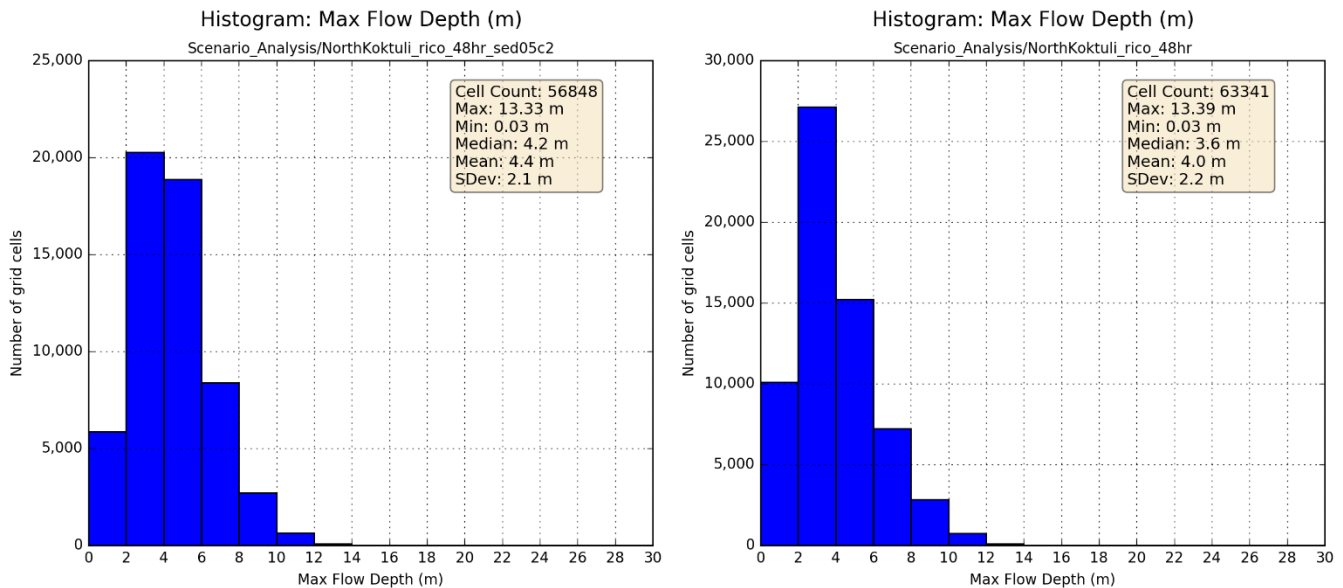


Figure 24. Histograms of the max flow depth cell values for the less viscous (left) and PLP-derived parameters (right) simulations

3.5 Sensitivity to Bingham Parameters

We examined two scenarios with variable mudflow parameters to examine the sensitivity of the model outputs to the yield stress properties of the non-Newtonian flow. Both sets of parameters were estimated using information provided in PLP reports (see section 4.2.4). This section outlines the model results from a “PLP-estimated” parameter simulation alongside a “less viscous” model simulation.

The FLO-2D model results using the less viscous mudflow parameters results in less volume stored within the floodplain while also producing a slightly larger area of inundation when compared to the PLP-estimated yield stress parameters. The inundated areas are similar in both model runs (261 km² for the less viscous simulation and 235 km² for the PLP yield stress simulation). The inundation maps also show that the model results have similar flow depths along the Kuktuli River (Figure 25). The floodplain hydrographs also show very similar results for the discharge hydrographs upstream and downstream of the Swan River confluence (Figure 26). Therefore, the model is largely considered to be insensitive to the range of yield stress parameters evaluated.

Table 15: Yield Stress Sensitivity Analysis – Model Output

Model Run	Bulked Breach Volume (million m ³)	Bulked Floodplain Storage (million m ³)	Bulked Outflow Volume (million m ³)	Storage as a % of Inflow	Outflow as a % of Inflow	Maximum Inundated Area (km ²)
Less viscous	341.9	28.4	313.6	8.3%	91.7%	261.9
PLP parameters	341.9	69.6	272.4	20.4%	79.7%	255.9

Table 16: Yield Stress Sensitivity Analysis – Hydrograph Output

Model Run	Koktuli River upstream of Swan River			Mulchatna River		
	Maximum Discharge (m ³ /s)	Time to Maximum Discharge (hours)	Total Discharge Volume (million m ³)	Maximum Discharge (m ³ /s)	Time to Maximum Discharge (hours)	Total Discharge Volume (million m ³)
Less viscous	9,140	17.4	335.9	2,710	36.9	315.5
PLP parameters	9,800	17.6	328.4	2,720	38.0	274.7

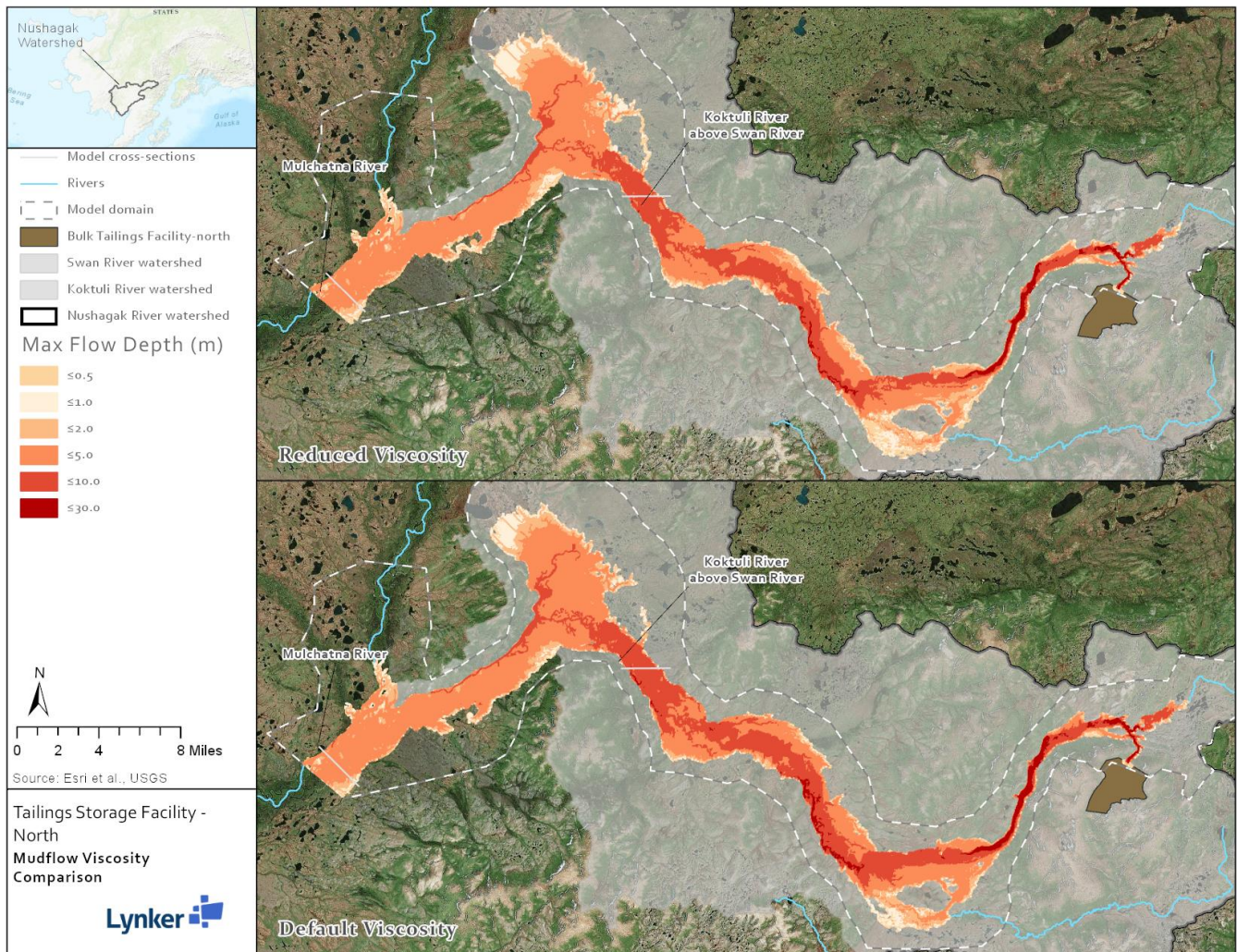


Figure 25: Max flow depth map of model sensitivity of breach discharge viscosity

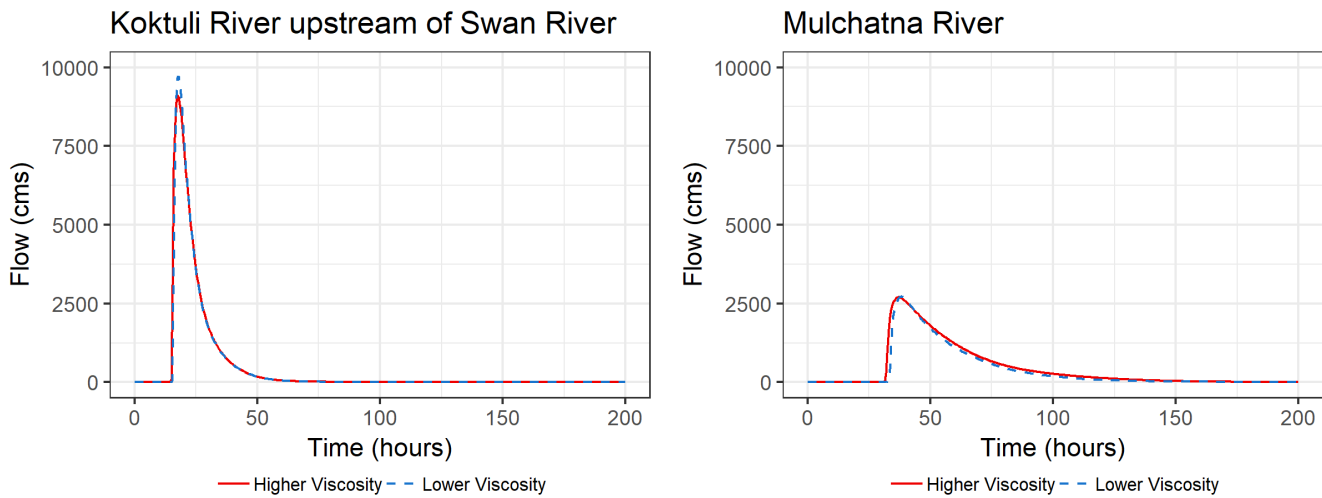


Figure 26: Mudflow Viscosity Sensitivity Analysis – Hydrograph

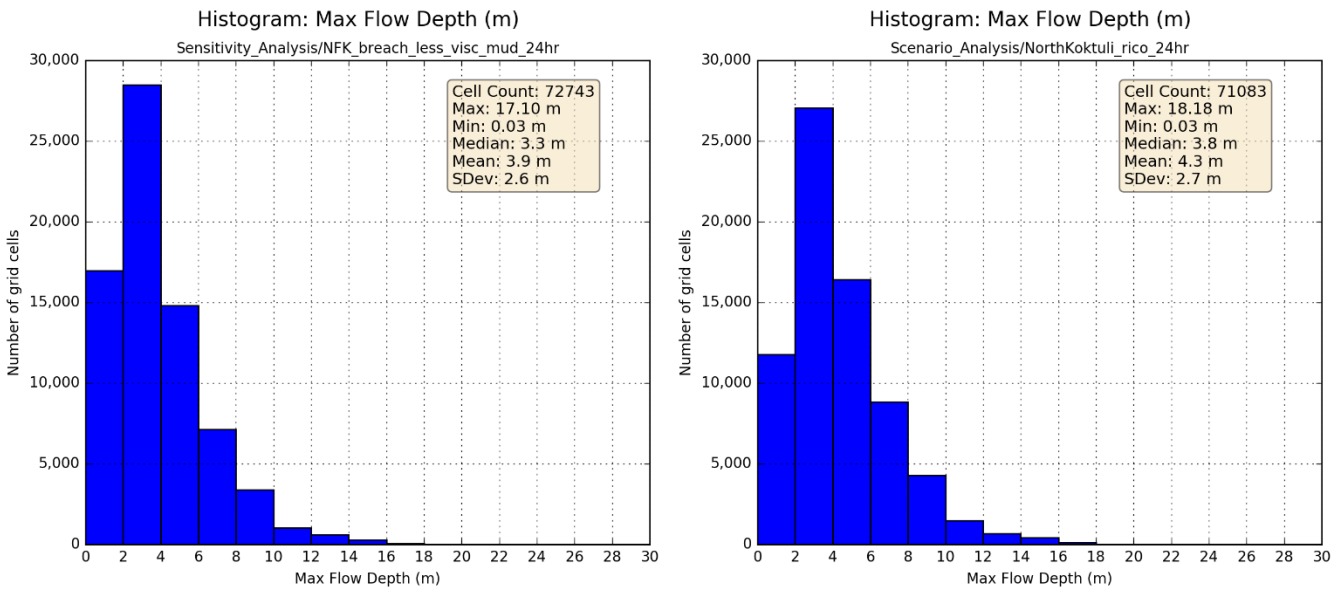


Figure 27. Histograms of the max flow depth cell values for the less viscous (left) and PLP-derived parameters (right) simulations

4 Dam Break Scenario Analysis

We developed dam break scenarios to characterize a suite of plausible different potential dam failure mechanisms. The failure scenarios are represented by two key parameters: the total volume of tailings released and the total duration of the dam breach. There is a significant amount of research into the volume of tailings dam releases, as discussed in Section 2.1. The Rico et al. (2008) curve (Figure 4) shows the likely release volume of 41.7%, but additional dam break releases of 10% and 60% were also tested to determine their impacts to the Nushagak River watershed. As discussed in Section 2.1.3, there is very little information available regarding the timing or duration of tailings releases from historical tailings dam breaches. We have relied on the 11-hour and 24-hour breaches as the most likely scenarios, and our results primarily illustrate the 24-hour breach, as it is a

more conservative estimate with a significantly lower peak flow compared with the 11-hour breach. The 11 hour breach is considerably more impactful.

Finally, we ran our scenarios over two model domains built and tested for this work: a higher resolution Kuktuli River watershed model and a lower resolution Nushagak River watershed model (see section 2.2.1 for discussion of model domains). The model results are discussed within their FLO-2D model domains of the Kuktuli and Nushagak Rivers.

4.1 Kuktuli River Model Results

The Kuktuli River FLO-2D model (see Figure 8) was tested on five different breach duration hydrographs (6-hours, 11-hours, 24-hours, 48-hours, and 96-hours) and two different breach volumes (10% of Rico and 60% of Rico) as shown in Table 17. Additional information regarding the development and calculation of these scenarios can be found in Section 2.1.

Table 17: Dam Break Scenario Analysis

Breach Release Volume (million m ³)	Peak Flow (cfs)	Duration of Breach Release (hours)	Maximum Sediment Concentration
Breach Duration Scenarios (Rico estimate volume)			
340	108,000	6	0.5
340	33,000	11	0.5
340	15,000	24	0.5
340	7,000	48	0.5
340	3,700	96	0.5
Breach Volume Scenarios			
82 (10%)	3,600	24	0.5
340 (42%)	15,000	24	0.5
490 (60%)	21,000	24	0.5

4.1.1 Breach Volume

Among the scenarios we evaluated, the volume of the tailings dam breach is the most significant factor in determining the spatial extent of deposited tailings from the bulk TSF. The 10% breach volume results in a total breach volume of 82 million m³, while the 60% breach volume results in breach of 492 million m³ of mine tailings. The 10% scenario inundates 158 km² of the watershed while the 60% breach scenario inundates 286 km², nearly double the area (Table 18). For reference, the dam breach volume predicted by the Rico et al. (2008) equation breach over 24 hours (41.7% of TSF storage capacity) results in a simulated inundated area of 256 km².

A map depicting the difference in inundated area and maximum depth for the 10% and 60% breach is shown in Figure 28. The difference in the depths of the inundated area between the three volume scenarios is depicted in the histograms showing maximum flow depths (Figure 29). The 10% breach has an average maximum flow depth of 2.3 meters, the 42% breach has an average maximum flow depth of 4.3 meters, and the 60% breach has an average maximum flow depth of 4.5 meters, with a maximum flow depth of 21 meters.

Table 18: Breach Volume Scenario Analysis – Model Output

Model Run	Bulked Breach Volume (million m ³)	Bulked Floodplain Storage (million m ³)	Bulked Outflow Volume (million m ³)	Storage as a % of Inflow	Outflow as a % of Inflow	Maximum Inundated Area (km ²)
10% of TSF storage capacity (24-hr breach)	82.0	28.9	53.1	35.3%	64.7%	158
42% of TSF storage capacity (24-hr breach)	341.9	69.6	272.4	20.4%	79.7%	256
60% of Rico breach volume (24-hr breach)	491.8	89.8	402.1	18.3%	81.8%	286

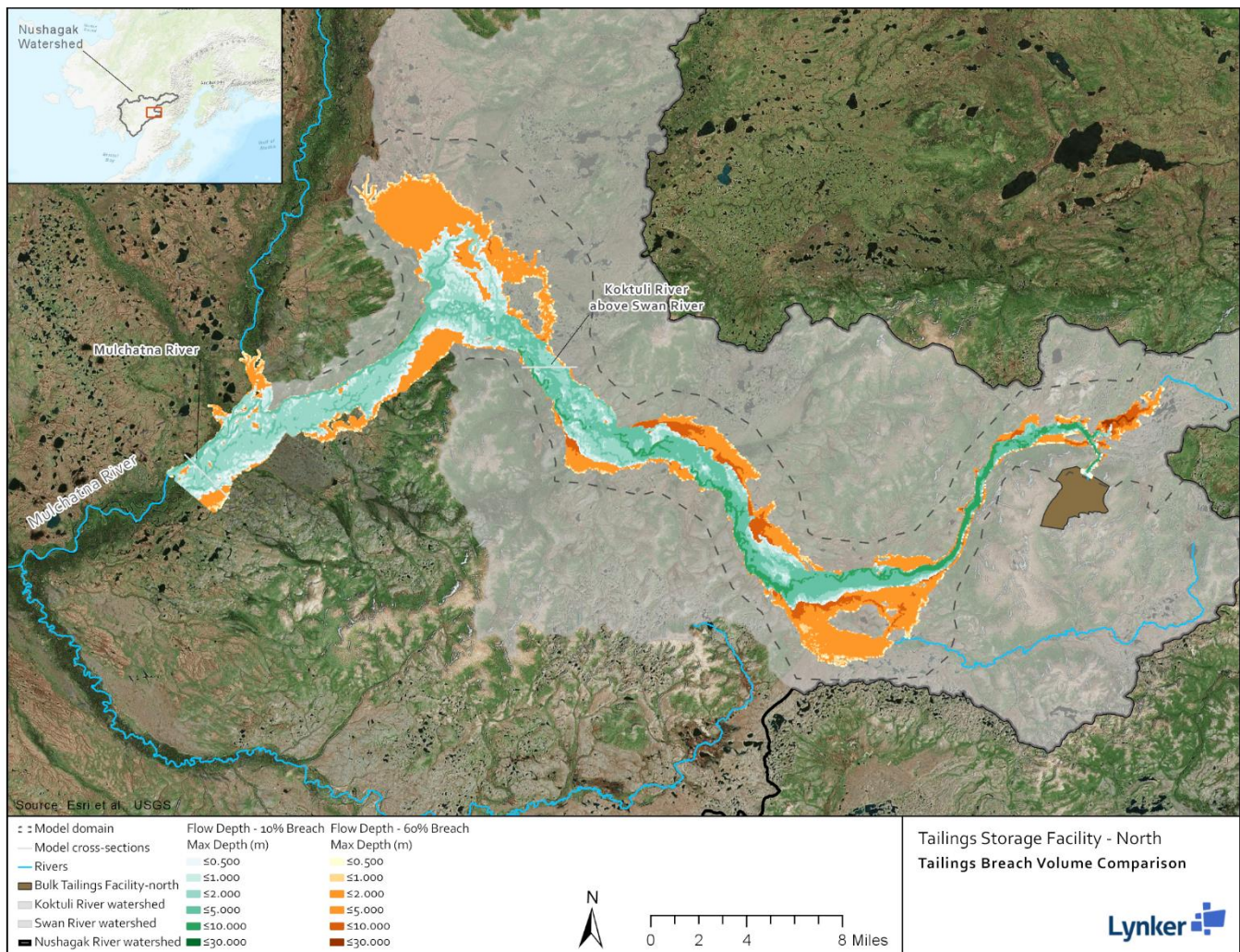


Figure 28. Breach volumes scenario analysis of max flow depth – 10% breach volume (green) vs. 60% breach volume (orange)

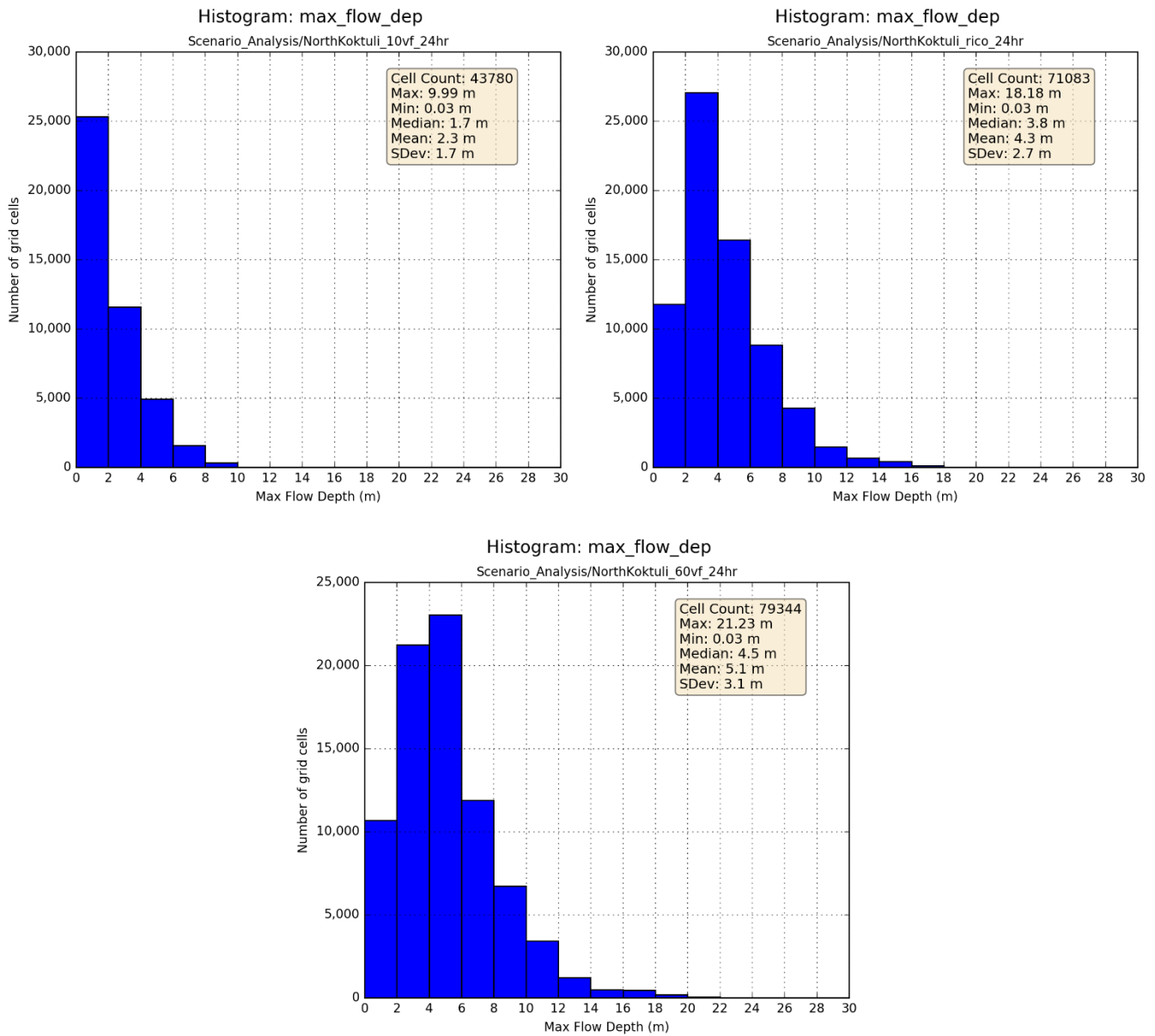


Figure 29. Histograms of the max flow depth cell values for the 10% (top left), 42% (top right), and 60% (bottom) breach volume simulations

The differences in impacts between the 10%, 42% and 60% release are readily observed from the cross-section hydrographs. The 10% breach has peak flow of 1,670 cfs, the 42% breach has a peak flow of 9,790 cfs, and the 60% breach has a peak flow of 14,000 cfs at the Koktuli River upstream of the Swan River. The results are shown in Table 19 and Figure 30. The hydrograph cross-section locations are shown in Figure 28.

Table 19: Breach Volume Scenario Analysis – Hydrograph Output

Model Run	Koktuli River upstream of Swan River			Mulchatna River		
	Maximum Discharge (m ³ /s)	Time to Maximum Discharge (hours)	Total Discharge Volume (million m ³)	Maximum Discharge (m ³ /s)	Time to Maximum Discharge (hours)	Total Discharge Volume (million m ³)
10% Breach Volume	1,670	24.6	74.3	483	60.7	55.1
41.7% Breach Volume	9,790	17.6	328.4	2,724	38.0	274.7
60% Breach Volume	14,270	16.5	478.4	4,140	34.0	404.2

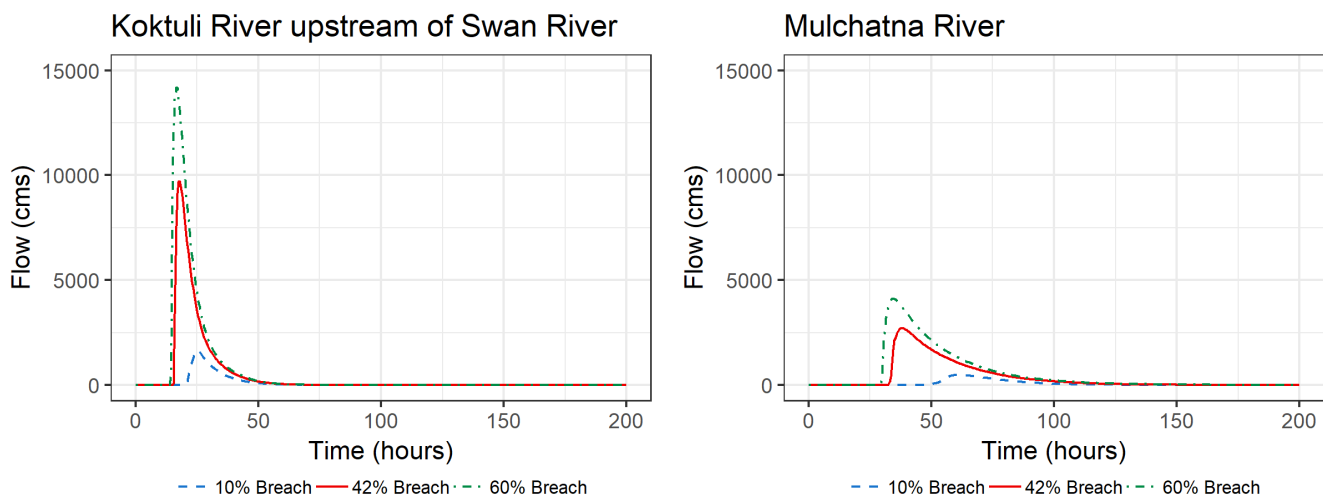


Figure 30: Hydrographs at the Koktuli and Mulchatna Rivers comparing breach volume scenarios

4.1.2 Breach Duration

A literature review of historical breach events yielded limited estimates of breach release duration (length of time from start of failure to end of breach release). The EPA assessment for mining impacts to Bristol Bay (U.S. EPA, 2014) examined a series for breach failure events ranging from 30-minutes to 4-hours in duration. The limited record of breach failure release duration data generally indicates that TSF breach events commonly occur quickly with event durations measured in hours (Wahl, 1998). Given the large scale of the planned Bulk TSF, we examined both short breach scenarios consistent with the observations from Wahl (1998), as well as much longer breaches. For these sensitivity analyses, we developed a series of inflow scenarios using a consistent release volume and altered the discharge hydrograph durations to generate a 6-hour, 11-hour, 24-hour, 48-hour and 96-hour events. Results from these simulations provides an overall assessment of the range of impacts that could be expected given the uncertainty surrounding what a possible failure might look like for the bulk TSF.

The results of the breach duration scenario analysis show a wide range of outcomes, in terms of the volume of tailings stored on the floodplain and the maximum watershed area inundated by the tailings breach. The 11-hour breach stores 99 million m³ on the floodplain with an inundated area of 272 km² while the 96-hour breach stores 66 million m³ on the floodplain with an inundated area of 203 km² (Table 20). A map comparing the maximum depth and the extent of the 6-hr and 96-hour breach events is shown in Figure 31. The 6-hour event has larger maximum flow depths (noted by more dark red coloring) as well as a larger inundation extent, which can be seen by a spill into the South Fork of the Koktuli River and a greater inundation in the Swan River basin to the north.

The difference in the flow depths of the inundated area between the 6-hour and 96-hour duration events is depicted in the histograms showing maximum flow depths (Figure 32). The 6-hour breach has an average maximum flow depth of 5.2 meters; the 24-hour breach has an average maximum flow depth of 4.3 meters; and the 96-hour breach has an average maximum flow depth of 3.6 meters.

Table 20: Breach Duration Scenario Analysis – Model Output

Model Run	Bulked Breach Volume (million m ³)	Bulked Floodplain Storage (million m ³)	Bulked Outflow Volume (million m ³)	Storage as a % of Inflow	Outflow as a % of Inflow	Maximum Inundated Area (km ²)
6-hr ¹	341.8	60.3	281.4	17.7%	82.4%	298
11-hr	341.9	98.8	243.1	28.9%	71.1%	272
24-hr breach	341.9	69.6	272.4	20.4%	79.7%	256
48-hr breach	341.9	67.2	274.7	19.7%	80.4%	228
96-hr breach	341.9	66.3	275.7	19.4%	80.6%	203

¹The 6-hr breach scenario was configured with an enhanced rising limb and peak which results in a different water/sediment composition compared to the event hydrograph used for the 11-hr to 96-hr simulations

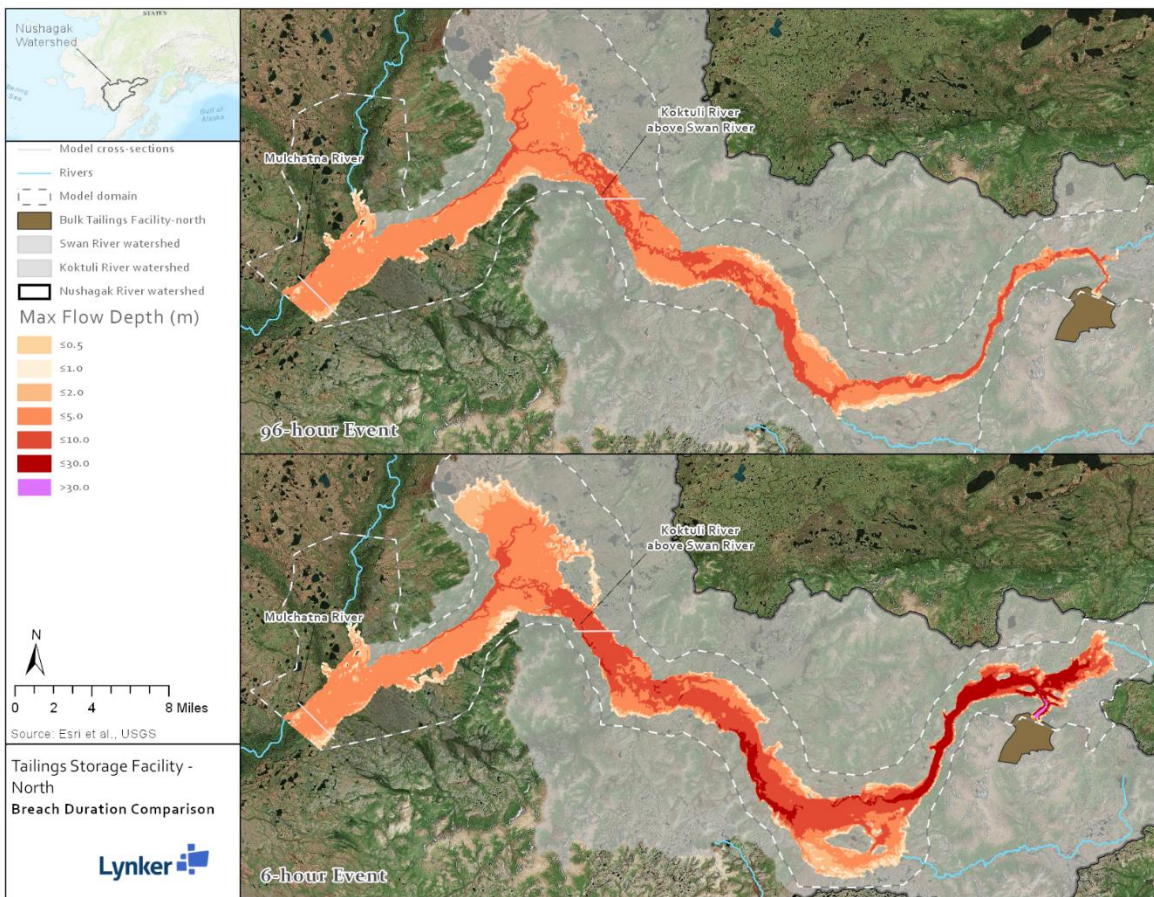


Figure 31: Breach Duration Scenario Comparison – 96-hr event (top) compared to a 6-hr event (bottom)

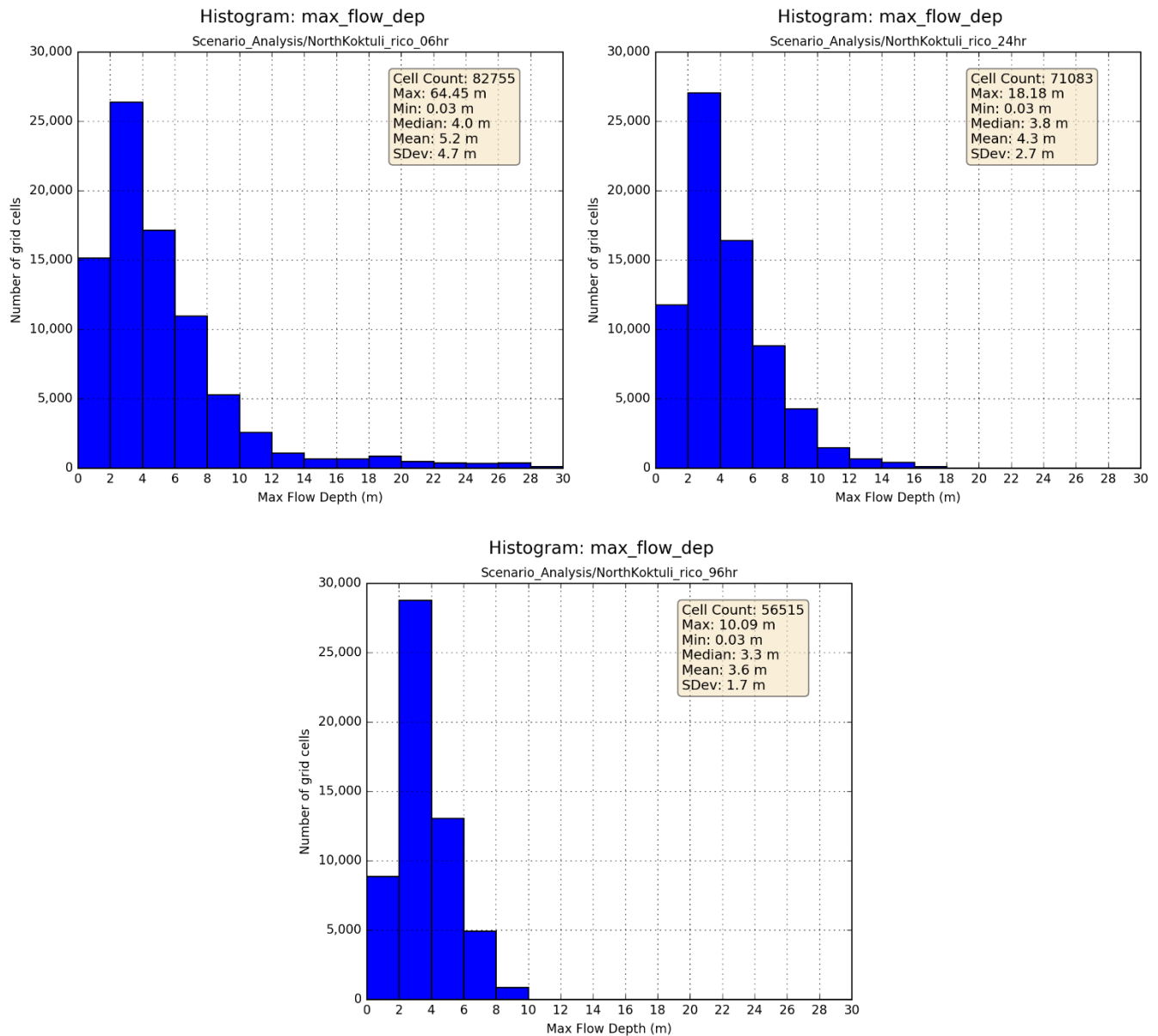


Figure 32. Histograms of the max flow depth cell values for the 6-hr (top left), 24-hr (top right), and 96-hr (bottom) breach duration simulations

The difference in tailings releases are shown for two floodplain cross-sections at the Koktuli River upstream of the Swan River and the Mulchatna River (cross section locations are shown in Figure 31). The 6-hour breach has a peak flow of 10,400 cfs at the Koktuli River upstream of the Swan River and a peak flow of 2,400 cfs at the Mulchatna River. The 96-hour breach has a peak flow of 5,200 cfs at the Koktuli River upstream of the Swan River and a peak flow of 2,300 cfs at the Mulchatna River. The similarities in the hydrographs at the Mulchatna River cross section are most likely caused by the wide flat valley at the confluence of the Swan River and the Koktuli River, which dampens the flow in both scenarios. As a result of this wide valley that gets filled with tailings in all scenarios, the magnitude of the peak flow is no longer sensitive to the initial conditions of the breach duration by the time the tailings dam breach reaches the Mulchatna River. However, the time of arrival of the breach floodwave is still sensitive to the initial conditions. The peak flow for the 6-hour breach reaches the

Mulchatna River in 33 hours, while the peak flow for the 96-hour breach reaches the Mulchatna River in 62 hours. The results of the hydrograph cross-section analysis are shown in Table 21 and Figure 33.

Table 21: Breach Duration Scenario Analysis – Hydrograph Output

Model Run	Koktuli River upstream of Swan River			Mulchatna River		
	Maximum Discharge (m ³ /s)	Time to Maximum Discharge (hours)	Total Discharge Volume (million m ³)	Maximum Discharge (m ³ /s)	Time to Maximum Discharge (hours)	Total Discharge Volume (million m ³)
6-hr Breach Duration	10,420	12.1	326.1	2,409	32.9	283.4
24-hr Breach Duration	9,788	17.6	328.4	2,724	38.0	274.7
96-hr Breach Duration	5,218	34.6	334.4	2,340	61.9	278.0

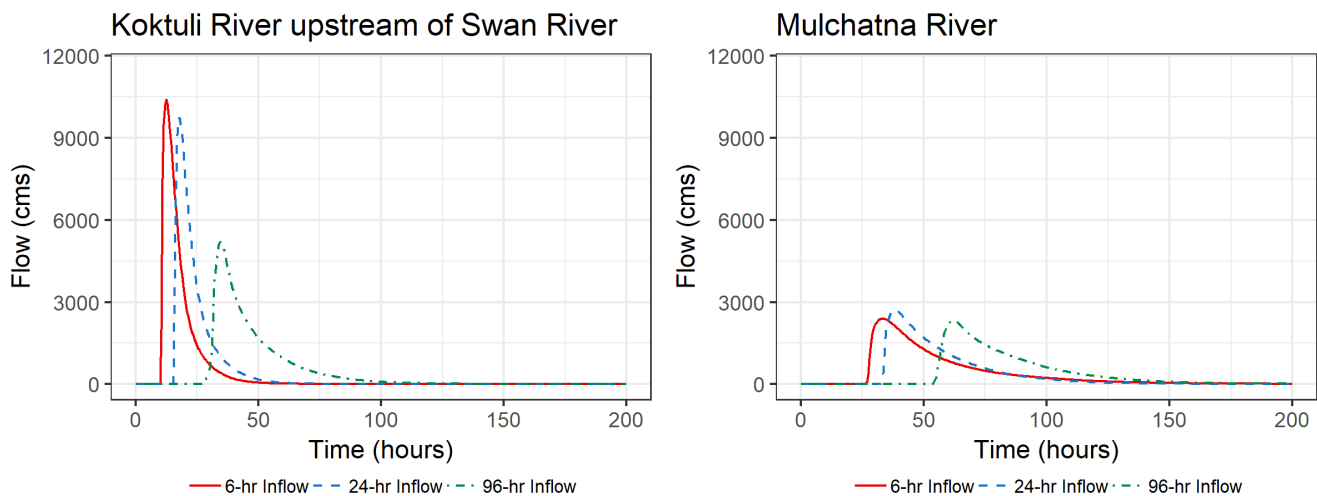


Figure 33. Floodplain Hydrographs showing different breach durations

4.2 Nushagak River Model Results

The Nushagak River watershed model domain spans from the bulk TSF in the Nork Fork of the Koktuli River to the Nushagak River approximately 142 km downstream. This larger model domain was run for two scenarios, a 41.7% breach volume (Rico volume) and a 10% breach volume. We selected these scenarios because our sensitivity analysis indicated that floodplain impacts were most sensitive to the breach release volume. The TSF breach volumes for the two scenarios are shown in Table 22.

As discussed in the DEM sensitivity analysis (Section 3.1), the Nushagak River watershed model uses a different DEM than was used in the Koktuli River watershed model. The ArcticDEM was the highest resolution DEM available for the full model domain. However, because of the way it was generated, the ArcticDEM is a “first-

return” rather than “bare-earth” representation of the land surface, meaning the elevations in the DEM can represent the tops of trees and shrubs in vegetated areas (Figure 34). This has implications for the quality of the results from the Nushagak River watershed model compared to that of the Koktuli River watershed model: particularly in the more vegetated river reaches further downstream, the ArcticDEM generates an artificially rough surface that could significantly influence the tailings transport results. Given these data constraints, the results from the Nushagak River watershed model should be interpreted with significant caution. However, the coarser ArcticDEM also creates a conservative bias in terms of impacts: since the ArcticDEM generates a “rougher” land surface by including the tops of vegetation, the tailings breach loses energy more quickly than it should as it moves downstream. These effects are evaluated in Section 3.1, where the ArcticDEM is shown to have peak flow 25% less than the higher resolution IfSAR DEM and a total flow release 6% less than the higher resolution IfSAR DEM at the Mulchatna River (bottom of the Koktuli model domain). For these reasons the modeled output of the Nushagak model are likely conservative and underestimate the flow downstream to the Nushagak River.

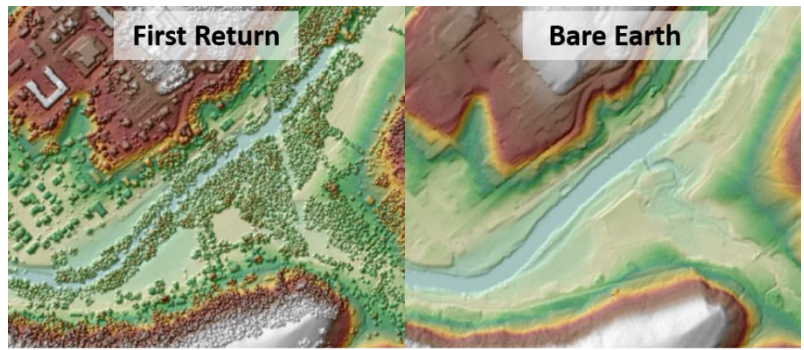


Figure 34. Example comparison of top of canopy first return vs. bare earth DEM

Table 22: Nushagak River Watershed Model Scenarios

Breach Release Volume (million m3)	Peak Flow (cfs)	Duration of Breach Release (hours)	Maximum Sediment Concentration
82 (10%)	3,600	24	0.5
340 (42%)	15,000	24	0.5

In the Nushagak model, the 10% of dam capacity release has a total model boundary outflow of 18 million m³ whereas the 42% of dam capacity release has an outflow of 196 million m³ (Table 23). In the 10% release scenario, most of the tailings release (78%) is deposited on the floodplain, while 22% continues downstream via the Nushagak River. In the 42% release scenario, 43% of the tailings release is deposited on the floodplain while 57% continues downstream via the Nushagak River. The maximum inundated area of the 42% release scenario is approximately double that of the 10% release scenario (480 km² compared to 260 km², respectively). The model results are presented in Table 23. The maximum flow depths for the two release volume scenarios are shown in Figure 35.

Due to the lower resolution of the underlying ArcticDEM, there is lower confidence in the flow depths and areal extent of the tailings release in the Nushagak model. However, both model scenarios show the tailings release continuing downstream to the Nushagak River. Therefore, despite the limitations from the ArcticDEM, there is high confidence that a breach of the bulk TSF would result in mine tailings reaching the Nushagak River. The difference in the flow depths of the inundated area between the 10% release and 42% release is depicted in the histograms showing maximum flow depths (Figure 36). The 10% breach has an average maximum flow depth of 1.8 meters, and the 42% breach has an average maximum flow depth of 3.1 meters.

Table 23. Model Results for Nushagak Model Runs

Model Run	Bulked Breach Volume (million m ³)	Bulked Floodplain Storage (million m ³)	Bulked Outflow Volume (million m ³)	Storage as a % of Inflow	Outflow as a % of Inflow	Maximum Inundated Area (km ²)
10% of Volume	82.0	64.0	17.9	78.1%	21.9%	261.7
41.7% of Volume	341.9	145.5	196.4	42.6%	57.4%	480.2

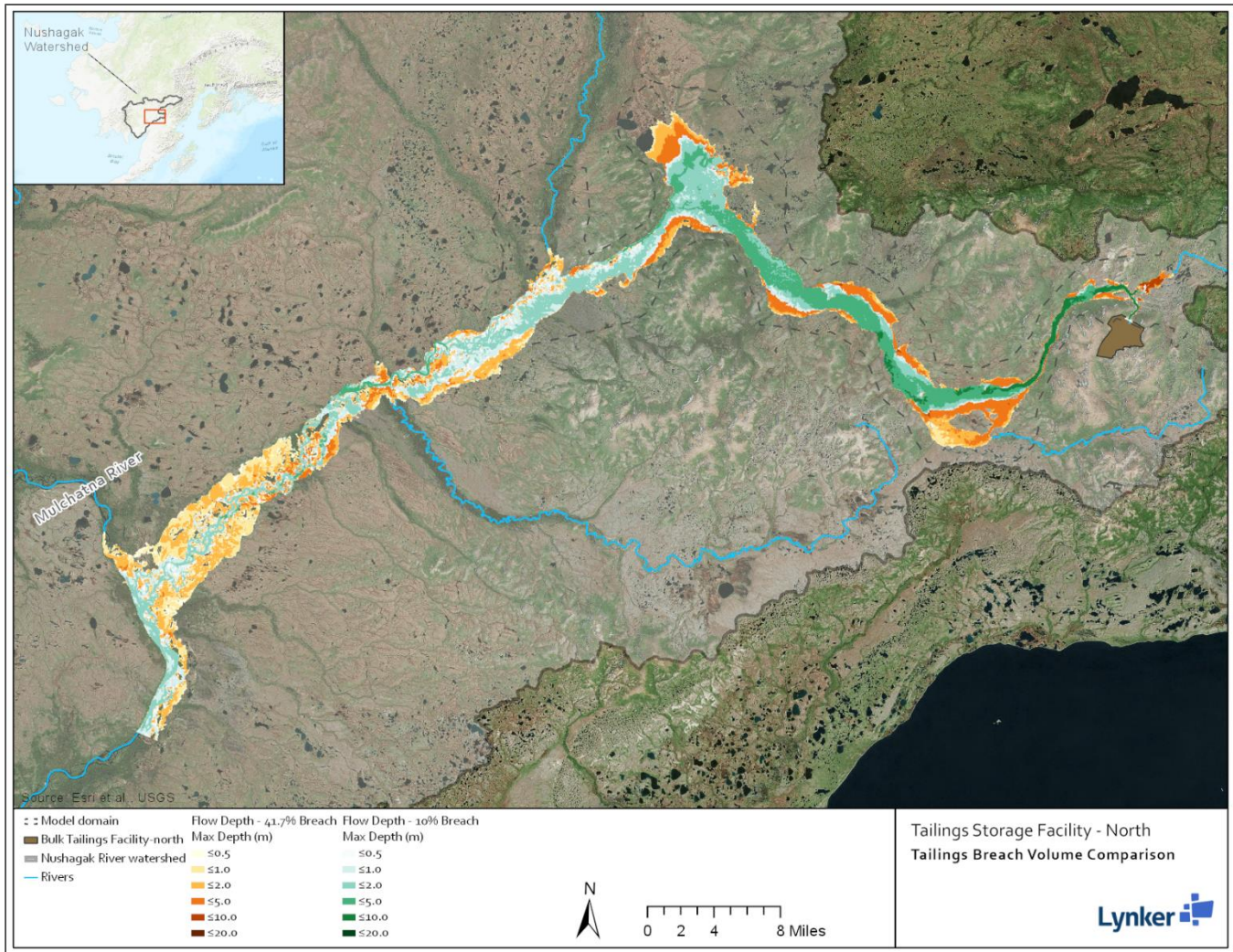


Figure 35. Max flow depth comparison between the 10% breach volume (green) and the 41.7% breach volume (orange) simulations

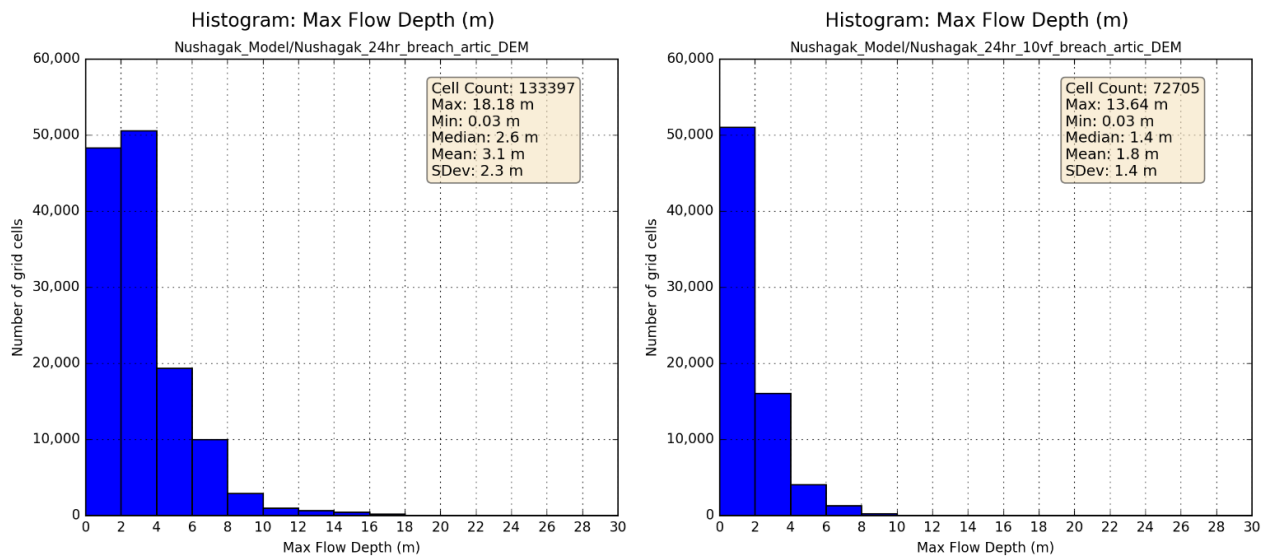


Figure 36. Histograms of the max flow depth cell values for the 41.7% breach volume (left) and 10% breach volume (right) for the Nushagak model domain simulations

4.3 Impacts to Salmon Habitat

Using the results of the simulated flood inundated area, we can infer potential impacts to downstream salmon habitat that would result from a TSF dam failure. The Anadromous Waters Catalog (AWC) (<https://www.adfg.alaska.gov/sf/SARR/AWC/index.cfm?ADFG=main.home>) specifies streams, rivers, and lakes that are identified as important to anadromous fish spawning, rearing, and migration (Johnson & Blossom, 2018). Water bodies identified in the catalog are afforded protection under AS 16.05.871. It is important to note that the AWC documentation (Johnson & Blanche, 2012) states that “anadromous fish often rear in small tributaries, flood channels, intermittent streams, and beaver ponds” but “due to the remote location, small size, or ephemeral nature of these systems, most have not been surveyed and are not included in the Catalog or Atlas”. Because the AWC does not account for the abundant off-channel habitat within the floodplains of the Nushagak watershed (see Figure 37), estimates of salmon habitat impacted by tailings releases are likely to be significant underestimates of true impacts.

Although the AWC is a very coarse representation of salmon habitat in the Nushagak watershed, as described above, the inundated areal extent from the 24-hour, 42% bulk TSF breach model directly impacts approximately 219 miles of AWC protected river reaches (Figure 38).

In addition to the AWC reaches and the off-channel habitat that would be directly impacted by a TSF breach, there are also hundreds of miles of river reaches that may become inaccessible to salmonids as an indirect result of a tailings dam failure. For example, the concentration of copper in water contacting bulk tailings is projected to be approximately 0.01 mg/L (DEIS, Table K4.18-2). This concentration is approximately 20 times higher than the concentration shown to create olfactory inhibition and avoidance behavior in salmonids (approximately 0.0005 mg/L in water collected from the Pebble site; see Morris et al., 2019). Although a complete analysis of copper concentrations in tailings and downstream waters is beyond the scope of this study, these data indicate that a tailings dam breach could potentially cause migrating salmonids to avoid the abundant habitat in the upper Nushagak and Mulchatna systems. More detailed study of the nature and long-term fate of tailings after deposition is warranted to evaluate whether migrating salmonids would respond to a tailings breach by avoiding up-migration into the Mulchatna-Nushagak system altogether, potentially eliminating salmon spawning and rearing habitat from a substantial fraction of the Bristol Bay fishery.

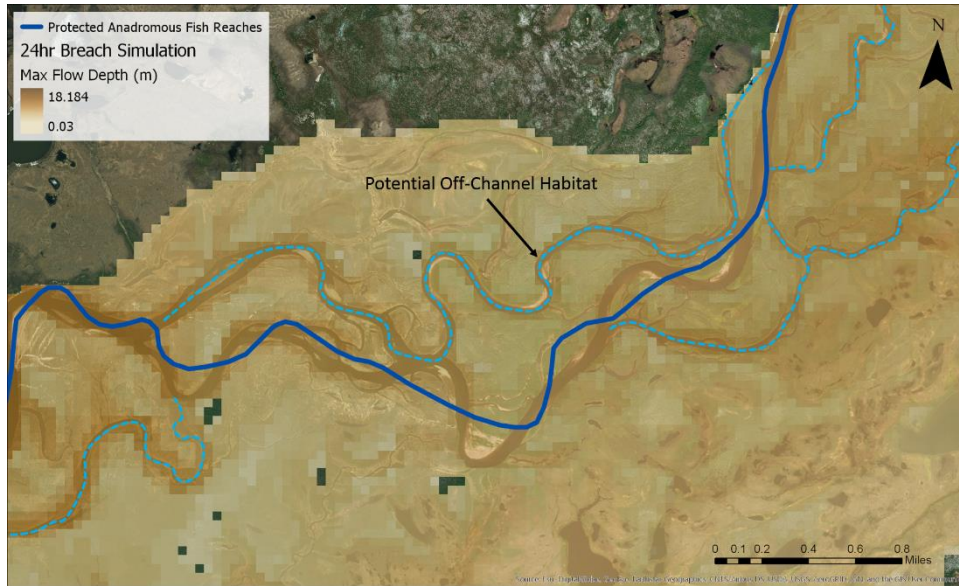


Figure 37. Example of potential off-channel reaches (dashed blue line) visible from satellite imagery that are not represented by the AWC designated reach (solid blue line)

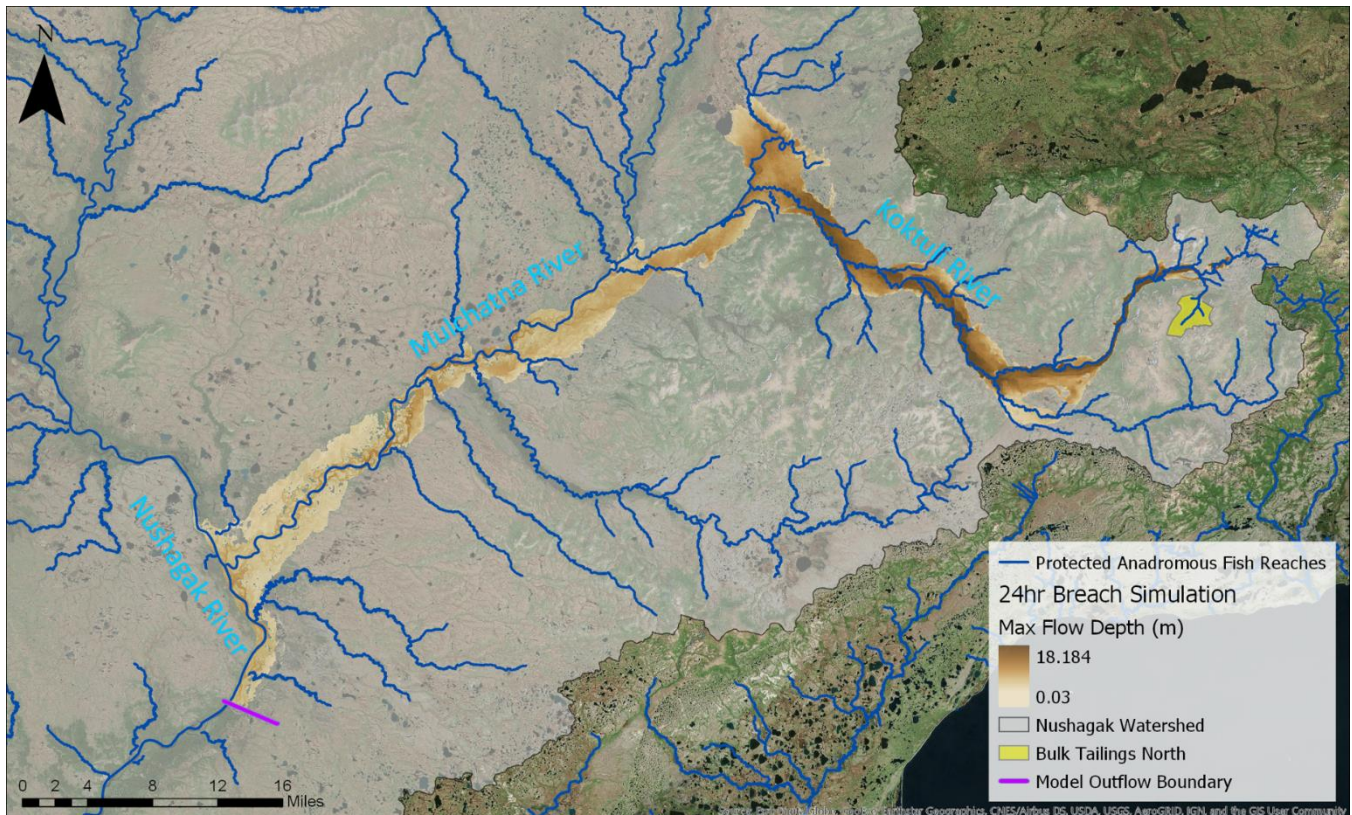


Figure 38. Map of the simulated max flow depth (41.7% breach volume) and the inundated protected anadromous fish reaches

Recent work using strontium isotopes from Pacific salmon otoliths (ear stones) to recreate the freshwater portion of the salmon lifecycle demonstrates the importance of the Nushagak-Mulchatna system to both Chinook and sockeye salmon (Brennan et al., 2019). The study analyzed data from 2011, 2014, and 2015 to explore how salmon populations are distributed across the watershed, and how these patterns shift year-to-year. The results demonstrate a high degree of inter-annual variability in which streams are most utilized during the freshwater parts of the salmon lifecycle, but also highlight the importance of the upper Nushagak-Mulchatna system as part of the habitat mosaic of Bristol Bay. As an example, Figure 39 and Figure 40 show relative salmon production metrics from 2015 from Brennan et al. (2019), overlaid with the simulated 24-hr bulk TSF flood inundation area. The production metrics indicate that there are numerous moderate to high production stream reaches that would be directly impacted from the simulated bulk TSF failure, as well as significant upstream high production reaches that may become inaccessible to salmon if copper concentrations create avoidance behavior as described above.

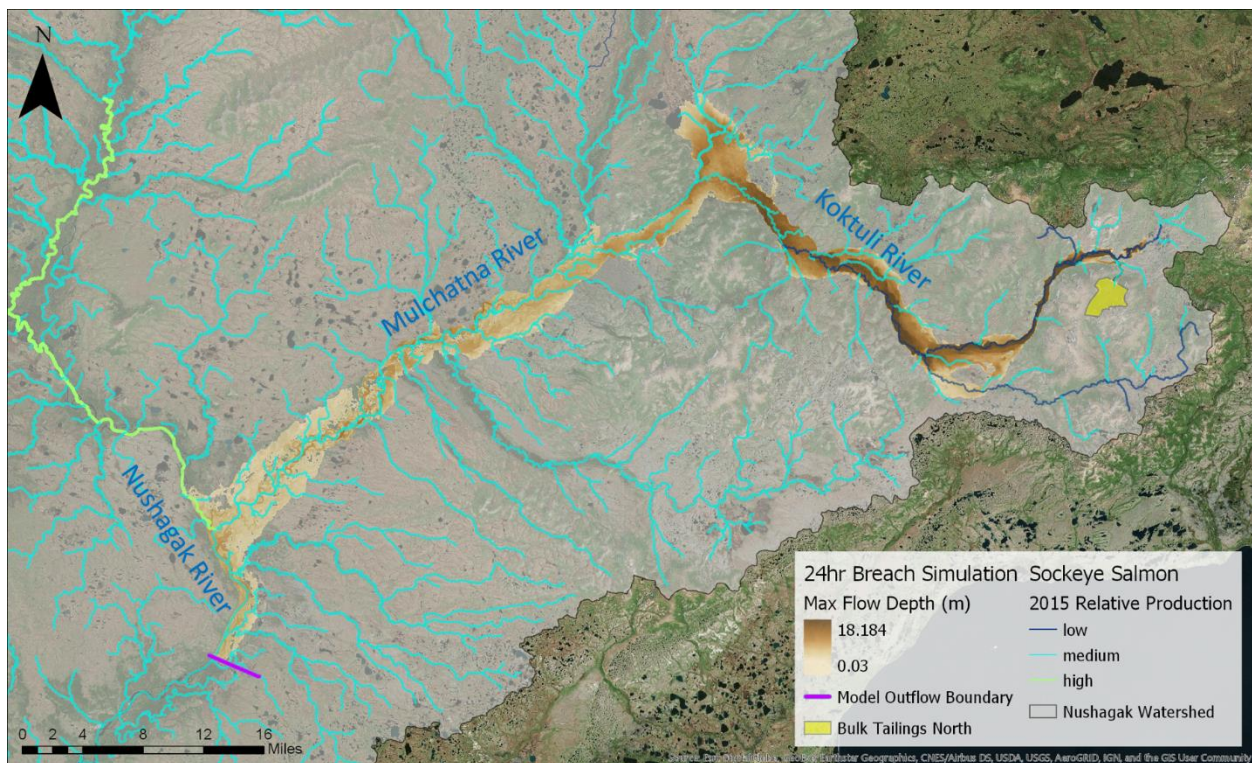


Figure 39. 2015 relative production of Sockeye salmon

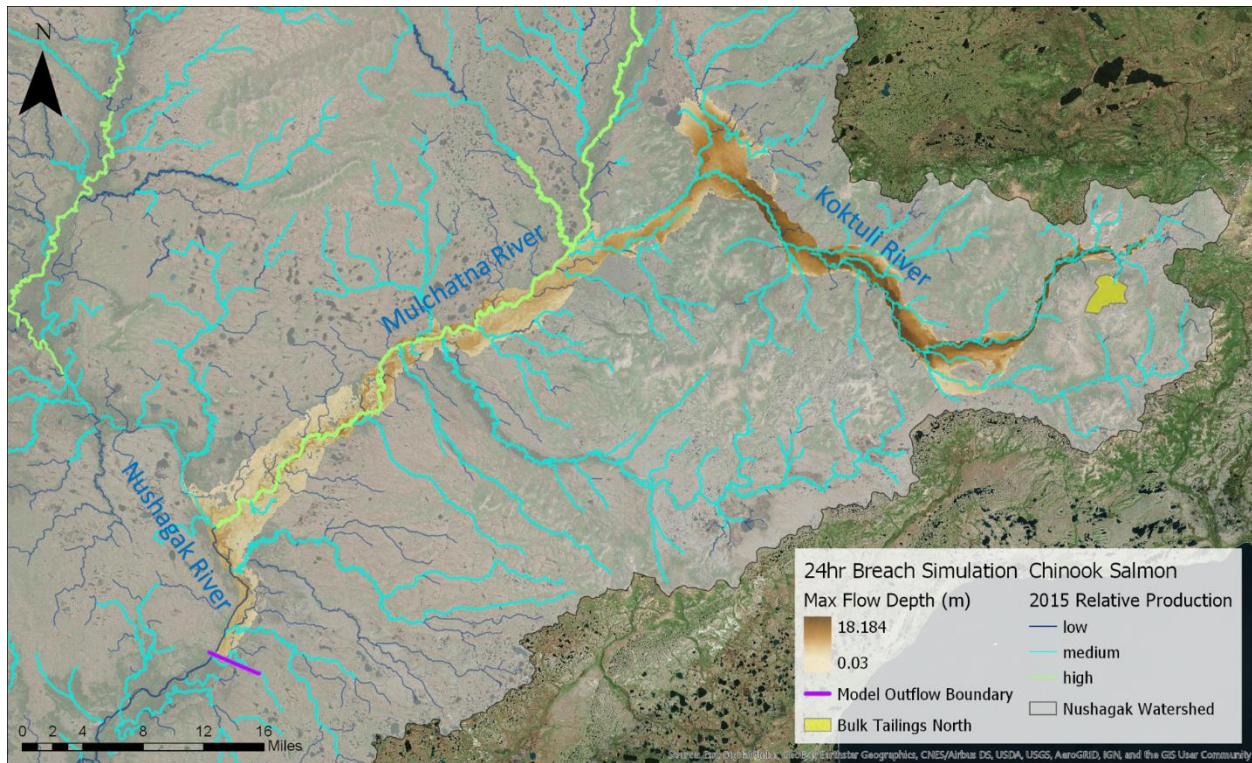


Figure 40. 2015 relative production of Chinook salmon

4.4 Long-term fate of tailings

The results of our modeling illustrate the maximum spatial extent of tailings across the floodplains of the Kuktuli, Mulchatna and Nushagak rivers resulting from a range of tailings failure scenarios. While some of these tailings would be deposited within the channels of the major rivers, the majority of them would be spread across the floodplain, draping the landscape with fine-grained mineral matter. As shown in Figure 41 and in our simulation results, while some of the tailings from TSF breaches are deposited in the active stream channel, the majority of the area affected is on the floodplain and valley side slopes.



Figure 41. Example of the landscape effects of a TSF failure in Brazil

Photo credit: <https://slate.com/news-and-politics/2015/12/brazil-mining-dam-disaster-toxic-sludge-and-irreversible-environmental-damage.html>

A quantitative evaluation of the long-term fate of the tailings deposited across the floodplain would require development of a distributed hydrologic model with high-resolution topographic data to simulate local processes such as rain splash, overland flow, and sediment transport in small channels across the landscape. While such an exercise would require topographic and climatic data that are not currently available, the DEIS describes in qualitative terms what the long-term fate of these materials might be.

First, because of the remoteness of the area, the DEIS notes that “Recovery of a massive release, especially one that reaches flowing water, would be extremely difficult.” (DEIS, p. 4.27-65). There are no roads leading to the vast majority of the streams that would be affected, and even if access were possible, it is not clear what sorts of remedial activities could be undertaken that would not cause further damage to the vegetation and the landscape.

Furthermore, because the majority of the tailings deposition would occur in off-channel areas, natural attenuation would also likely take a very long time: naturally high river discharge events in the spring and fall may gradually flush tailings out of active channels through time, but the tailings deposited on the floodplain and off-channel habitat would take much longer to recover, and could also be a long-term source of contamination. As described in the DEIS:

“Unrecovered tailings that are exposed to oxygen could generate acid on a timescale of years to decades...acid and heavy metals that accumulate in streambed sediments, wetland soils, or isolated waterbodies could impact water quality on a timescale of decades.” (DEIS, page 4.27-65).

5 Summary

With more than 130 years of sustainable harvest, Bristol Bay ranks among the most important wild salmon fisheries on earth (Hilborn et al. 2003, Knapp et al 2013): the region contains thousands of miles of mainstem and off-channel salmon habitat, with virtually no imprint of human activity. Based on our analysis, a tailings dam failure at the proposed Pebble Mine would directly impact hundreds of miles of this habitat, and could indirectly impact many hundreds of miles more. These impacts were documented using the best available information from the Pebble Partnership and the Draft EIS, using hydrologic and hydraulic modeling software well-known and used by the mining industry.

Despite these potential impacts, and the public availability of data and software to model them, the Draft Environmental Impact Statement that is currently under review ignores the risk of a TSF dam failure. In doing so, the DEIS cites the low likelihood of dam failure in just the first 20-years of dam life, for a structure that must maintain its integrity forever. As described in NEPA (40 C.F.R. § 1502.22), the EIS's cumulative impacts analysis must include quantified and detailed information about past, present and reasonably foreseeable future actions. Importantly, "reasonably foreseeable" includes impacts that would have catastrophic consequences, even if their probability of occurrence is low. Our analysis provides the quantified and detailed information that the DEIS is lacking, and that we believe should be repeated by USACE and incorporated into the final EIS.

6 References

- AECOM. 2018. Pebble EIS-phase failure modes and effects analysis workshop report. December 2018.
- Alaska Department of Natural Resources. (2017). Guidelines for Cooperation with the Alaska Dam Safety Program. Retrieved from http://dnr.alaska.gov/mlw/water/dams/AK_Dam_Safety_Guidelines072817rev2.pdf
- Azam, S., & Li, Q. (2010). Tailings dam failures: A review of the last one hundred years. *Geotechnical News*, 28(4), 50–53. <https://doi.org/10.1373/clinchem.2008.105395>
- Baker, B., & Schaefer, M. (2007). *Dam Safety Guidelines: Dam Break Inundation Analysis and Downstream Hazard Classification* (Vol. 92–55E). Olympia, WA. Retrieved from <https://fortress.wa.gov/ecy/publications/documents/9255e.pdf>
- Bowker, L.N. and Chambers, D.M. In *The Dark Shadow of The Supercycle: Tailings Failure Risk & Public Liability Reach All Time Highs*, *Environments* 2017, 4(4), 75; doi:10.3390/environments4040075
- Brennan, A. S. R., Schindler, D. E., Cline, T. J., Walsworth, T. E., Buck, G., & Fernandez, D. P. (2019). Shifting habitat mosaics and fish production across river basins. Manuscript submitted for publication
- Brennan, S. R., Schindler, D. E., & Fernandez, D. P. (2017). Using strontium in otoliths to determine the natal origin and habitat use of sockeye salmon in the Nushagak River; Final Report to Bristol Bay Science Research Institute.
- CNN, 2018. "Inside Alaska's battles over land, sea and life." Available: <https://www.cnn.com/2018/07/23/us/alaska-environment-battles-weir/index.html> Accessed 24 January, 2019
- Concha Larrauri, P., & Lall, U. (2018). Tailings Dams Failures: Updated Statistical Model for Discharge Volume and Runout. *Environments*, 5(2), 28. <https://doi.org/10.3390/environments5020028>
- CVT News, 2016 "Mt Polley mine owner sues engineering firms over tailings dam failure" Available: <https://www.ctvnews.ca/business/mount-polley-mine-owner-sues-engineering-firms-over-tailings-dam-failure-1.2979873> Accessed 24 January, 2019

- Federal Energy Regulatory Commission. (2015). Engineering Guidelines: Chapter II Selecting and Accommodating Inflow Design Floods for Dams.
- Fernandes, G. W., Goulart, F. F., Ranieri, B. D., Coelho, M. S., Dales, K., Boesche, N., et al. (2016). Deep into the mud: ecological and socio-economic impacts of the dam breach in Mariana, Brazil. *Natureza & Conservação*, 14(2), 35–45. <https://doi.org/10.1016/j.ncon.2016.10.003>
- FLO-2D. (2017). FLO-2D Reference Manual. Nutrioso, AZ. Retrieved from <https://www.flo-2d.com/download/>
- FLO-2D. (n.d.). FLO-2D Simulating Mudflows Guidelines.
- Gee, M. (n.d.). Comparison of Dam Breach Parameter Estimators. Corps of Engineers Hydrologic Engineering Center. Davis, CA. Retrieved from <http://citeseerx.ist.psu.edu/viewdoc/download?doi=10.1.1.897.9923&rep=rep1&type=pdf>
- Hilborn, R., Quinn, T. P., Schindler, D. E., & Rogers, D. E. (2003). Biocomplexity and fisheries sustainability. *Proceedings of the National Academy of Sciences*, 100(11), 6564–6568. <https://doi.org/10.1073/pnas.1037274100>
- Homer, C.G., Dewitz, J., Yang, L., Jin, S., Danielson, P., Xian, Coulston, J., Herold, N., Wickham, J. and K. Megown. 2015. Completion of the 2011 National Land Cover Database for the conterminous United States – representing a decade of land cover change information, *Photogrammetric Engineering and Remote Sensing*, Vol. 81, 345-353.
- Independent Expert Engineering Investigation and Review Panel. (2015). Report on Mount Polley Tailings Storage Facility Breach, 1–147. Retrieved from <https://www.mountpolleyreviewpanel.ca/final-report>
- Johnson, J., and B. Blossom. 2018. Catalog of Waters Important for Spawning, Rearing, or Migration of Anadromous Fishes—Southwestern Region, Effective June 1, 2018. Alaska Department of Fish and Game, Divisions of Sport Fish and Habitat Special Publication No. 18-06, Anchorage.
- Julien, P. Y., & Leon S., C. A. (2000). Mud Floods, Mudflows and Debris Flows Classification, Rheology and Structural Design. In *Int. Workshop on the Debris Flow Disaster of December 1999 in Venezuela*. Caracas, Venezuela: Universidad Central de Venezuela. Retrieved from http://www.engr.colostate.edu/~pierre/ce_old/resume/Paperspdf/Julien-LeonCar00.PDF
- Knight Piésold Ltd. (2014). Dam breach analyses and inundation studies for the Afton Tailings Storage Facility (TSF). Retrieved from: http://mssi.nrs.gov.bc.ca/AftonAjax/AftonAjaxAbacus_2014_inundation.pdf
- Knight Piésold Ltd. (2018). Operations Water Management Plan Rev 1.
- Knight Piésold Ltd. (2018b). RE: Pebble Project: EIS-FMEA Failure Scenario for the Bulk Tailings Storage Facility.
- Knight Piésold Ltd. (2018c). RE: Pebble Project: EIS-FMEA Failure Scenario for the Pyritic Tailings Storage Facility.
- Major, J. J., & Pierson, T. C. (1992). Debris flow rheology: Experimental analysis of fine-grained slurries. *Water Resources Research*, 28(3), 841–857. <https://doi.org/10.1029/91WR02834>
- Marshall, J. (2018). Tailings dam spills at Mount Polley and Mariana Chronicles of Disasters Foretold. Retrieved from [https://www.policyalternatives.ca/sites/default/files/uploads/publications/BC Office/2018/08/CCPA-BC_TailingsDamSpills.pdf](https://www.policyalternatives.ca/sites/default/files/uploads/publications/BC%20Office/2018/08/CCPA-BC_TailingsDamSpills.pdf)
- Martin, V., & Akkerman, A. (2017). Challenges with conducting tailings dam breach assessments. In *85th Annual Meeting of International Commission on Large Dams*. Prague, Czech Republic.
- Miguel, H. A., Daniel, P. E., & Mishel, M. B. (2015). Considerations on dam breach analysis of tailing storage facilities. *3rd International Seminar on Tailings Management*, 1–13.
- Morris, J. M., Brinkman, S. F., Takeshita, R., McFadden, A. K., Carney, M. W., & Lipton, J. (2019). Copper toxicity in Bristol Bay headwaters: Part 2—Olfactory inhibition in low-hardness water. *Environmental toxicology and chemistry*, 38(1), 198-209.
- O'Brien, J. S., & Julien, P. Y. (1988). Laboratory Analysis of Mudflow Properties. *Journal of Hydraulic Engineering*, 114(8), 877–887. [https://doi.org/10.1061/\(ASCE\)0733-9429\(1988\)114:8\(877\)](https://doi.org/10.1061/(ASCE)0733-9429(1988)114:8(877))

- O'Brien, J. S., Gonzalez-Ramirez, N., Tocher, R. J., Chao, K. C., & Overton, D. D. (2015). Predicting Tailings Dams Breach Release Volumes for Flood Hazard Delineation. In Association of State Dam Safety Officials. New Orleans. Retrieved from https://issuu.com/asdso/docs/asdso-conference_program-print_fina
- O'Brien, J. S., Julien, P. Y., & Fullerton, W. T. (1993). Two-Dimensional Water Flood and Mudflow Simulation. *Journal of Hydraulic Engineering*, 119(2), 244–261. [https://doi.org/10.1061/\(ASCE\)0733-9429\(1993\)119:2\(244\)](https://doi.org/10.1061/(ASCE)0733-9429(1993)119:2(244))
- Orman, M., et al. 2017. Tailings Dam Classification and Breach Analyses; perspectives from the Canadian Dam Association. Presentation for the 25th Annual Mine Design, Operations & Closure Conference. Available: https://www.mtech.edu/mwtp/2017_presentations/wednesday/marc-orman.pdf. Accessed 24 January, 2019
- Pierson, T. C., & Scott, K. M. (1985). Downstream Dilution of a Lahar: Transition From Debris Flow to Hyperconcentrated Streamflow. *Water Resources Research*, 21(10), 1511–1524. <https://doi.org/10.1029/WR021i010p01511>
- Porter, Claire; Morin, Paul; Howat, Ian; Noh, Myoung-Jon; Bates, Brian; Peterman, Kenneth; Keeseey, Scott; Schlenk, Matthew; Gardiner, Judith; Tomko, Karen; Willis, Michael; Kelleher, Cole; Cloutier, Michael; Husby, Eric; Foga, Steven; Nakamura, Hitomi; Platson, Melisa; Wethington, Michael, Jr.; Williamson, Cathleen; Bauer, Gregory; Enos, Jeremy; Arnold, Galen; Kramer, William; Becker, Peter; Doshi, Abhijit; D'Souza, Cristelle; Cummins, Pat; Laurier, Fabien; Bojesen, Mikkel, 2018, "ArcticDEM", <https://doi.org/10.7910/DVN/OHHUKH>, Harvard Dataverse, V1, February 21, 2019.
- Rico, M., Benito, G., & Díez-Herrero, A. (2008). Floods from tailings dam failures. *Journal of Hazardous Materials*, 154(1–3), 79–87. <https://doi.org/10.1016/j.jhazmat.2007.09.110>
- Rico, M., Benito, G., Salgueiro, A. R., Díez-Herrero, A., & Pereira, H. G. (2008). Reported tailings dam failures. *Journal of Hazardous Materials*, 152(2), 846–852. <https://doi.org/10.1016/j.jhazmat.2007.07.050>
- Schindler, D. E., Hilborn, R., Chasco, B., Boatright, C. P., Quinn, T. P., Rogers, L. A., & Webster, M. S. (2010). Population diversity and the portfolio effect in an exploited species. *Nature*, 465(7298), 609–612. <https://doi.org/10.1038/nature09060>
- Schoenberger, E. (2016). Environmentally sustainable mining: The case of tailings storage facilities. *Resources Policy*, 49, 119–128. <https://doi.org/10.1016/j.resourpol.2016.04.009>
- Tetra Tech. (2015). Treasury Metals Goliath Project TSF Breach Impact Assessment Water Quality Model. Retrieved from <https://www.ceaa.gc.ca/050/documents/p80019/101536E.pdf>
- The Pebble Partnership. (2011). North Fork Koktuli River Basin, Reaches, and Instream Flow Study Sites.
- U.S. Department of the interior Bureau of Reclamation. (2012). Embankment Dams. Chapter 6. Freeboard. Design Standards No. 13: Embankment Dams, 4(13). Retrieved from <https://www.usbr.gov/tsc/techreferences/designstandards-datacollectionguides/finalds-pdfs/DS13-6.pdf>
- U.S. Department of the interior Bureau of Reclamation. (2012). Embankment Dams. Chapter 6. Freeboard. Design Standards No. 13: Embankment Dams, 4(13).
- U.S. EPA. (2014). An Assessment of Potential Mining Impacts on Salmon Ecosystems of Bristol Bay, Alaska. EPA 910-R-14-001a, 1(January). <https://doi.org/10.1145/1391978.1391983>
- USEPA (U.S. Environmental Protection Agency). 2014. An Assessment of Potential Mining Impacts on Salmon Ecosystems of Bristol Bay, Alaska. Region 10, Seattle, WA. EPA 910-R-14-001.
- USGS (2019). About 3DEP Products and Services. Website accessed January 2, 2019. <https://www.usgs.gov/core-science-systems/ngp/3dep/about-3dep-products-services>
- Wahl, T. L. (1998). Prediction of Embankment Dam Breach Parameters: Literature Review and Needs Assessment, Dam Safety Research Report. DSO-98-004. Retrieved from <https://www.nrc.gov/docs/ML0901/ML090150051.pdf>
- Woll, C., Albert, D., & Whited, D. (2012). A Preliminary Classification and Mapping of Salmon Ecological Systems in the Nushagak and Kvichak Watersheds, Alaska. Retrieved from <https://pdfs.semanticscholar.org/43d8/6d6c0d2f5167db66563c30f8a327ab2ffa7d.pdf>

7 Appendices

7.1 Additional Model Sensitivity Assessments

7.1.1 Sensitivity to Maximum Sediment Concentration

The FLO-2D model was found to be moderately sensitive to the sediment concentration of the inflow breach hydrograph. Model results using a maximum sediment concentration of 50% were compared to results using a maximum sediment concentration of 35%. A literature review of dam failure mudflow events results in hyperconcentrated sediment flows are typically characterized by sediment concentration by volume values ranging from 10% to 55% (Julien & Leon S., 2000; Major & Pierson, 1992; J. S. O'Brien et al., 1993; Jim S. O'Brien & Julien, 1988). The FLO-2D Reference Manual and Mudflow Guidelines documentation (FLO-2D, 2017) also defines hyperconcentrated sediment flows as flows with average sediment concentrations greater than 20% by volume. Therefore, all simulations implemented breach hydrographs with greater than 20% average sediment concentration to adequately represent a breach from a tailings pond. As described in section 4.2, the breach hydrograph includes both a water and sediment component over a given time. Just as water discharge changes over time, so does the sediment concentration. We use the term maximum sediment concentration for clarity, since the breach inflow hydrograph does not have a static sediment concentration over time.

The FLO-2D model results using a maximum sediment concentration of 50% distribute more sediment on the floodplain compared to the 35% results (67 million m³ versus 27 million m³, respectively). However, the inundated areas are similar in both model runs (228 million m² for 50% and 235 million m² for 35%). The inundation maps show that the 50% model results have deeper flow depths for more cells along the Koptuli River (Figure 42). The floodplain hydrographs are different from the dam breach until the Swan River, where the large, flat topography allows the floodwave to dissipate across the valley. The flood hydrograph for the 50% maximum sediment concentration has a larger peak flow than the 35% hydrograph (Figure 43). The cross section hydrographs are very similar at the Mulchatna River. Thus, the model is sensitive to the maximum sediment concentration, but this sensitivity decreases in importance from upstream to downstream.

Table 24: Maximum Sediment Concentration Sensitivity Analysis – Model Output

Model Run	Bulked Breach Volume (million m ³)	Bulked Floodplain Storage (million m ³)	Bulked Outflow Volume (million m ³)	Storage as a % of Inflow	Outflow as a % of Inflow	Maximum Inundated Area (km ²)
35% max sediment concentration	341.9	27.3	314.6	8.0%	92.0%	235.1
50% max sediment concentration	341.9	67.2	274.7	19.7%	80.4%	228.0

Table 25: Maximum Sediment Concentration Sensitivity Analysis – Hydrograph Output

Model Run	Koptuli River upstream of Swan River (XS-7)			Mulchatna River (XS-4)		
	Maximum Discharge (m ³ /s)	Time to Maximum Discharge (hours)	Total Discharge Volume (million m ³)	Maximum Discharge (m ³ /s)	Time to Maximum Discharge (hours)	Total Discharge Volume (million m ³)
35% max sediment concentration	6,600	23.0	337.4	2,540	44.0	316.6

50% max sediment concentration	7,900	23.5	332.3	2,660	46.1	276.8
--------------------------------	-------	------	-------	-------	------	-------

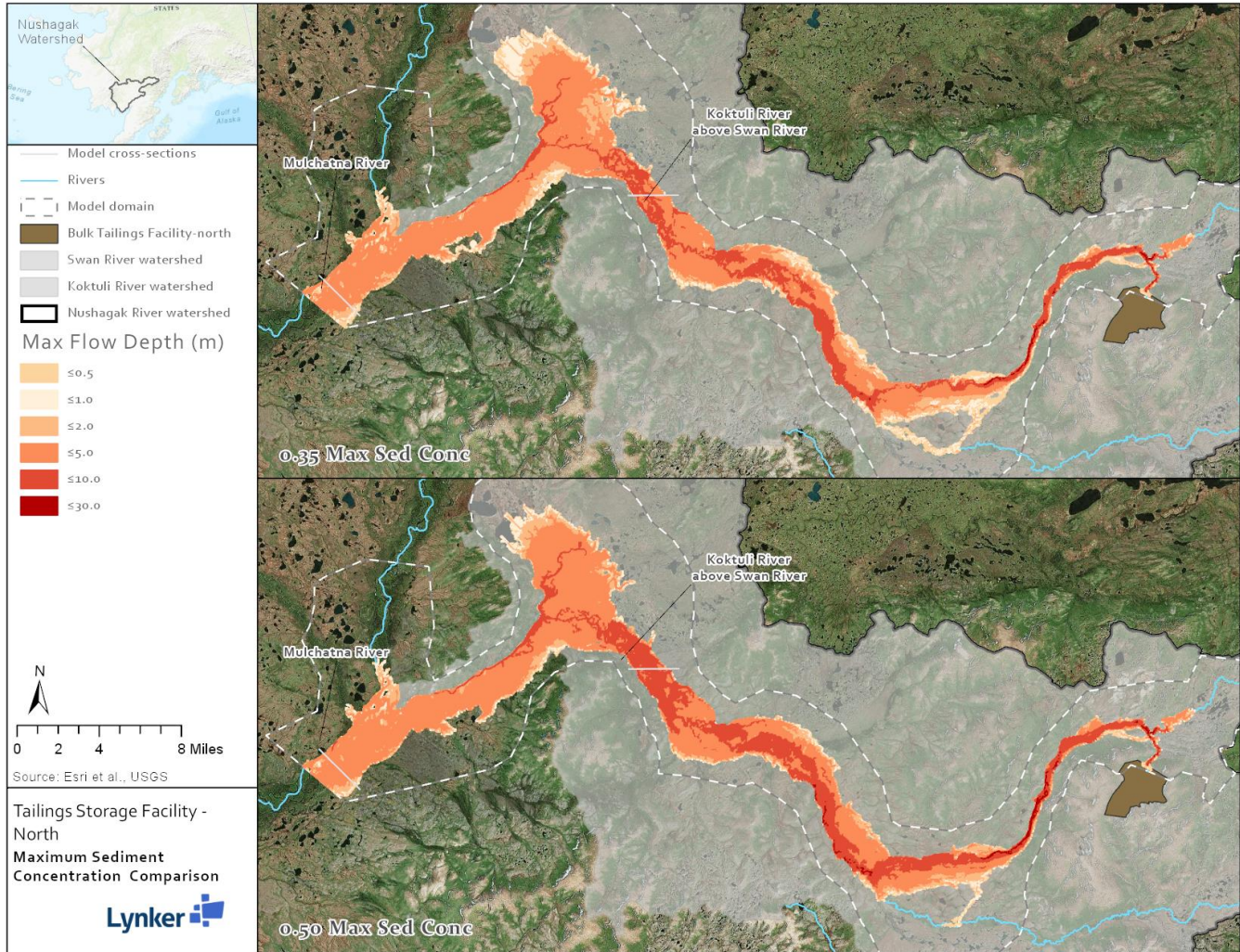


Figure 42: Max flow depth map of model sensitivity to sediment concentration of breach discharge

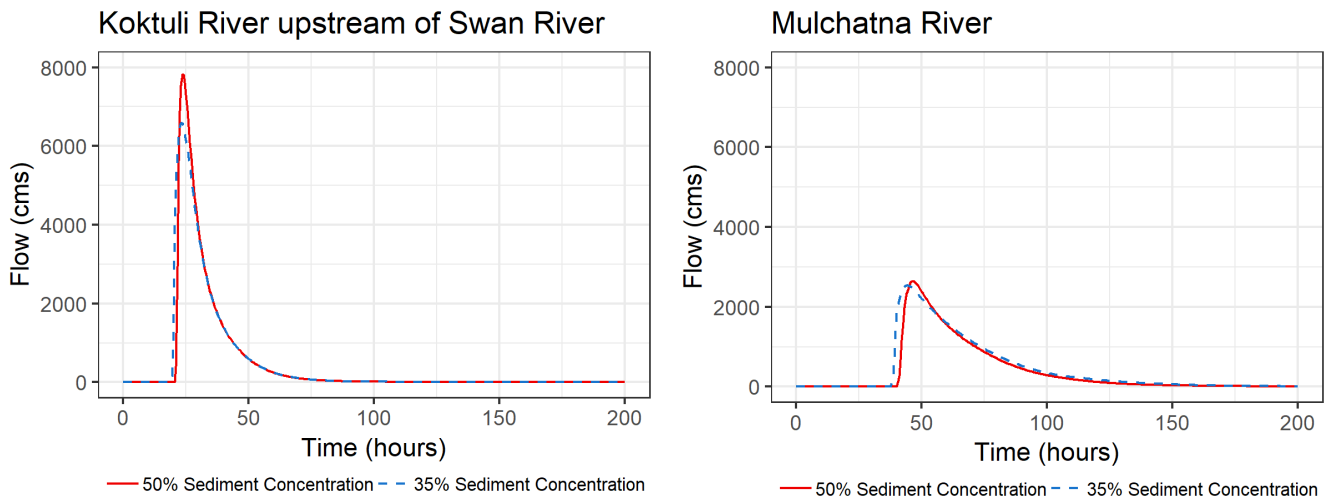


Figure 43: Sediment Concentration Sensitivity Analysis – Hydrograph

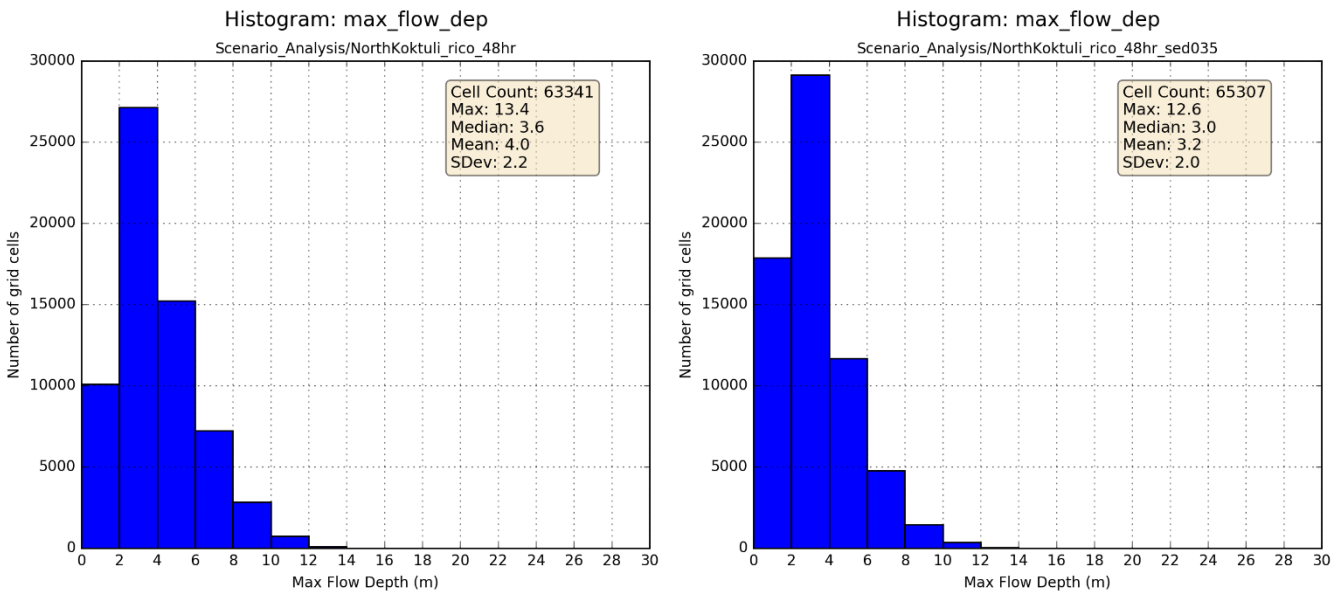


Figure 44. Histograms of the max flow depth cell values for the 50% (left) and 35% (right) max sediment concentration simulations

7.1.2 Laminar Flow Resistance Sensitivity

We examined two scenarios to examine the sensitivity of the model outputs to the variable laminar flow resistance properties of the non-Newtonian flow. An initial estimate of the laminar flow resistance ($K = 2,480$) was developed from Table 8 in the FLO-2D Reference Manual based on the surface vegetation coverage. A second value ($K = 4,960$) was implemented for the sensitivity comparison simulation. This section outlines the model results from the “standard” laminar flow resistance parameter simulation alongside the “increased” laminar flow resistance model simulation.

The FLO-2D model results using the increased laminar flow resistance results in increased bulked breach volume stored within the floodplain. The inundated areas are similar in both model runs (253.4 km² for the increased

laminar flow simulation and 255.9 km² for the standard laminar flow simulation). The floodplain hydrographs also show very similar results for the discharge hydrographs upstream and downstream of the Swan River confluence (Figure 45). Therefore, the model is largely considered to be insensitive to the range of yield stress parameters evaluated.

Table 26: Laminar Flow Sensitivity Analysis – Model Output

Model Run	Bulked Breach Volume (million m ³)	Bulked Floodplain Storage (million m ³)	Bulked Outflow Volume (million m ³)	Storage as a % of Inflow	Outflow as a % of Inflow	Maximum Inundated Area (km ²)
Increased laminar flow resistance	341.9	81.6	260.3	23.9%	76.1%	253.4
Standard laminar flow resistance	341.9	69.6	272.4	20.4%	79.7%	255.9

Table 27: Laminar Flow Sensitivity Analysis – Hydrograph Output

Model Run	Koktuli River upstream of Swan River			Mulchatna River		
	Maximum Discharge (m ³ /s)	Time to Maximum Discharge (hours)	Total Discharge Volume (million m ³)	Maximum Discharge (m ³ /s)	Time to Maximum Discharge (hours)	Total Discharge Volume (million m ³)
Increased laminar flow resistance	9,580	17.7	325.6	2,630	39.2	262.6
Standard laminar flow resistance	9,800	17.6	328.4	2,720	38.0	274.7

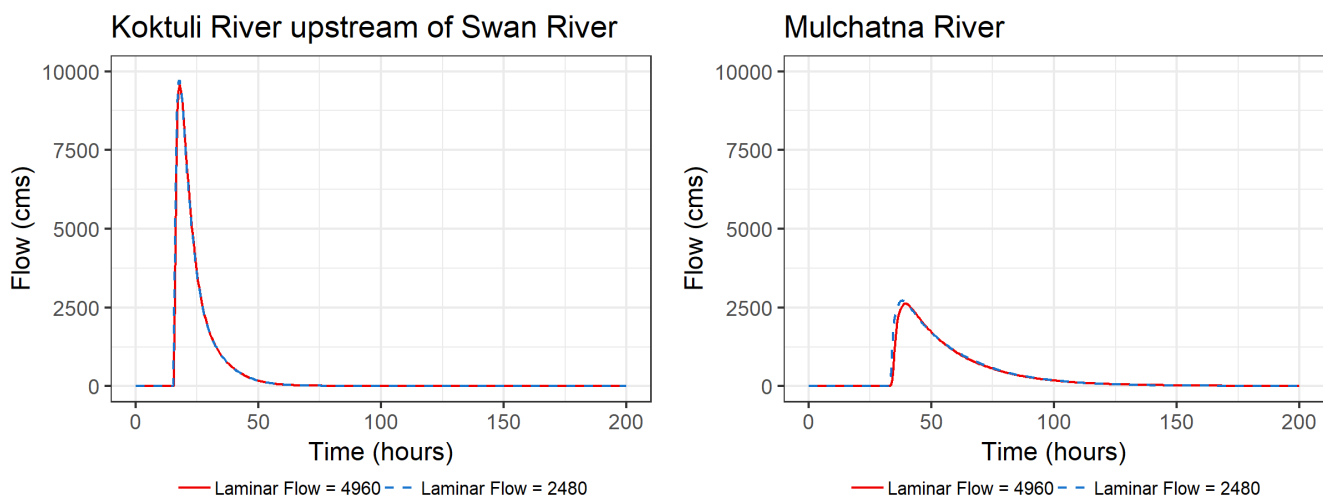


Figure 45: Laminar Flow Resistance Sensitivity Analysis – Hydrograph

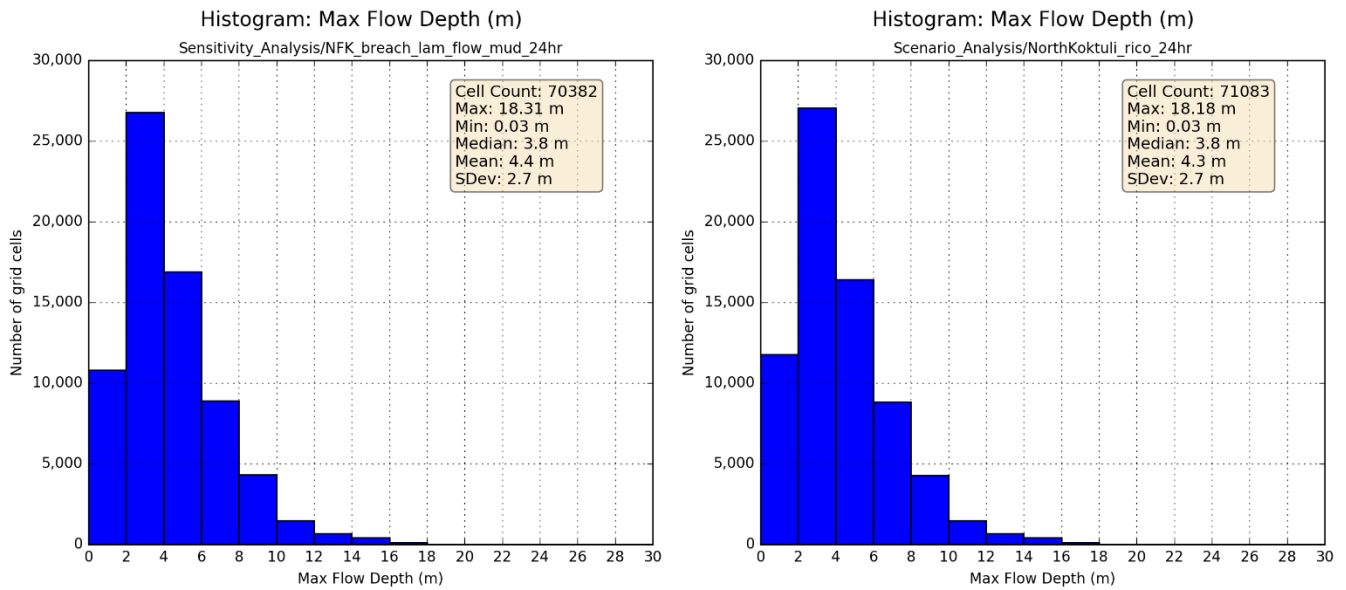


Figure 46. Histograms of the max flow depth cell values for the increased laminar flow (left) and default laminar flow (right) simulations

7.2 Reach-Scale Analysis of Salmon Habitat Characteristics

A TNC study of the relative distribution and abundance of salmon by species and life state developed a reach-scale analysis of salmon habitat characteristics and estimates of salmon abundance throughout the Nushagak watershed (Woll et al., 2012). The study used a multitude of reach-scale properties from satellite imagery, topographic data, and hydrography data (e.g. stream order, elevation, gradient, mean annual flow, channel width, etc.) to develop a database of salmon habitat characteristics. The maps on the following pages illustrate the spawning and rearing habitat suitability classifications for Chinook, Sockeye, and Coho Salmon developed in the TNC study. Reach segments are ranked from 1 (low suitability) to 4 (high suitability) to identify important salmon habitat areas as well as estimates of potential salmon abundance.

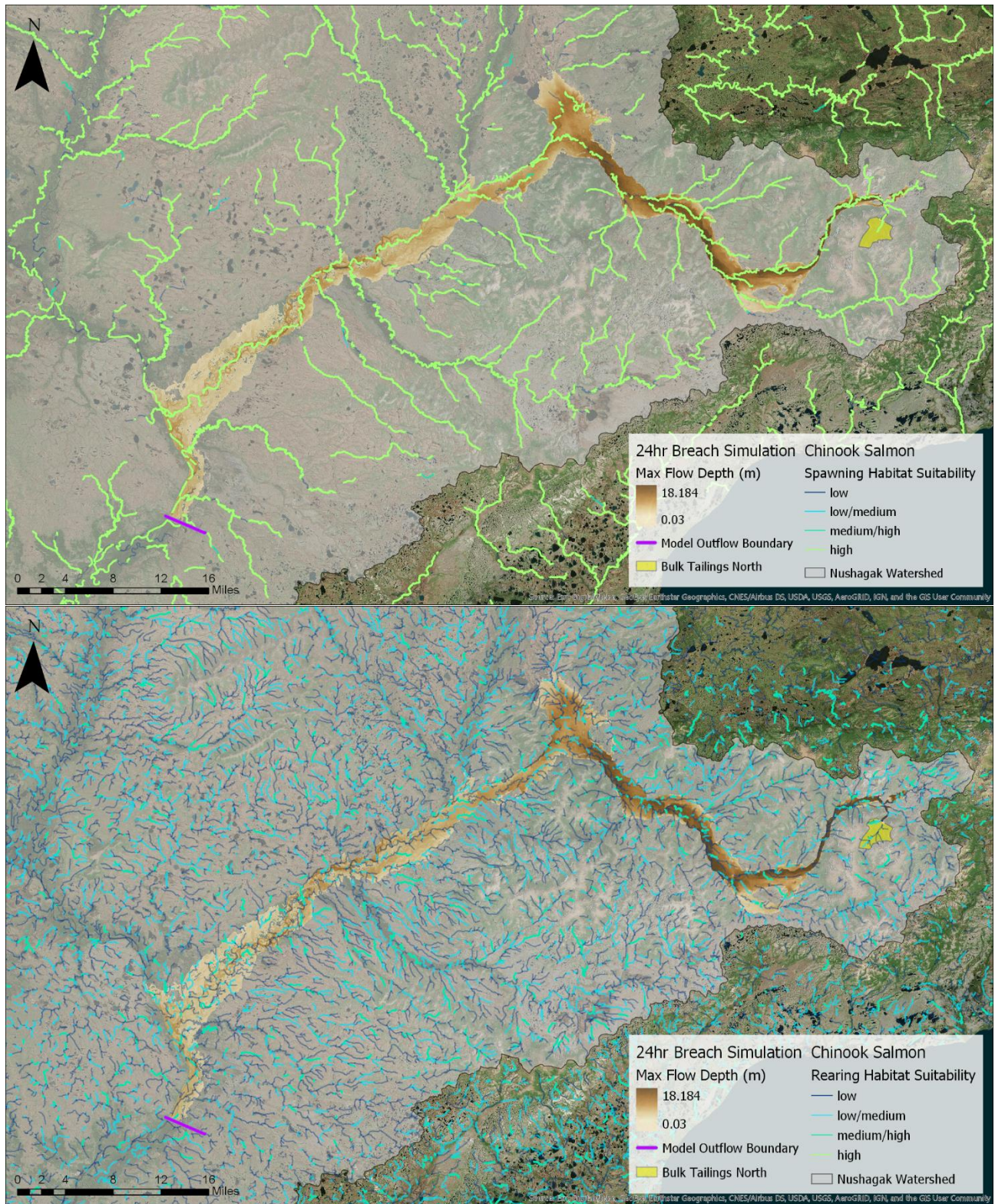


Figure 47. Map of 24-hr breach inundation and Chinook Salmon spawning (top) and rearing (bottom) habitat suitability reach scores.

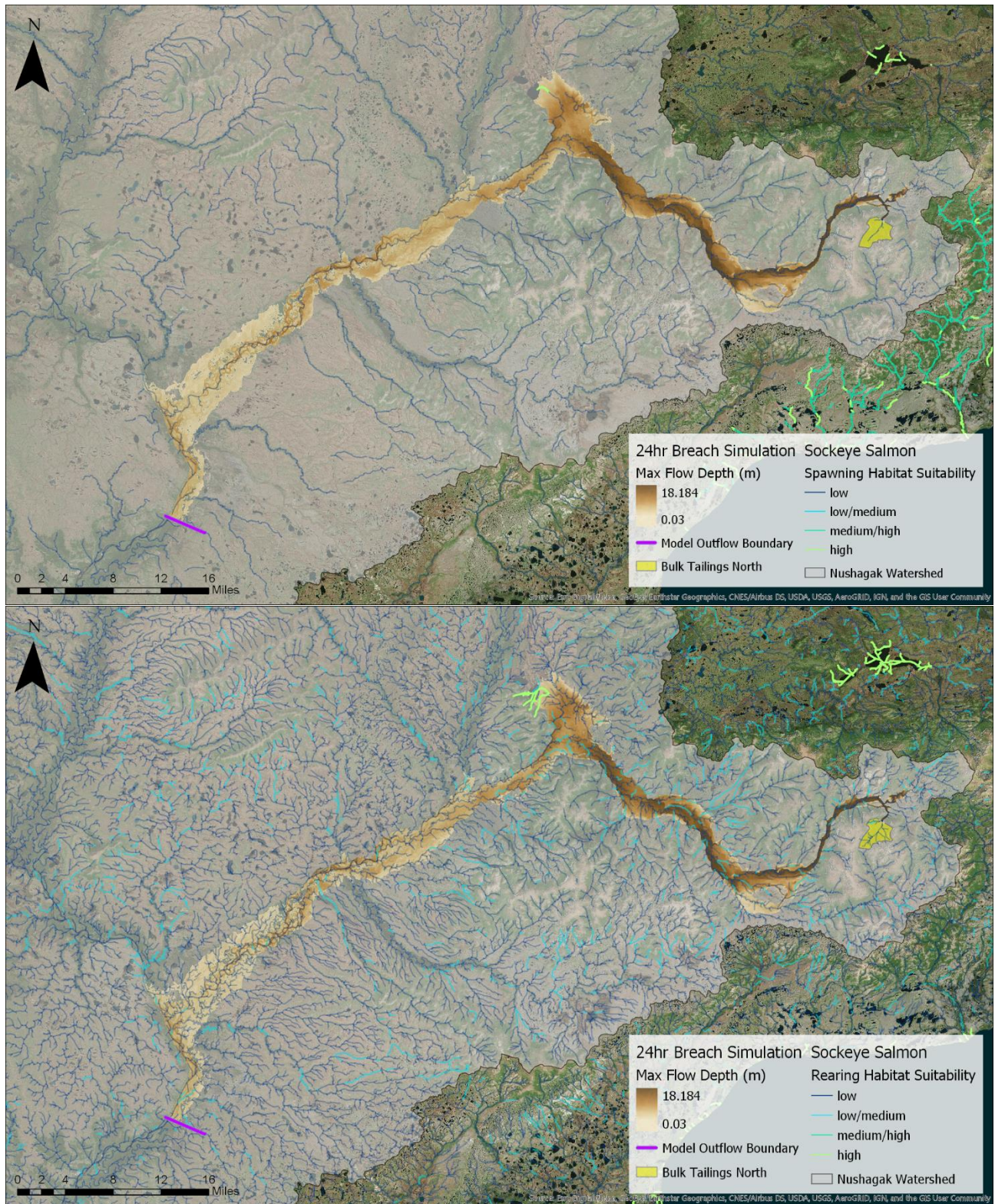


Figure 48. Map of 24-hr breach inundation and Sockeye Salmon spawning (top) and rearing (bottom) habitat suitability reach scores.

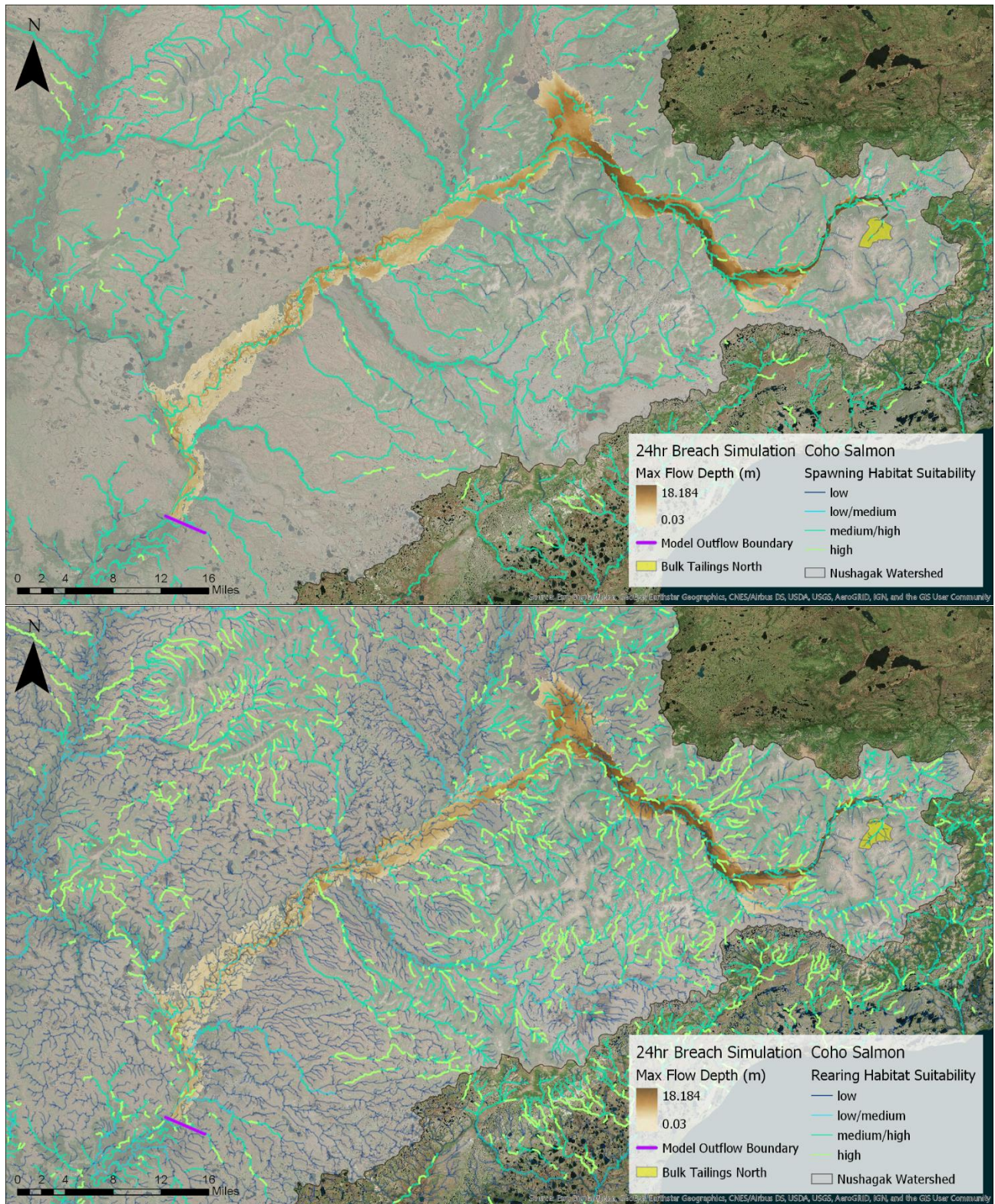


Figure 49. Map of 24-hr breach inundation and Coho Salmon spawning (top) and rearing (bottom) habitat suitability reach scores.

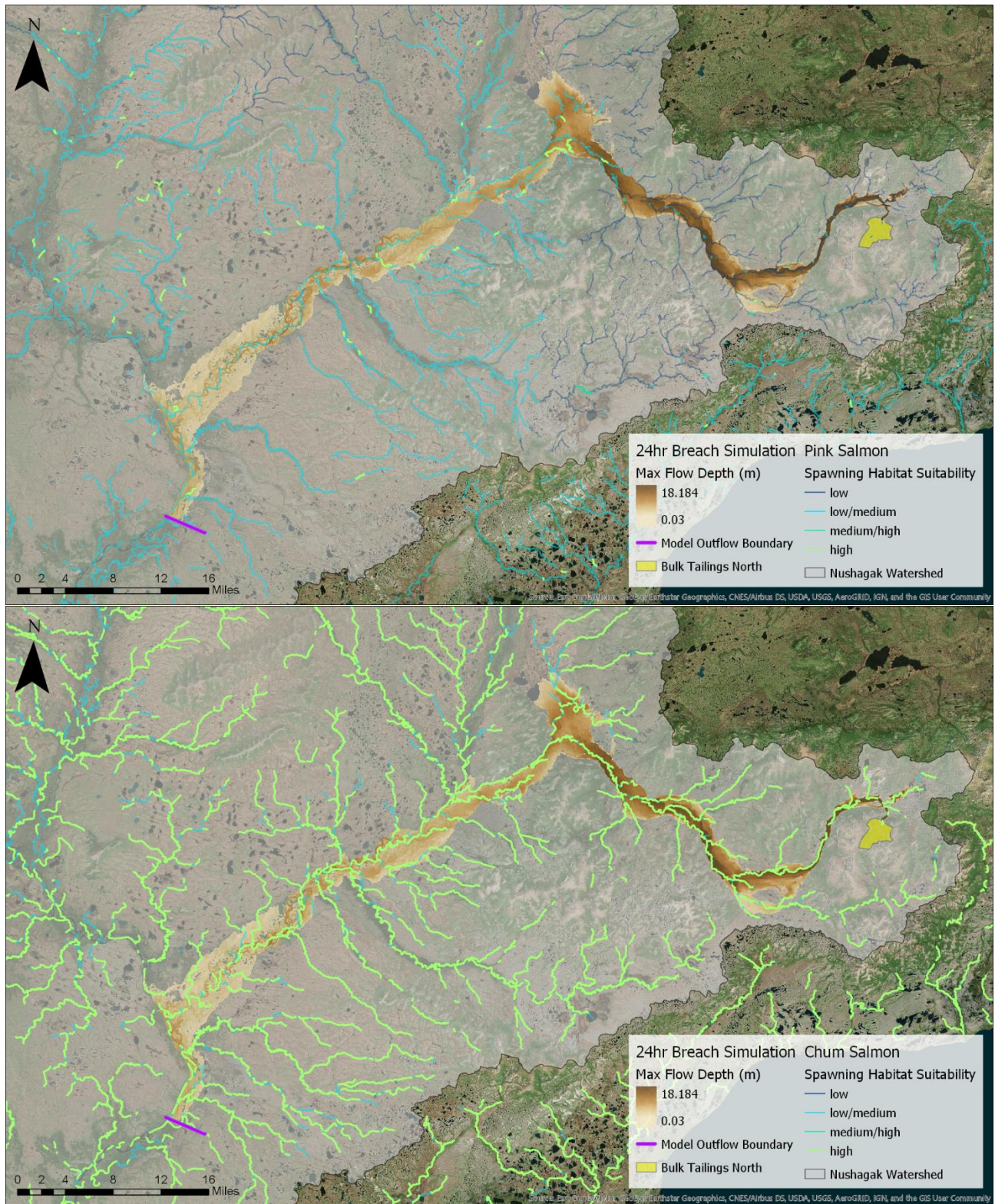


Figure 50. Map of 24-hr breach inundation and Pink Salmon spawning (top) and Chum Salmon spawning (bottom) habitat suitability reach scores.

7.3 Report Authors and Funding

This study was conducted under contract # LYNK-2018-179 from the Nature Conservancy (TNC) to Lynker, with funding provided to TNC by the Bristol Bay Regional Seafood Development Authority (BBRSDA). The model setup, breach hydrographs, and model runs were conducted by Ryan Spies, MS, and Bill Szafranski, MS, under the direction of Cameron Wobus, PhD. Mr. Spies, Mr. Szafranski and Dr. Wobus are all employees of the Water and Environmental Resources division at Lynker. Mapping and technical support were provided by James DePasquale, MS and Dave Albert, MS, both of TNC. Biographies of the three modeling leads are summarized below.

Ryan Spies, MS, is a hydrologic scientist with Lynker Technologies in Boulder, CO. He is experienced in hydrometeorological data analysis, statistical hydrology assessments, and surface water modeling applications using spatially-distributed hydrologic modeling tools. With experience spanning both the public and private sectors, Mr. Spies has conducted hydrologic and hydraulic modeling studies throughout the United States including river forecast model development and calibration for the National Weather Service Alaska-Pacific River Forecast Center. Recent project experiences also include developing and optimizing automated flood warning systems, flood inundation mapping applications, and reservoir water supply optimization studies.

Bill Szafranski, MS, is a water resources scientist at Lynker with experience in hydrology, water resources engineering, watershed and water quality modeling, and watershed planning. Mr. Szafranski is passionate about using modeling tools to help local, state and federal organizations improve their understanding of their water supply and better quantify their vulnerability to extreme events such as drought. This includes developing a more robust understanding of system reliability and resilience using synthetic hydrology, paleohydrology data, and climate-adjusted hydrology. Mr. Szafranski has developed numerous reservoir operations models for the National Weather Service (NWS) River Forecast Centers, completed hydrologic analyses evaluating projected impacts from climate change, and worked with diverse multi-stakeholder agencies to develop modeling solutions for their watersheds.

Cameron Wobus, PhD, is a broadly trained Earth scientist with specific expertise in geomorphology, surface and groundwater hydrology, and numerical modeling and data analysis. For approximately 10 years, he has supported Federal, State and nongovernmental clients on topics including environmental impacts of hard rock mining, climate change impact analyses, and environmental litigation. Between 2010 and 2015, Dr. Wobus served as an expert supporting the State of Louisiana in its natural resource claims related to the Deepwater Horizon oil spill, leading a team of academic experts to provide data-driven solutions to support inter-agency discussions and settlement negotiations. Prior to his career in consulting, Dr. Wobus was a research scientist at the University of Colorado, where he led a field-based, multi-investigator study of climate change and coastal erosion on the North Slope of Alaska. Dr. Wobus holds a PhD in earth sciences from MIT, an MS in hydrology from Dartmouth College, and a BA in geology and economics from Bowdoin College.